Qualitative and Quantitative Phase Analysis

James A. Kaduk
Poly Crystallography Inc.
Naperville IL 60540
kaduk@polycrystallography.com

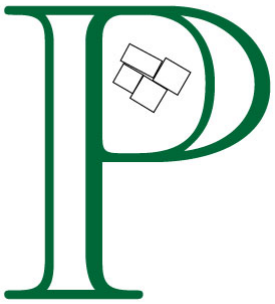

NORTH CENTRAL COLLEGE 1861

ILLINOIS INSTITUTE OF TECHNOLOGY

Qualitative Phase Identification

The peak positions in a powder diffraction pattern are determined by the size, shape, and symmetry of the unit cell. The relative intensities are determined by the arrangement of atoms. The powder pattern is thus an excellent "fingerprint" for phase identification.

To what do we compare our experimental data?

- PDF-4+ (annual) – 444,133 entries (2021)
- WebPDF-4, PDF-4 Minerals (48,946), PDF-4/Axiom (97,789)
- PDF-4 Organics (annual) – 547,295 (2021)
- PDF-2 (5 year) – 316,820 (2021)

Databases and Indexes

- A database is a compilation of many similar records of identical format.
- An index is a subset of the database, and is used to yield potential matches.

Search/Match Methods

The phase identification process actually involves several steps:

- *Search* – search an index for possible hits
- *Match* – check the experimental pattern against the reference pattern
- *Identify* – decide whether the match is reasonable
- *Repeat* for more phases
- *(Quantify)*

Phase Identification

- Pattern matching
- Boolean searches

(often most effective in combination)

History of Search/Match

Crystallographic databases and powder diffraction, J. A. Kaduk, Chapter 3.7 in *International Tables for Crystallography Volume H: Powder Diffraction* (2019).

Search/Match Examples

Crystallographic databases and powder diffraction, J. A. Kaduk, Chapter 3.7 in *International Tables for Crystallography Volume H: Powder Diffraction* (2019).

More Examples in Kaduk_ICDD.pptx/PDF

Now to quantitative phase analysis…

Harry Potter and the Sorcerer's (Philosopher's) Stone

Ron: Seeker? But first years never make the house team. You must be the youngest Quiddich player in …

Harry: … a century. According to McGonagall.

Fred/George: Well done, Harry. Wood's just told us.

Ron: Fred and George are on the team, too. Beaters.

Fred/George: Our job is to make sure *you* don't get bloodied up too bad.

Alastor “Mad-Eye” Moody – “Constant Vigilance”

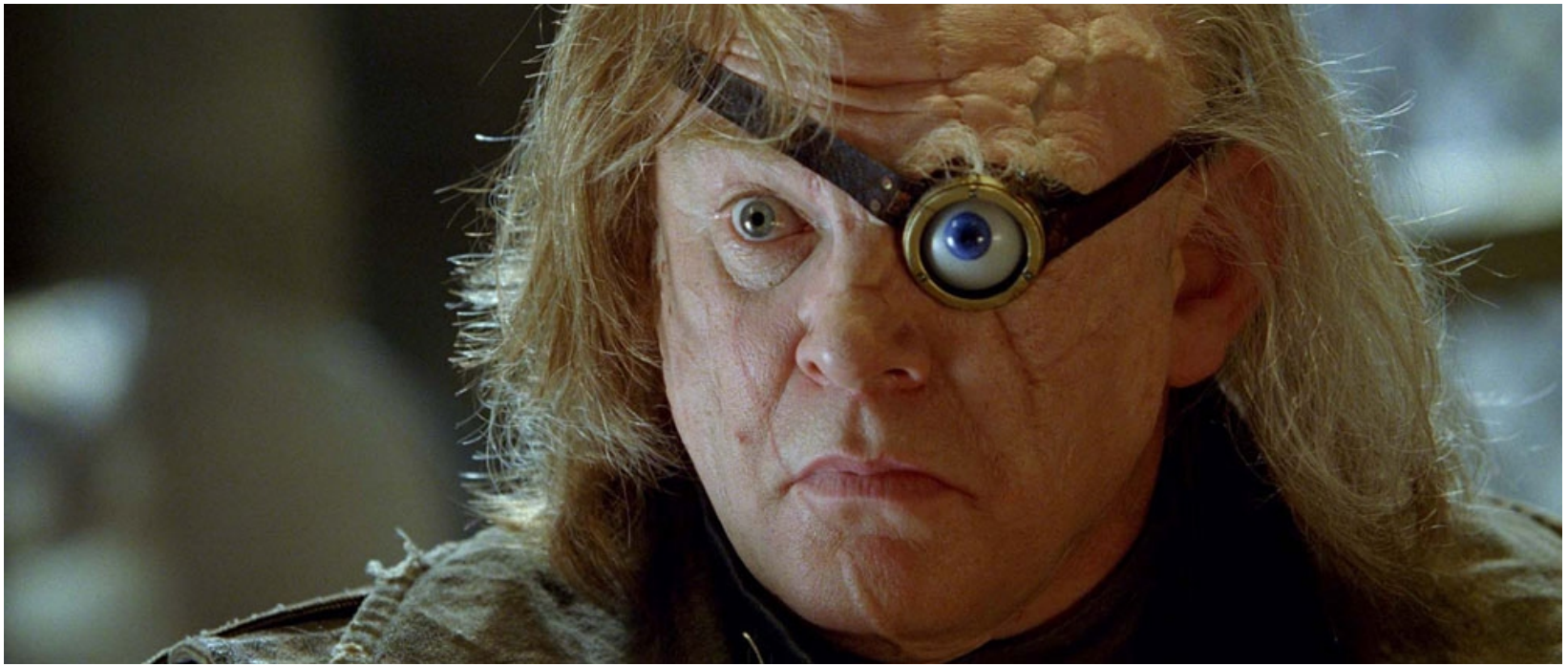

Harry Potter and the Goblet of Fire (2005)

Ian Madsen, Nicola Scarlett, Reinhard Kleeberg, and Karsten Knorr, "Quantitative Phase Analysis", Chapter 3.9 in *International Tables for Crystallography Volume H: Powder Diffraction* (2019).

Quantitative Analysis

Quantitative analysis by X-ray diffraction is the best method to determine **phase** composition.

"C. P. NaF" = NaF + $NaHF_2$

Albert W. Hull (GE),

"New Method of Chemical Analysis",

J. Amer. Chem. Soc., **41**, 1168-1175 (1919)

Quantitative Phase Analysis by X-ray Diffraction Papers in *Google Scholar*

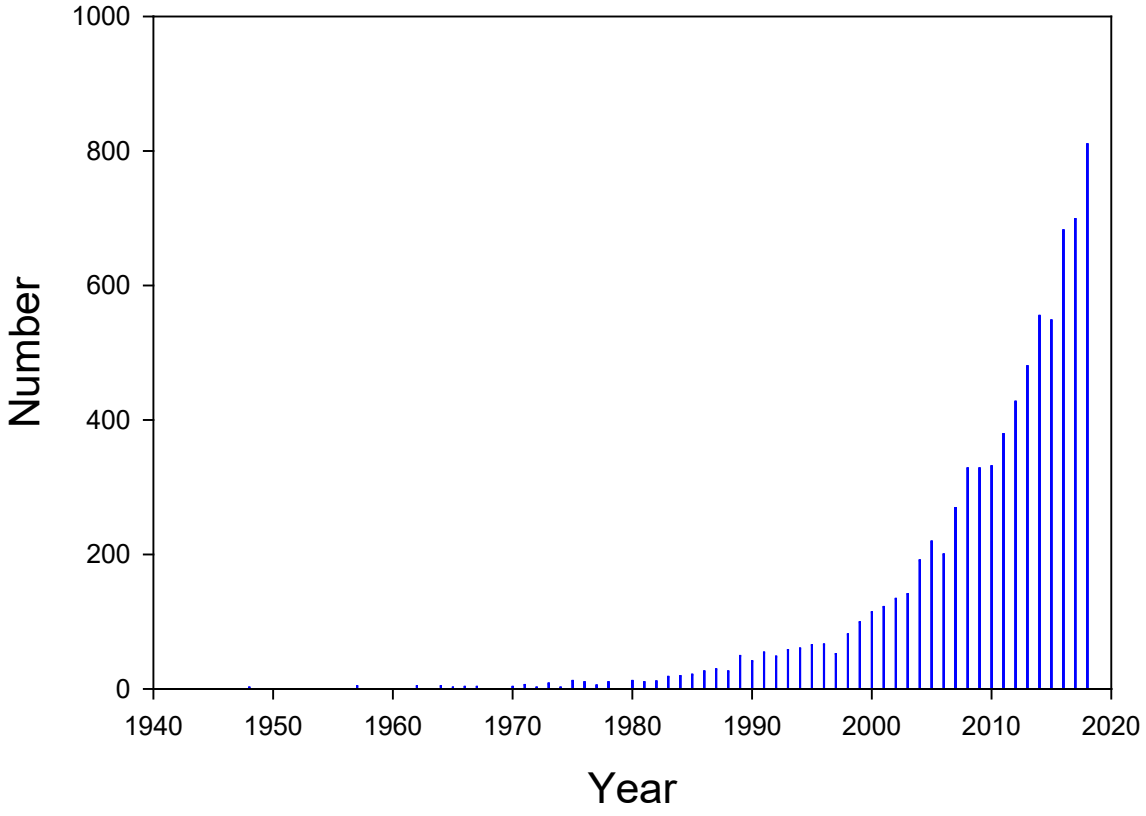

Early QPA Bibliography

- P. Debye and P. Scherrer, “Interferenzen an regellos orientierten teilchen in röntgenlicht”, *Physikalische Zeitschrift*, **17**, 277-283 (1916).
- P. Debye and P. Scherrer, “Interferenzen an regellos orientierten teilchen in röntgenlicht”, *Physikalische Zeitschrift*, **18**, 291-301 (1917).
- A. W. Hull, “A new method of x-ray crystal analysis”, *Phys. Rev.*, **10**, 661-661 (1917).
- A. W. Hull, “A new method of chemical analysis”, *J. Amer. Chem. Soc.*, **41**, 1168-1195 (1919).
- A. L. Navais, “quantitative determination of the development of mullite in fired clays by an x-ray method”, *J. Amer. Ceram. Soc.*, **8**, 296-302 (1925).

Significant Papers in Quantitative Analysis (1)

- L. E. Alexander and H. P. Klug, "Basic Aspects of X-ray Absorption in Quantitative Diffraction Analysis of Powder Mixtures", *Anal. Chem.*, **20**, 886-889 (1948).
- J. Leroux, D. H. Lennox, and K. Kay (Occupational Health Lab., Ottawa), "Direct quantitative X-ray Analysis by Diffraction-Absorption Technique", *Anal. Chem.*, **25**, 740-743 (1953).
- L. E. Copeland and R. H. Bragg (Portland Cement Assoc.), "Quantitative X-ray Diffraction Analysis", *Anal. Chem.*, **30**, 196-201 (1958).

Significant Papers in Quantitative Analysis (2)

- P. M. de Wolff and J. W. Visser, "Absolute Intensities – Outline of a Recommended Practice", *Powder Diffraction*, **3**, 202-204 (1988).
- R. F. Karlak and D. S. Burnett (Lockheed), "Quantitative Phase Analysis by X-ray", *Anal. Chem.*, **38**, 1741 (1996).
- F. H. Chung (Sherwin-Williams), "Quantitative Interpretation of X-ray Diffraction Patterns of Mixtures. I. Matrix-Flushing Method for Quantitative Multicomponent Analysis", *J. Appl. Cryst.*, **7**, 519-525 (1974).

Significant Papers in Quantitative Analysis (3)

- F. H. Chung, "Quantitative Interpretation of X-ray Diffraction Patterns of Mixtures. II. Adiabatic principle of X-ray Diffraction Analysis of Mixtures", *J. Appl. Cryst.*, **7**, 526-531 (1974).
- F. H. Chung, "Quantitative Interpretation of X-ray Diffraction Patterns of Mixtures. III. Simultaneous Determination of a Set of Reference Intensities", *J. Appl. Cryst.*, **8**, 17-19 (1975).
- R. L. Snyder, C. R. Hubbard, and N. C. Panagiotopoulos, "A Second Generation Automated Powder Diffractometer Control System", *Adv. X-ray Anal.*, **25**, 245-260 (1982).

Significant Papers in Quantitative Analysis (4)

- T. H. Starks, J. H. Fang, and L. S. Zevin (SIU), "A Standardless Method of Quantitative X-ray Diffractometry Using Target-Transformation Factor Analysis", *J. Int. Assn. Math. Geol.*, **16**, 351-367 (1984).
- D. K. Smith, G. G. Johnson Jr., A. Scheible, A. M. Wims, J. L. Johnson, and G. Ullmann, "Quantitative X-ray Powder Diffraction Method Using the Full Diffraction Pattern", *Powd. Diff.*, **2**, 73-81 (1987).
- D. L. Bish and S. A. Howard, "Quantitative Phase Analysis Using the Rietveld Method", *J. Appl. Cryst.*, **21**, 86-91 (1988).

Significant Papers in Quantitative Analysis (5)

- D. K. Smith, G. G. Johnson Jr., M. J. Kelton, and C. A. Andersen, "Chemical Constraints in quantitative X-ray Powder Diffraction for Mineral Analysis of the Sand/Silt Fractions of Sedimentary Rocks", *Adv. X-ray Anal.,* **32**, 489-496 (1989).

- Plus the usual treatments of powder diffraction:

  Pecharsky & Zavalij, Jenkins & Snyder,

  Klug & Alexander, Cullity & Stock,

  Clearfield, Reibenspies & Bhuvanesh, Dinnebier & Billinge, Mittemeijer & Welzel …

Quantitative phase analysis relies on measurement of *intensities*. Intensities (especially absolute) are the weakest aspect of a powder diffraction measurement. QPA is thus hard!

Intensity is a function of

- Crystal structure
- Instrument (kV, mA, slits, …)
- Specimen
- Measurement technique
- Data processing technique
- Concentration

Which intensity?

- (Peak height)
- Single peak integrated intensity
- Peak cluster(s)
- Whole pattern

Intensity of a Diffraction Peak

$$I_{(hkl)\alpha} = \frac{I_0 \lambda^3}{64\pi r}\left(\frac{e^2}{m_e c^2}\right)^2 \frac{M_{(hkl)}}{V_\alpha^2}\left|F_{(hkl)\alpha}\right|^2 \left(\frac{1+\cos^2(2\theta)\cos^2(2\theta_m)}{\sin^2\theta\cos\theta}\right)_{hkl} \frac{v_\alpha}{\mu_s}$$

I_0	incident beam intensity	μ_s	linear absorption coefficient of specimen	V_α	volume of the unit cell of phase α
r	distance from specimen to detector	v_α	volume fraction of phase α	$2\theta_m$	diffraction angle of the monochromator
λ	X-ray wavelength	M_{hkl}	multiplicity of reflection hkl of phase α	$F_{(hkl)\alpha}$	structure factor for reflection hkl of phase α
$(e^2/m_e c^2)^2$	square of classical electron radius	()	Lorentz-polarization correction		

or, in terms of weight fraction:

$$I_{(hkl)\alpha} = \left[\frac{I_0\lambda^3}{64\pi r}\left(\frac{e^2}{m_e c^2}\right)^2\right]\left[\frac{M_{(hkl)}}{V_\alpha^2}\left|F_{(hkl)\alpha}\right|^2\left(\frac{1+\cos^2(2\theta)\cos^2(2\theta_m)}{\sin^2\theta\cos\theta}\right)_{hkl}\right]\left[\frac{X_\alpha}{\rho_\alpha\left(\mu/\rho\right)_s}\right]$$

$$I_{(hkl)\alpha} = \frac{K_e K_{(hkl)\alpha} X_\alpha}{\rho_\alpha\left(\mu/\rho\right)_s}$$

X_α	weight fraction of phase α	ρ_α	density of phase α
$(\mu/\rho)_s$	mass attenuation coefficient of the polyphase specimen	μ	linear absorption coefficient

Absorption is the fundamental problem in quantitative phase analysis. Absorption needs to be measured, estimated, ignored, or calculated:

$$\left(\frac{\mu}{\rho}\right)_s = \sum_j \left(\frac{\mu}{\rho}\right)_j X_j$$

The single intensity equation contains two unknowns - X_α and $(\mu/\rho)_s$ – how do we get the extra information necessary to solve the problem?

Journal of Applied Crystallography

IUCr IT WDC

search IUCr Journals

home archive editors for authors for readers submit subscribe open access

research papers

JOURNAL OF APPLIED CRYSTALLOGRAPHY

ISSN: 1600-5767

Volume 51 | **Part 3** | June 2018 | Pages 789-795
https://doi.org/10.1107/S1600576718005228
Viewed by 60

Quantitative X-ray diffraction and X-ray fluorescence analyses of mixtures – unified and simplified

Frank H. Chung[a*]

[a]Analytical Research Department, Sherwin-Williams Research Center, 10909 Cottage Grove Avenue, Chicago, IL 60628, USA
[*]Correspondence e-mail: fhchung1@gmail.com

Edited by Th. Proffen, Oak Ridge National Laboratory, USA (Received 30 November 2017; accepted 2 April 2018; online 18 May 2018)

Owing to the complex matrix effects, the current approach to quantitative X-ray diffraction (XRD) and X-ray fluorescence (XRF) analyses of mixtures requires calibration lines from standards, and is hence tedious and time consuming. New insights reveal that both the matrix effects and the calibration lines can be eliminated mathematically. Any complex mixture can be transformed into a set of simple binary mixtures. One straightforward formula decodes both XRD and XRF. A single XRD or XRF scan quantifies the chemical compounds or chemical elements in any mixture. The unified and simplified procedure reduces by some 80% the laboratory work associated with current practice. Five sets of experimental data are presented to verify its applications. Statistical evaluation of this new procedure gives a precision of ±5% or better, which is normally expected from XRD and XRF analyses.

Keywords: **X-ray diffraction**; **X-ray fluorescence**; **powder diffraction**; **X-ray spectrometry**; **matrix effects**; **adiabatic principle**; **specific intensity**.

Similar articles **PowerPoint slides**

The Absorption-Diffraction Method

Consider the intensity of a line of phase α
in a mixture and in the pure phase:

$$\frac{I_{(hkl)\alpha}}{I^{0}_{(hkl)\alpha}} = \frac{\left(\mu/\rho\right)_{\alpha}}{\left(\mu/\rho\right)_{s}} X_{\alpha}$$

Calculate from bulk chemical analysis.

If the mass absorption coefficients of the analyte and the mixture are the same,

$$\frac{I_{(hkl)\alpha}}{I^{0}_{(hkl)\alpha}} = X_{\alpha}$$

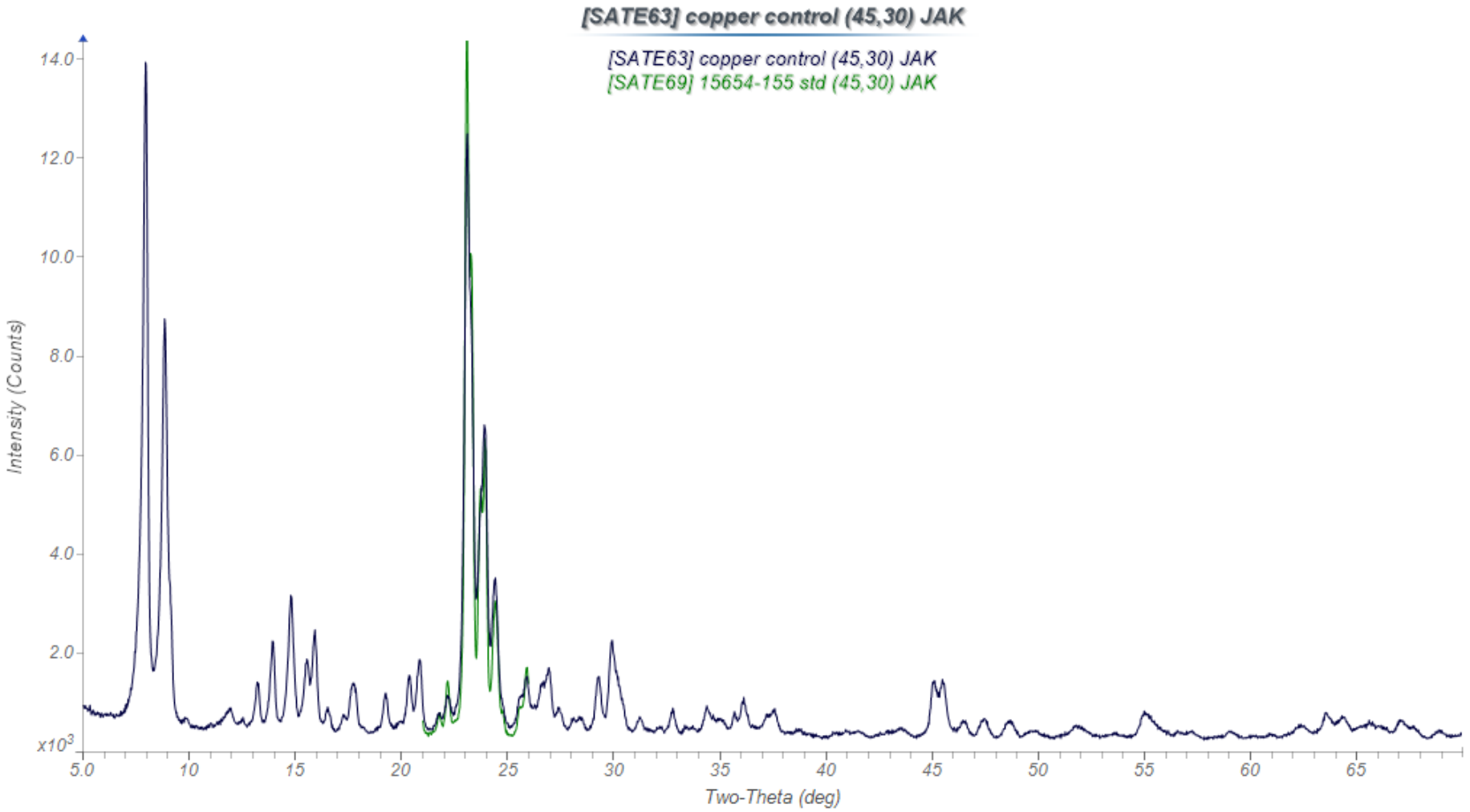
[SATE63] copper control (45,30) JAK
[SATE63] copper control (45,30) JAK
[SATE69] 15654-155 std (45,30) JAK
Intensity (Counts)
x10^3
14.0
12.0
10.0
8.0
6.0
4.0
2.0
5.0
10
15
20
25
30
35
40
45
50
55
60
65
Two-Theta (deg)

ASTM D5758-01

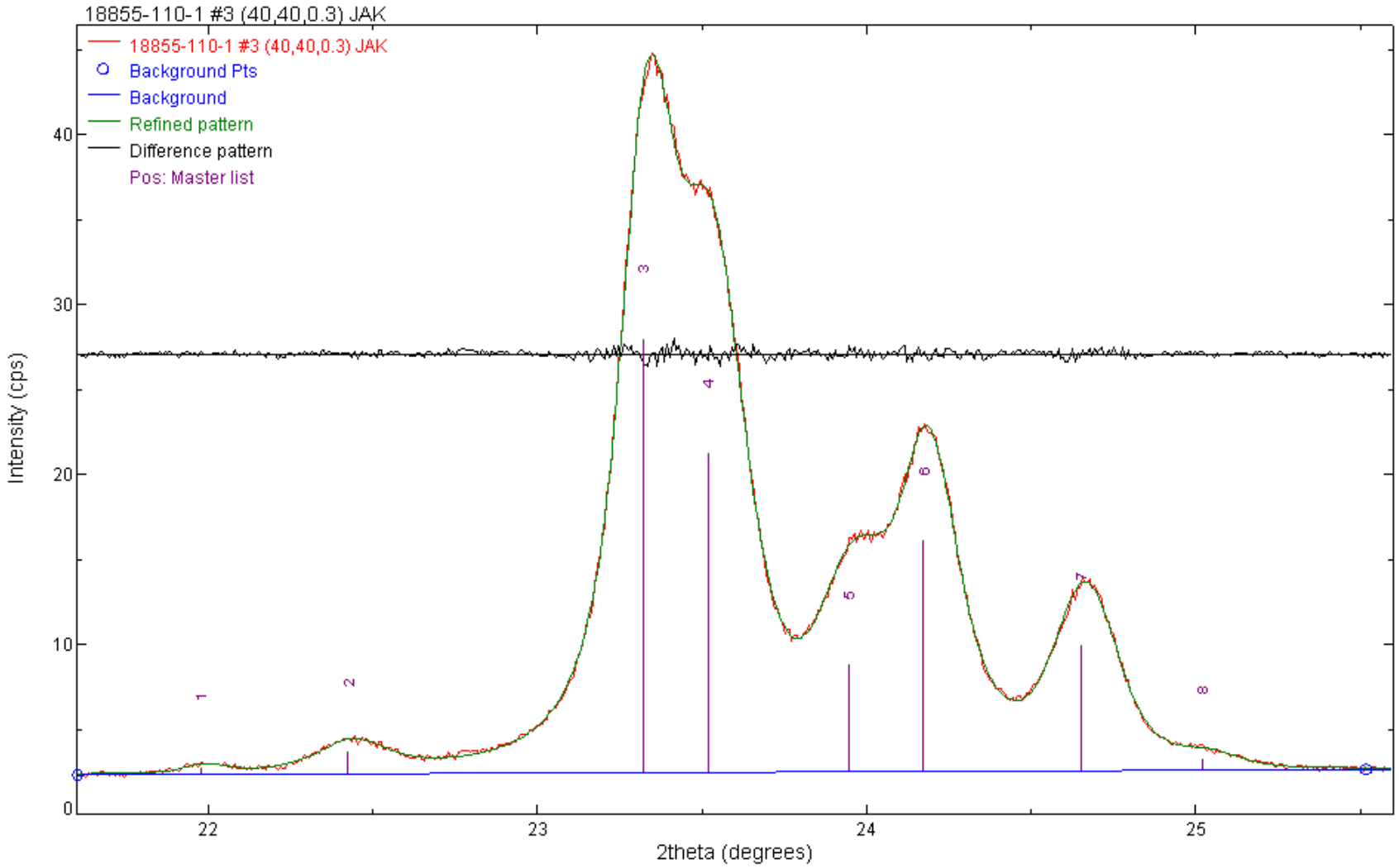

How well (or poorly) can you do? B-MFI HAMS-1B-3

Sample #	16171-106-1	18855-110-1	18855-112-1	18855-11-2
Area 16/6/05	33.26(4)	32.18(8)	29.66(17)	34.69(16)
σ_{rel}, %	0.1	0.2	0.6	0.5
Crystallinity, %	95.9(4)	92.8(5)	85.5(6)	100
Area 22/6/05		28.76(5)	27.39(13)	30.09(14)
		29.40(6)	28.19(9)	30.18(8)
σ_{rel}, %		0.2	0.5	0.5
σ_{rel}, %		0.2	0.3	0.3
Average		29.08(45)	27.79(56)	30.14(6)
σ_{rel}, %		1.5	2.0	0.2
Crystallinity, %		96.5(15)	92.2(20)	100
Area 11/2/99	3386(37)			3731(20)
σ_{rel}, %	1.1			0.5
Crystallinity, %	90.7(11)			100
Area 22/12/97	3446(32)			3574(68)
σ_{rel}, %	0.9			1.9
Crystallinity, %	96.4(20)			100
Grand average	94(3)	95(3)	89(5)	100

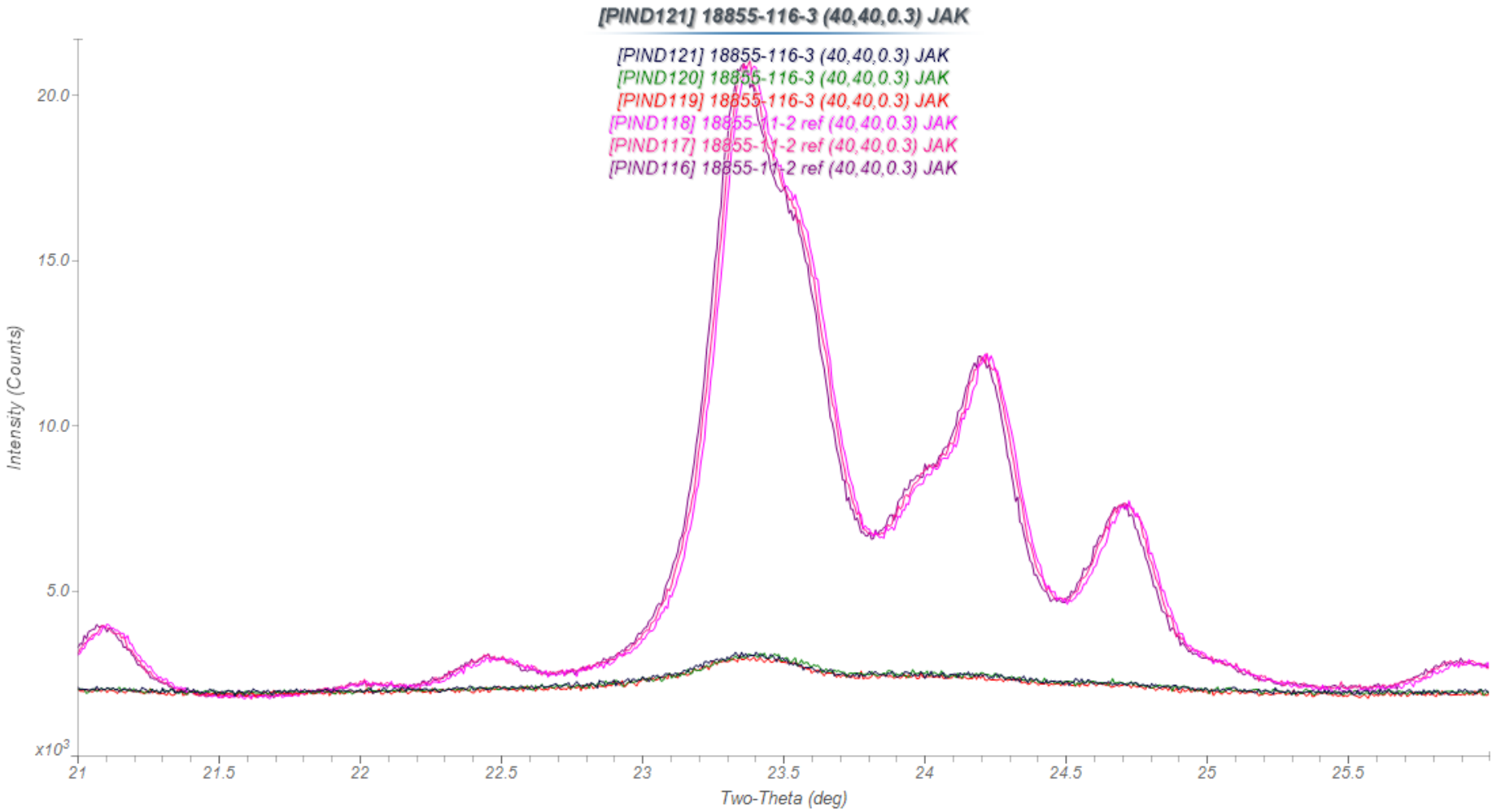
[PIND121] 18855-116-3 (40,40,0.3) JAK
[PIND121] 18855-116-3 (40,40,0.3) JAK
[PIND120] 18855-116-3 (40,40,0.3) JAK
[PIND119] 18855-116-3 (40,40,0.3) JAK
[PIND118] 18855-11-2 ref (40,40,0.3) JAK
[PIND117] 18855-11-2 ref (40,40,0.3) JAK
[PIND116] 18855-11-2 ref (40,40,0.3) JAK
Intensity (Counts)
x10^3
20.0
15.0
10.0
5.0
21
21.5
22
22.5
23
23.5
24
24.5
25
25.5
Two-Theta (deg)

HAMS-1B-3 Catalysts

Sample	Area 1 cps-deg	Area 2 cps-deg	Area 3 cps-deg	Average cps-deg	Crystallinity
18855-116-1	4.06(2)	4.51(3)	4.42(2)	4.33(24)	10.4(6)%
18855-116-2	3.92(2)	4.31(4)	4.29(5)	4.17(22)	10.0(5)%
18855-116-3	4.01(3)	3.93(2)	4.08(4)	4.00(11)	9.6(2)%
18855-116-4	4.34(6)	4.31(3)	4.14(6)	4.26(11)	10.2(3)%
18855-116-5	4.31(4)	3.99(6)	4.03(4)	4.11(17)	9.9(4)%
18855-116-6	3.74(6)	3.84(7)	3.74(4)	3.77(6)	9.1(1)%
18855-116-7	4.22(4)	4.25(13)	4.30(5)	4.26(4)	10.2(1)%
18855-11-2 reference	41.55(30)	41.65(16)	41.80(17)	41.67(12)	100%

Now take extra care…

Heroic Measures?

Naperville and Hull Analyses of B-MFI Concentration in AMSAC Catalysts

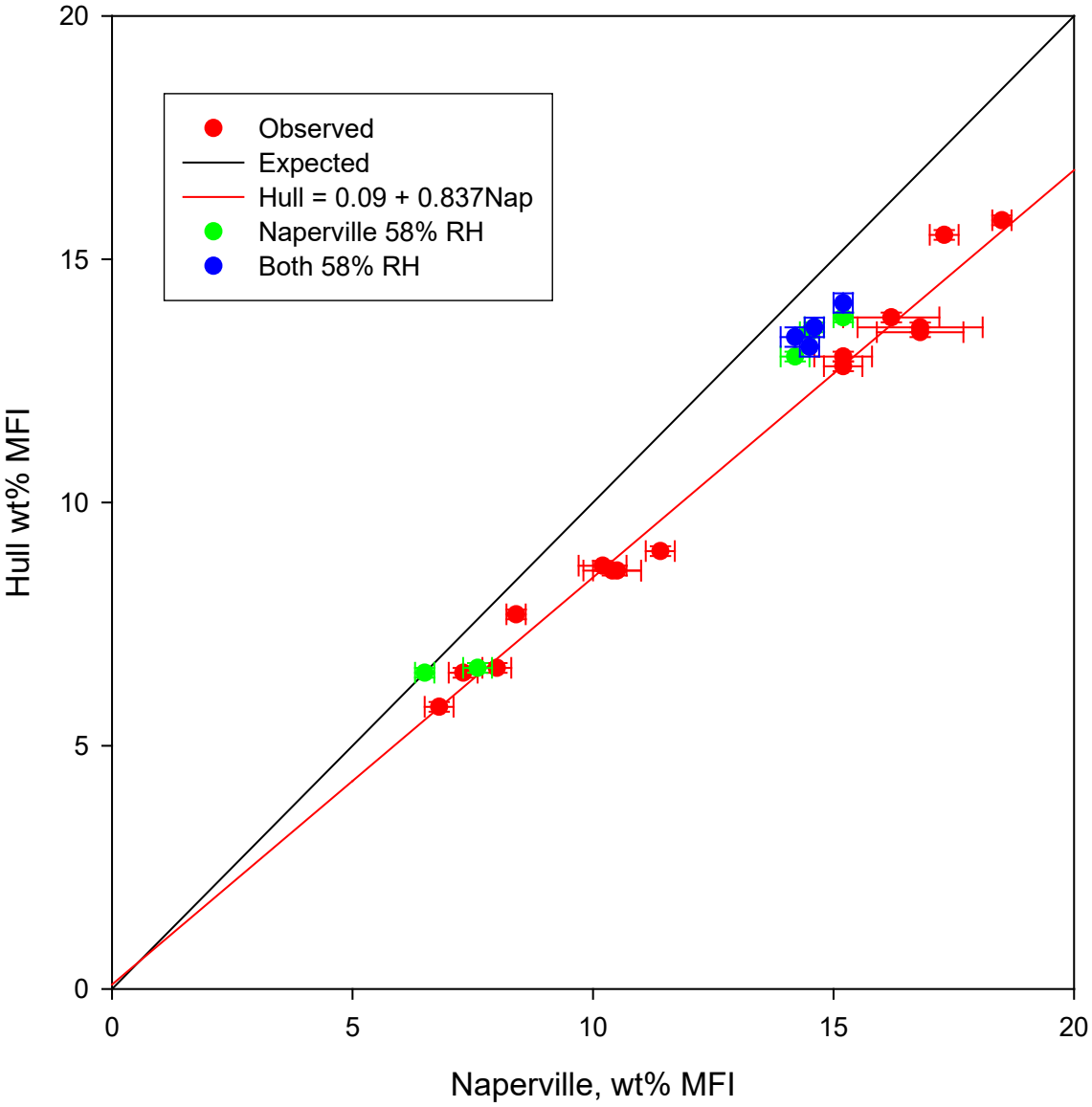

Weight Gain (16% RH) of Sieve and Catalyst Dehydrated at 350C

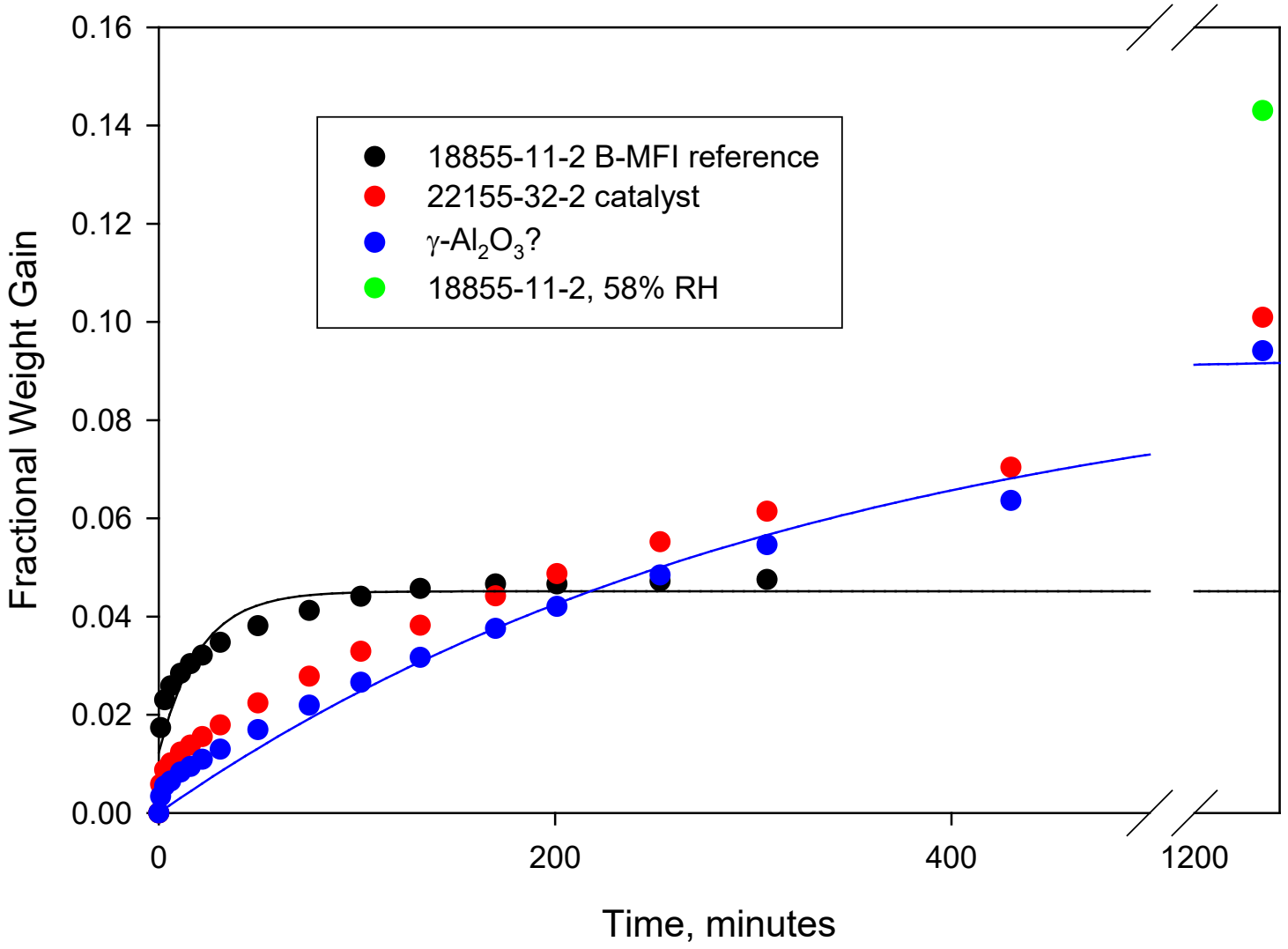

Naperville and Hull Processing of Hull MFI Crystallinity Data

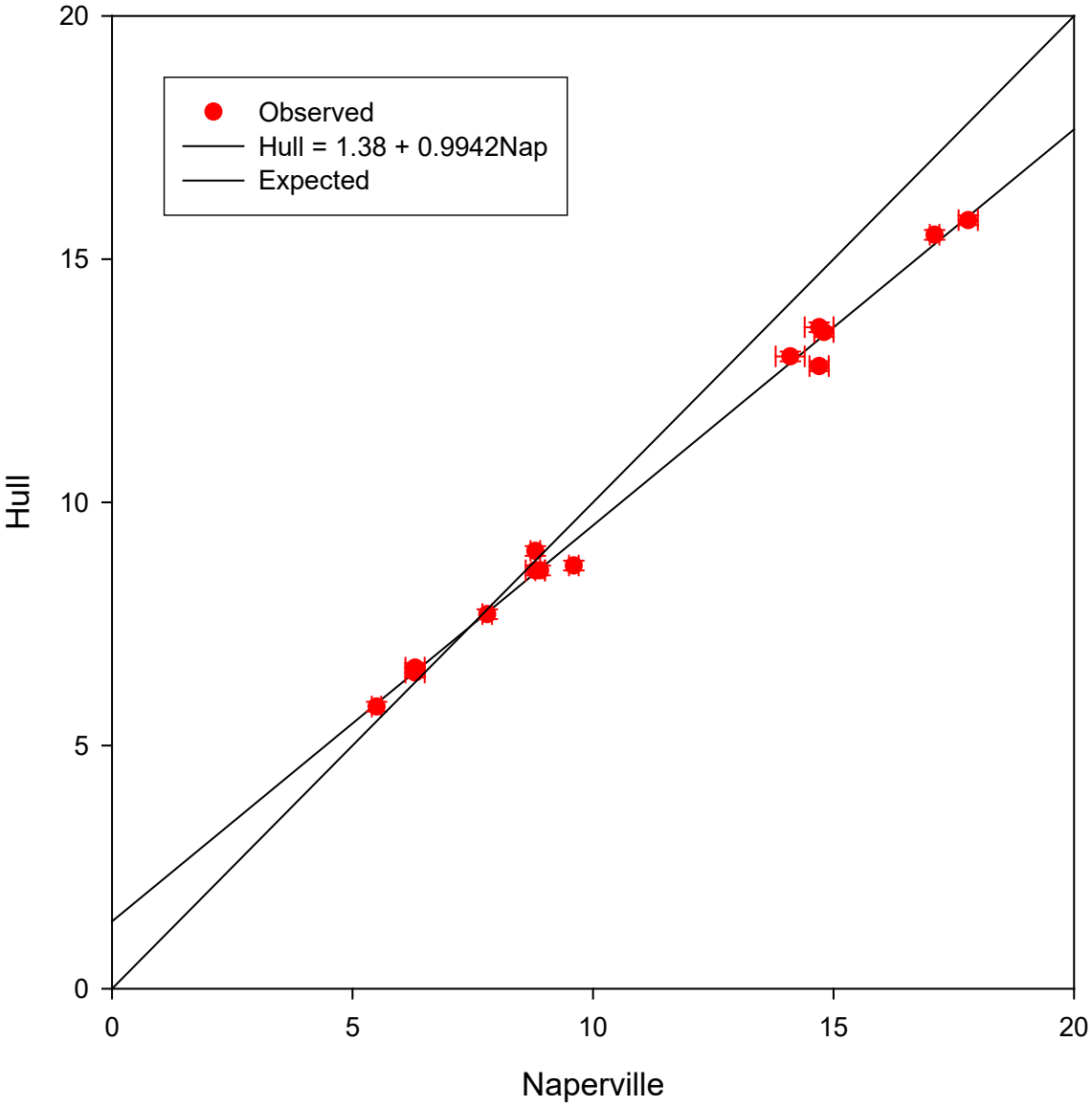

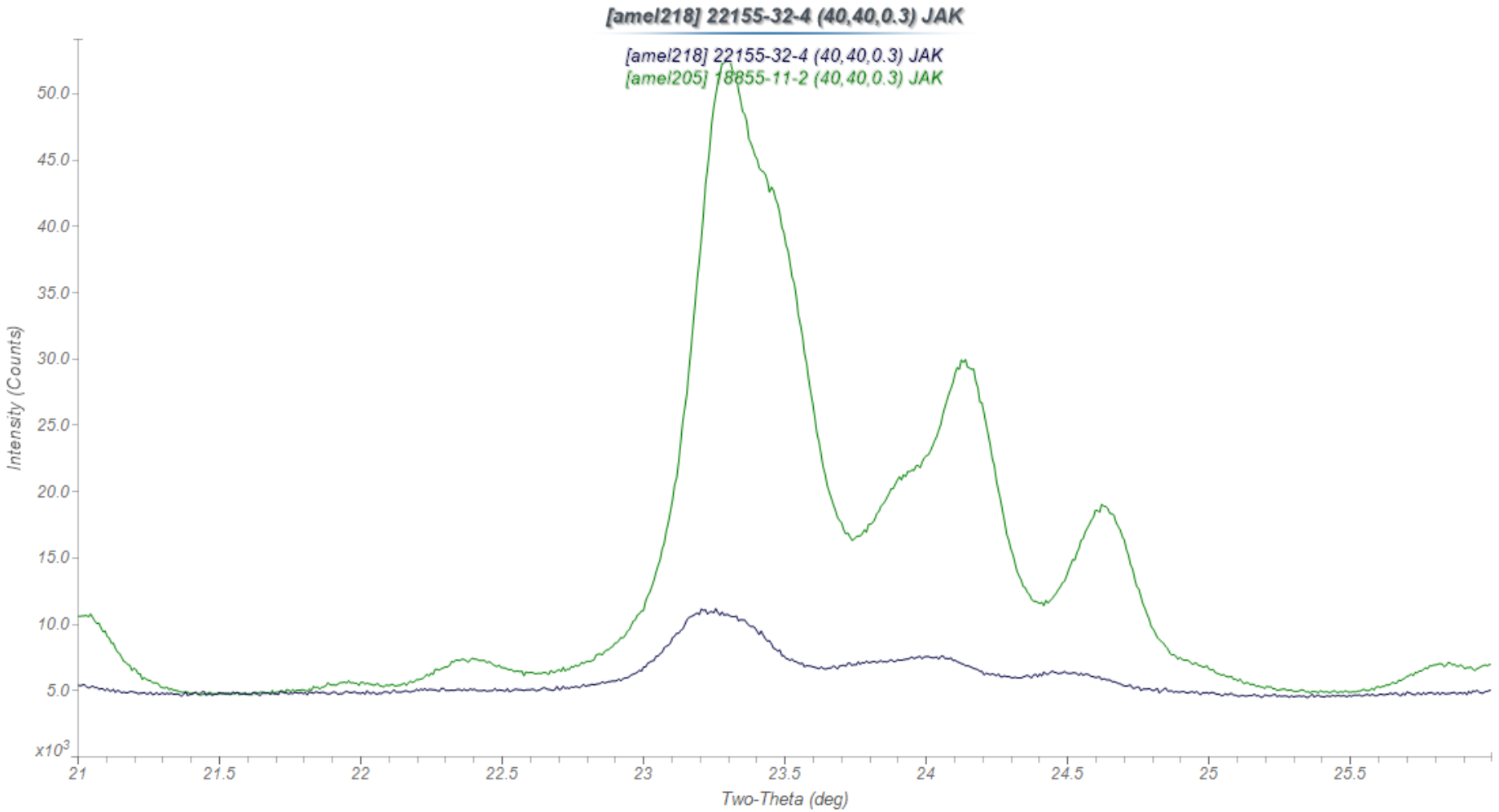
[amel218] 22155-32-4 (40,40,0.3) JAK
[amel218] 22155-32-4 (40,40,0.3) JAK
[amel205] 18855-11-2 (40,40,0.3) JAK
Intensity (Counts)
x10^3
50.0
45.0
40.0
35.0
30.0
25.0
20.0
15.0
10.0
5.0
21
21.5
22
22.5
23
23.5
24
24.5
25
25.5
Two-Theta (deg)

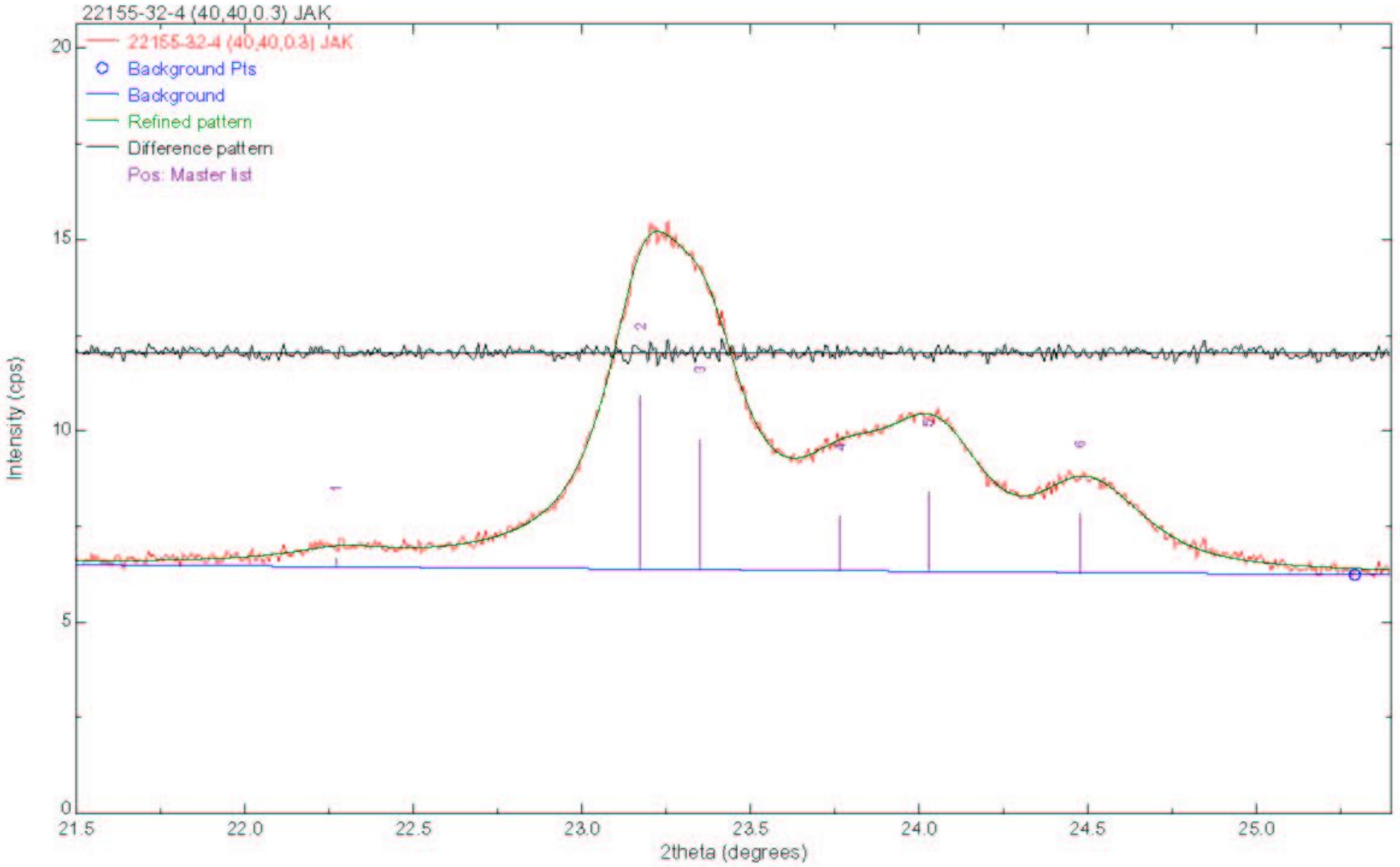
22155-32-4 (40,40,0.3) JAK
22155-32-4 (40,40,0.3) JAK
Background Pts
Background
Refined pattern
Difference pattern
Pos. Master list
Intensity (cps)
2theta (degrees)
0
5
10
15
20
21.5
22.0
22.5
23.0
23.5
24.0
24.5
25.0

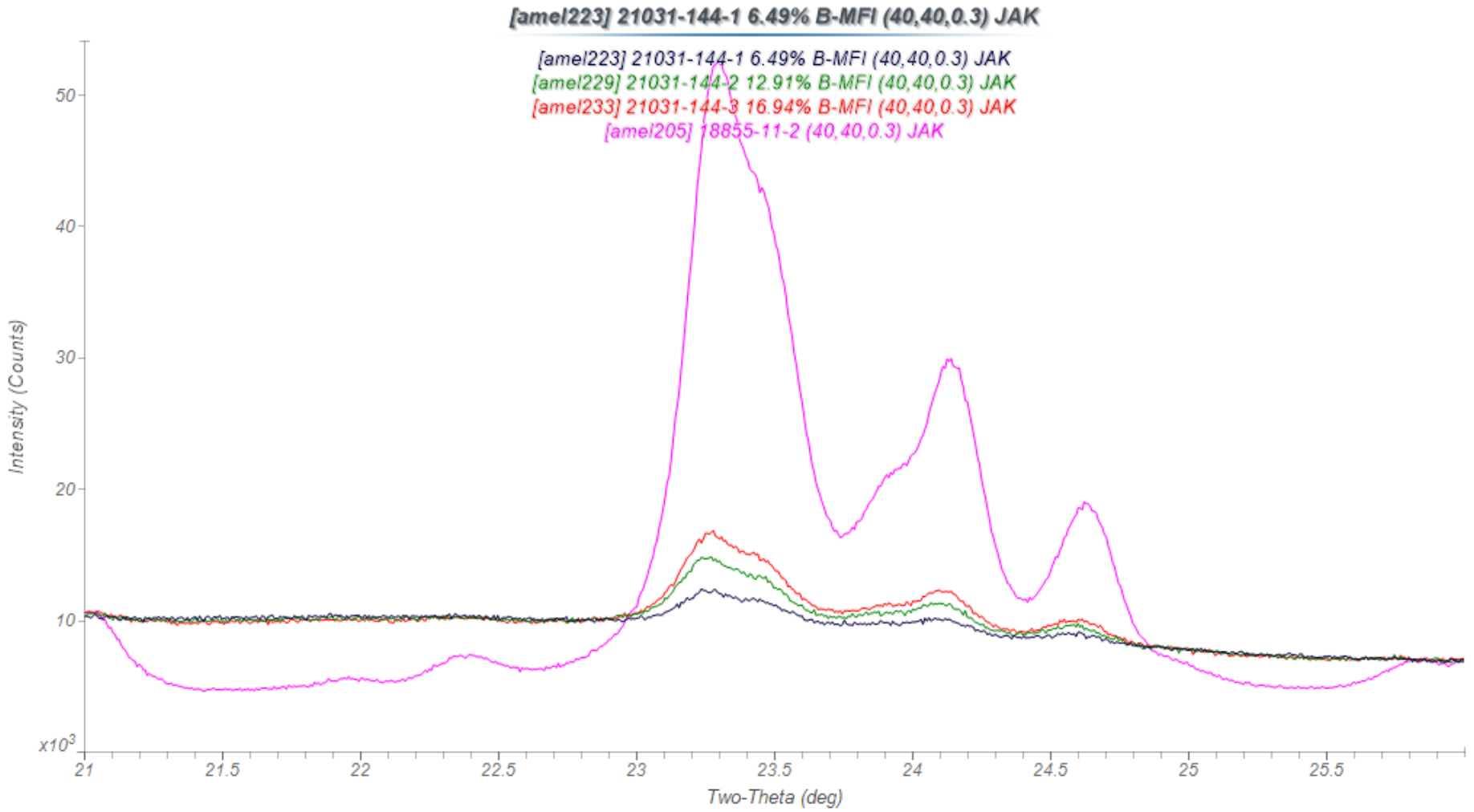
[amel223] 21031-144-1 6.49% B-MFI (40,40,0.3) JAK
[amel223] 21031-144-1 6.49% B-MFI (40,40,0.3) JAK
[amel229] 21031-144-2 12.91% B-MFI (40,40,0.3) JAK
[amel233] 21031-144-3 16.94% B-MFI (40,40,0.3) JAK
[amel205] 18855-11-2 (40,40,0.3) JAK
Intensity (Counts)
x10^3
50
40
30
20
10
21
21.5
22
22.5
23
23.5
24
24.5
25
25.5
Two-Theta (deg)

Physical Mixtures of B-MFI Reference 18855-11-2 and Amorphous Silica/Alumina 9743-58-1

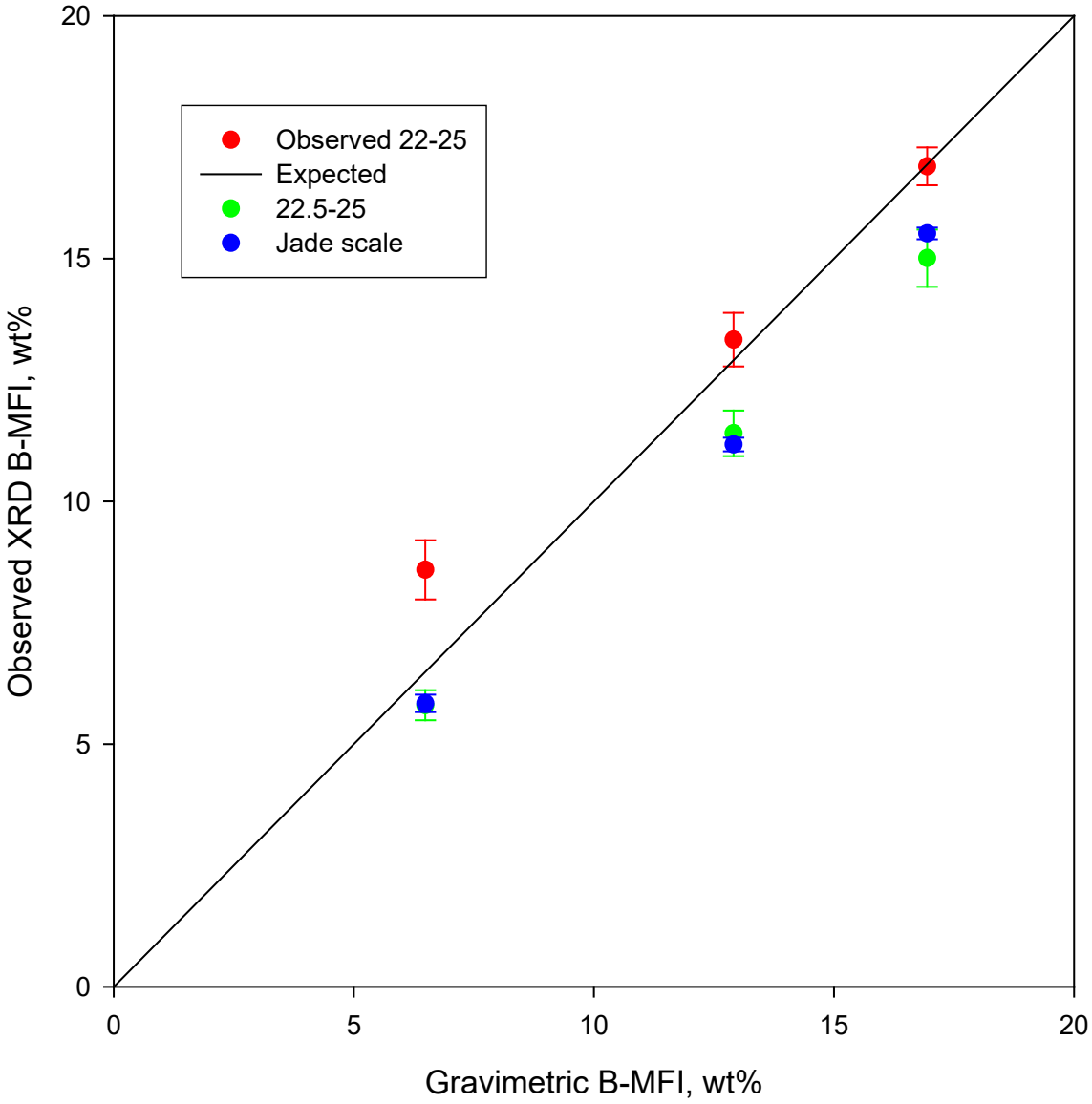

B-MFI Concentrations in Mixtures of
18855-11-2 and ASTM N10131 γ-Alumina
(Equilibrated at 58% RH)

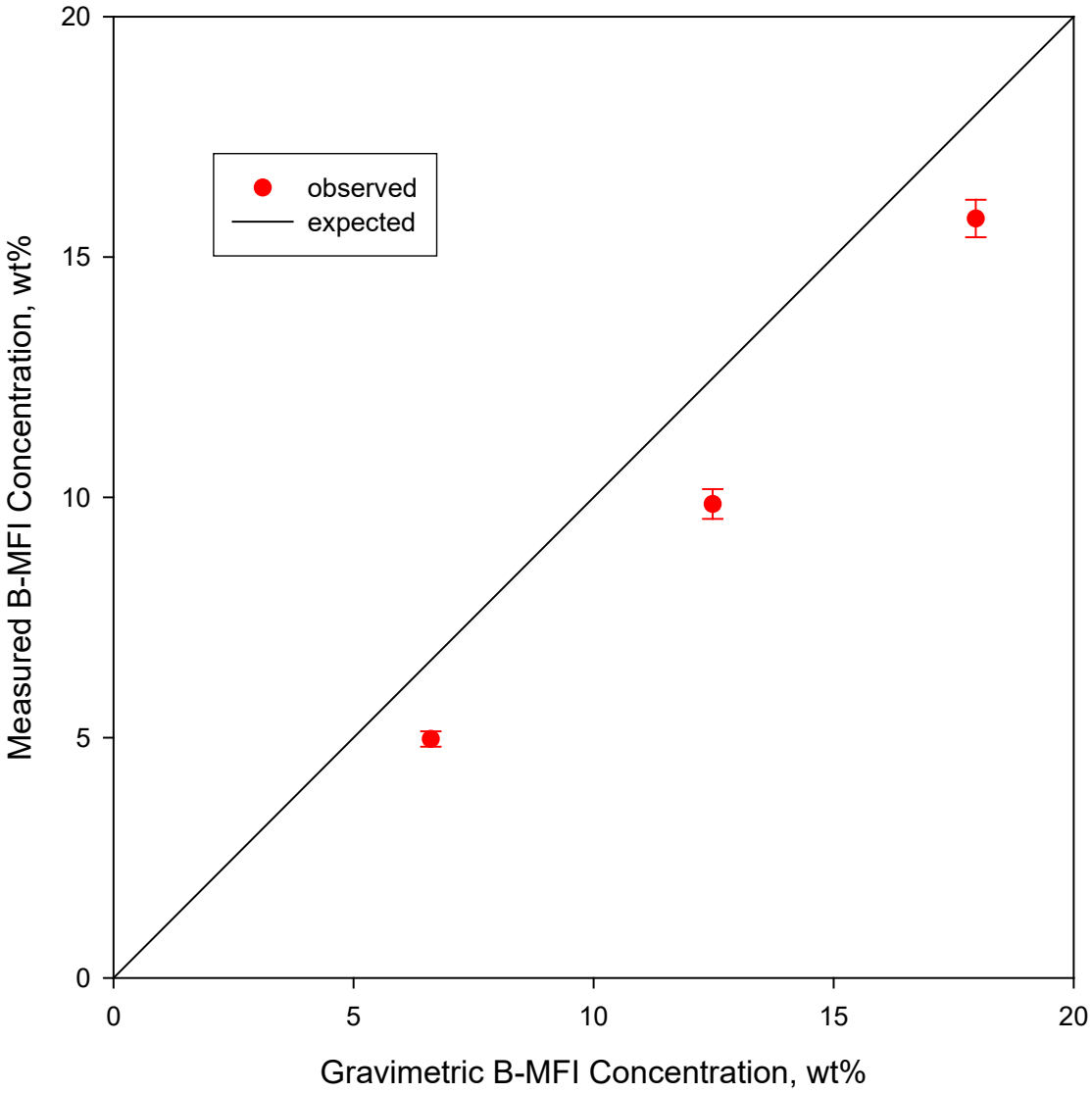

B-MFI Concentrations in Mixtures of
18855-11-2 and Micronized ASTM N10131 γ-Al_2O_3
(Equilibrated at 58% RH)

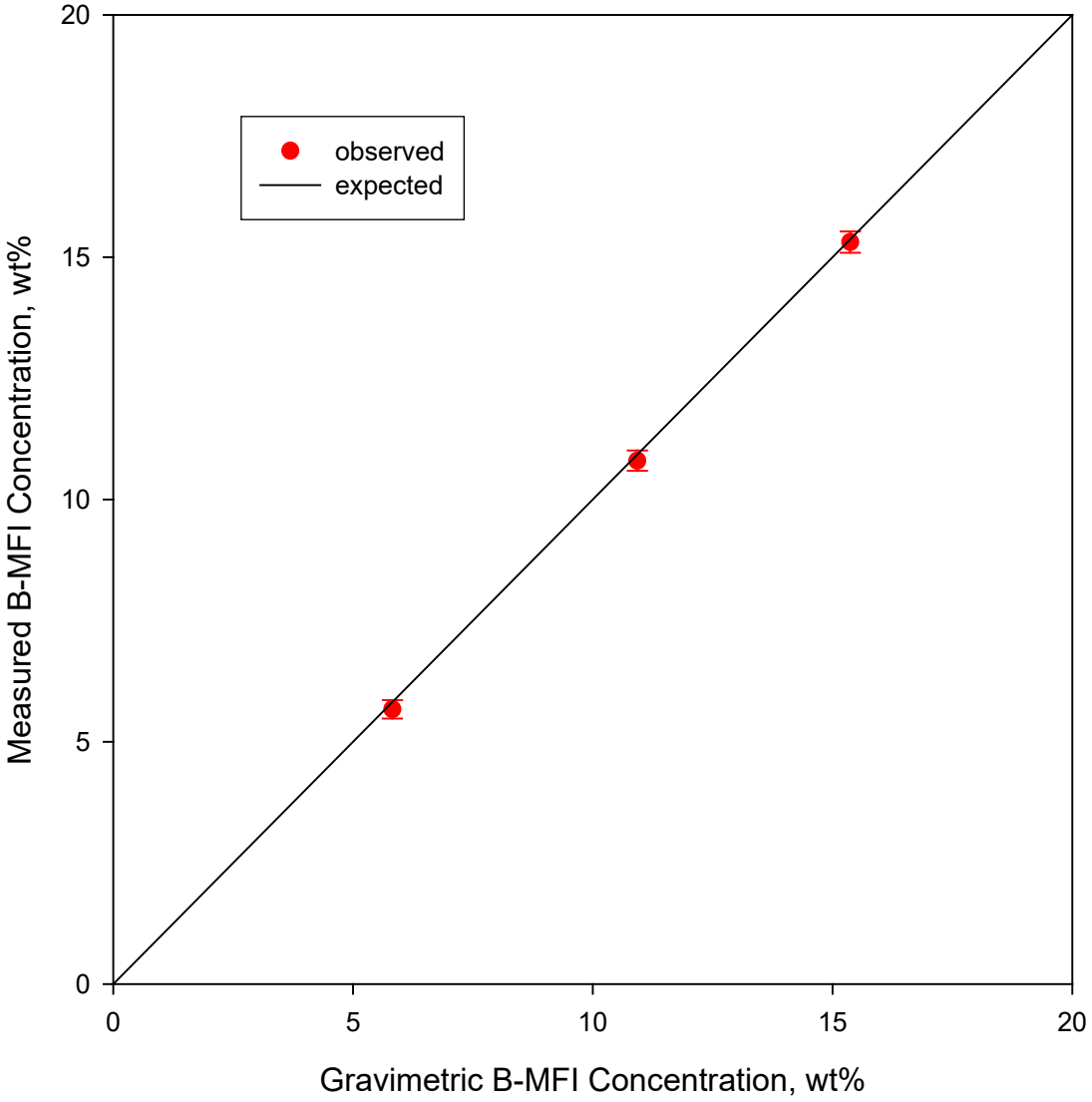

Al-MFI

Large-Particle Al-MFI 21455-77-1

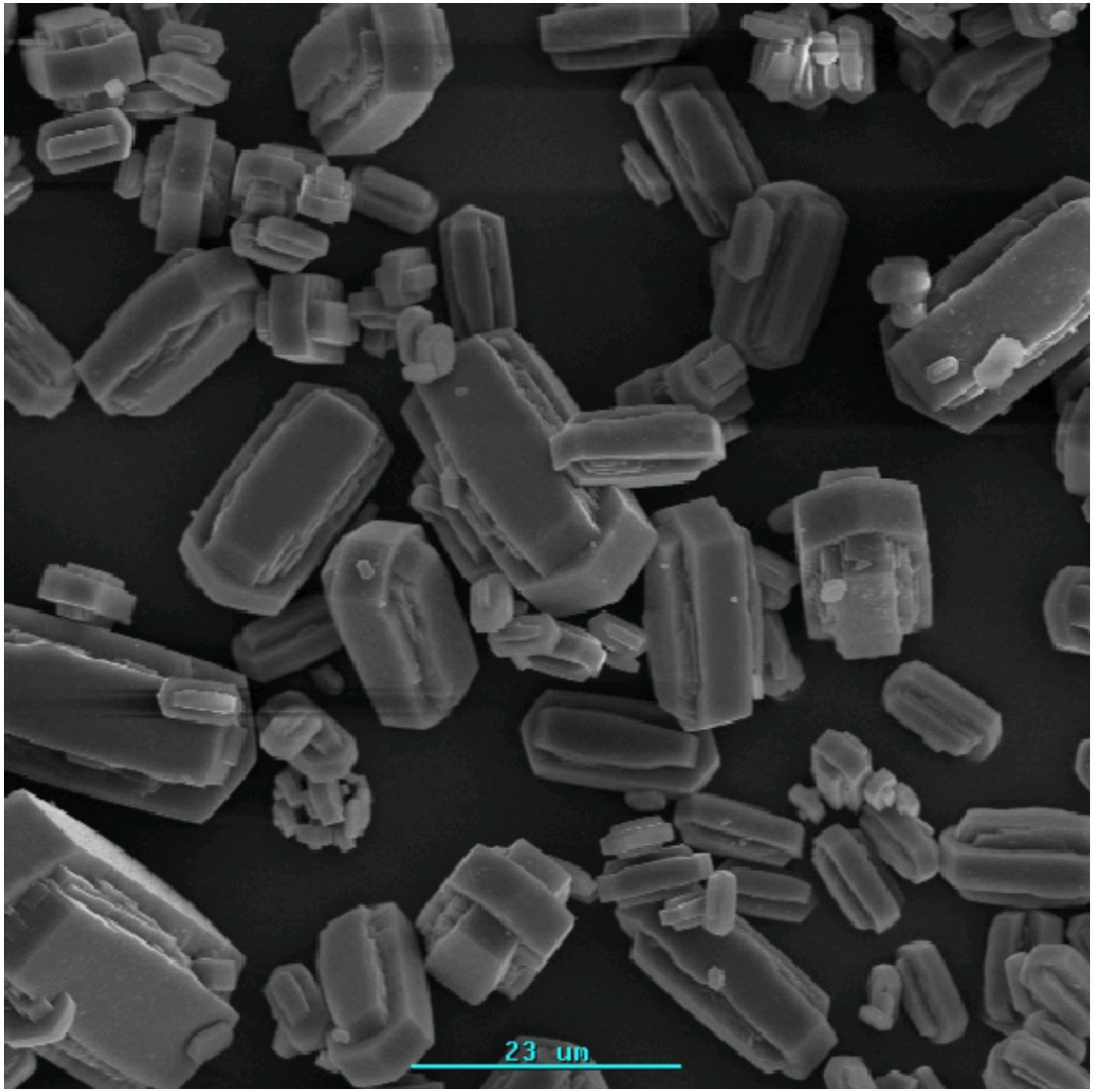

Al-MFI Raw Data

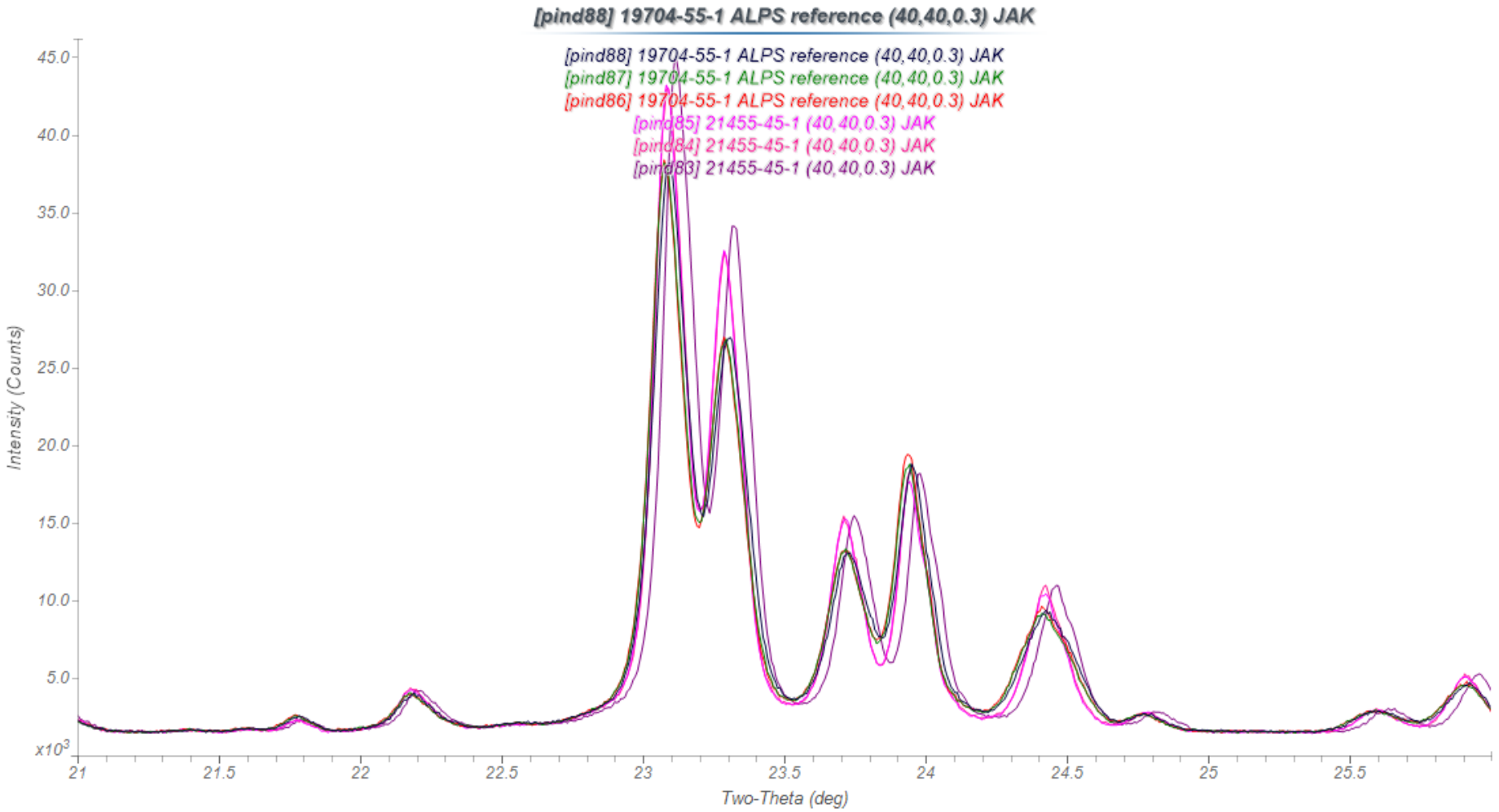

Al-MFI Corrected for Displacement

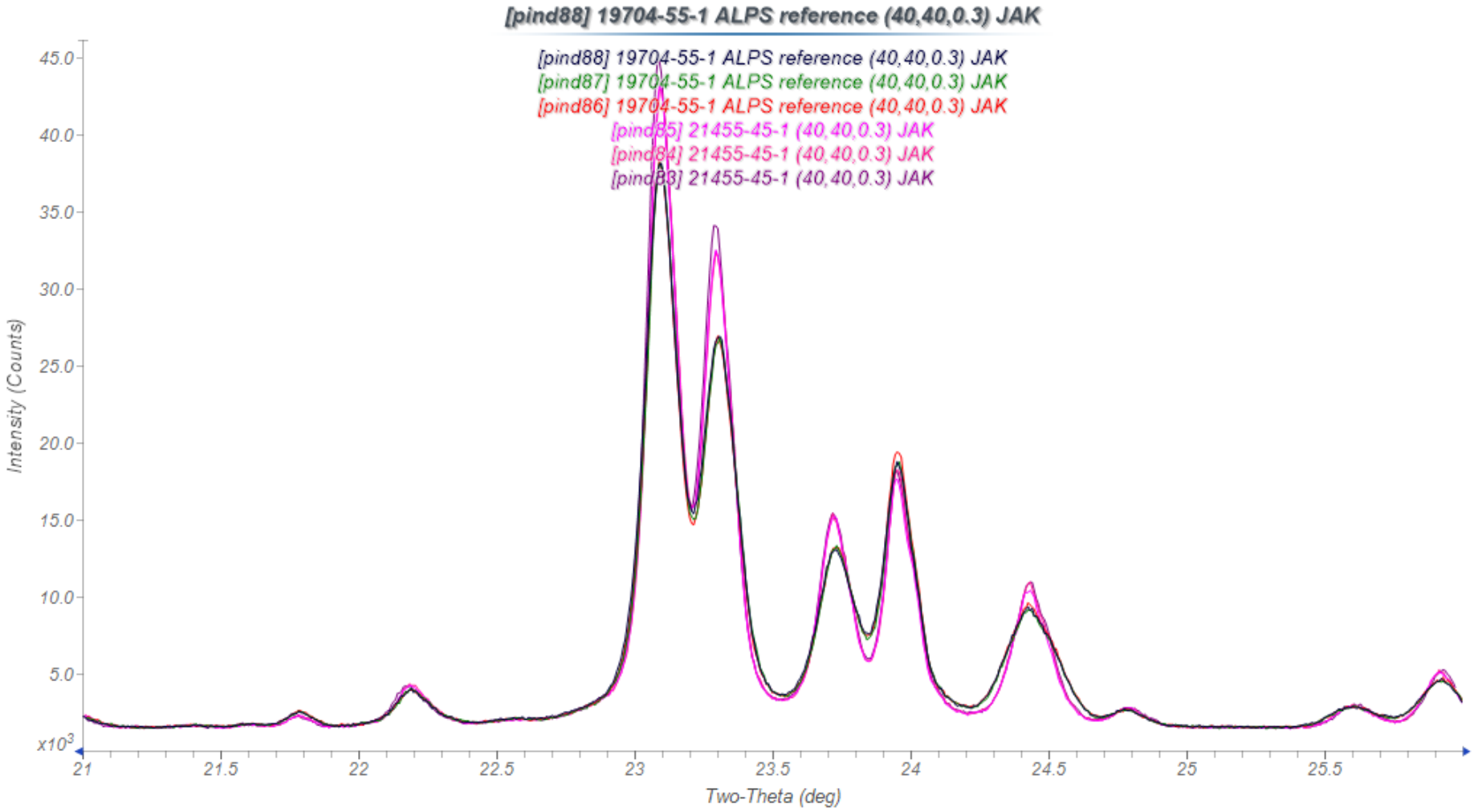

Typical Profile Fit

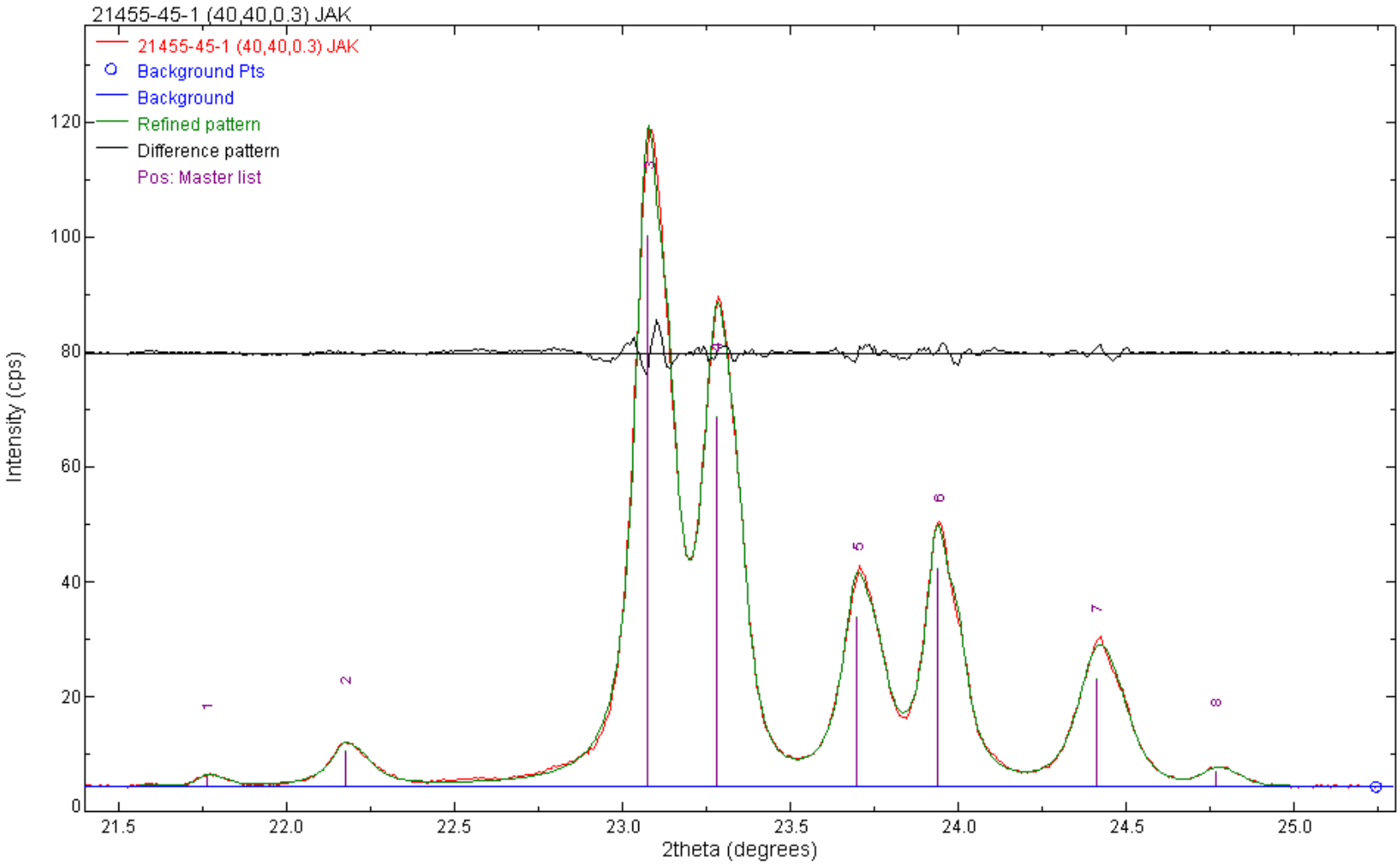

Peak Cluster Areas
ALPS Lot SD05301S

Sample #	21455-45-1	19704-55-1 Reference
501/051/151/303/133 area, cps/channel-deg	47.07(12) 47.31(12) 49.05(11)	47.39(10) 46.34(9) 46.62(9)
Average $\sigma_{relative}$, %	47.81(108) 2.2	46.78(54) 1.2
Crystallinity, %	103(3)	100

Error Propagation

$$\sigma^2(area) = \sigma^2(501) + \sigma^2(051) + \sigma^2(151) + \sigma^2(303) + \sigma^2(133)$$

$$d\frac{x}{y} = \frac{1}{y}dx - \frac{x}{y^2}dy$$

$$\sigma^2(crystallinity) = \left(\frac{\sigma(sample)}{area(reference)}\right)^2 + \left(\frac{area(sample)\sigma(reference)}{area^2(reference)}\right)^2$$

A favorable case - polymorphs

Consider rutile and anatase
(pigments, catalyst supports)

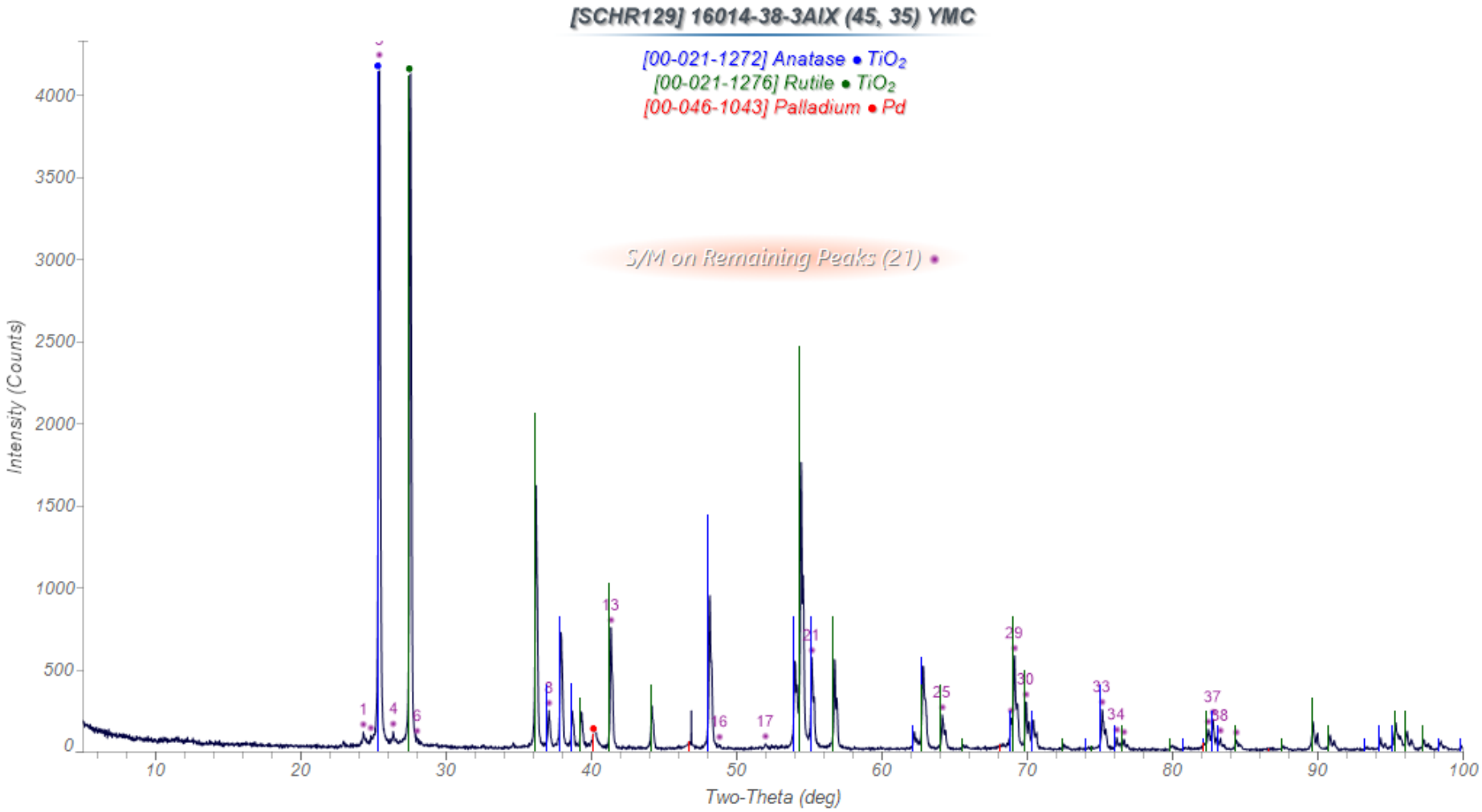
[SCHR129] 16014-38-3AIX (45, 35) YMC
[00-021-1272] Anatase • TiO2
[00-021-1276] Rutile • TiO2
[00-046-1043] Palladium • Pd
S/M on Remaining Peaks (21) •
Intensity (Counts)
Two-Theta (deg)
0
500
1000
1500
2000
2500
3000
3500
4000
10
20
30
40
50
60
70
80
90
100
1
4
6
8
13
16
17
21
25
29
30
33
34
37
38

$$\frac{X_r}{X_a} = \frac{I^0_{(101)a}}{I^0_{(110)r}} \frac{I_r}{I_a}$$

The ratio of the intensities of the lines in the pure phases is a measure of their absolute intensities, or a *relative intensity ratio* (RIR). For anatase/rutile, this ratio is 1.33.

For a binary mixture

$$X_r = 1 - X_a$$

$$X_a = \frac{1}{1 + 1.33\left(I_r / I_a\right)}$$

Klug's equation for binary mixtures

$$I_{(hkl)\alpha} = \frac{K_e K_{(hkl)\alpha} X_\alpha}{\rho_\alpha \left[X_\alpha \left(\mu/\rho \right)_\alpha + X_\beta \left(\mu/\rho \right)_\beta \right]}$$

For pure phase α:

$$I^0_{(hkl)\alpha} = \frac{K_e K_{(hkl)\alpha}}{\rho_\alpha \left(\mu/\rho \right)_\alpha}$$

$$\frac{I_{(hkl)\alpha}}{I^{0}_{(hkl)\alpha}} = \frac{X_{\alpha}\left(\mu/\rho\right)_{\alpha}}{X_{\alpha}\left(\mu/\rho\right)_{\alpha} + X_{\beta}\left(\mu/\rho\right)_{\beta}}$$

For a binary mixture,

$$X_{\alpha} + X_{\beta} = 1$$

$$\frac{I_{(hkl)\alpha}}{I^{0}_{(hkl)\alpha}} = \frac{X_{\alpha}\left(\mu/\rho\right)_{\alpha}}{X_{\alpha}\left[\left(\mu/\rho\right)_{\alpha} - \left(\mu/\rho\right)_{\beta}\right] + \left(\mu/\rho\right)_{\beta}}$$

$$X_{\alpha} = \frac{\left(I_{(hkl)\alpha}/I^{0}_{(hkl)\alpha}\right)\left(\mu/\rho\right)_{\beta}}{\left(\mu/\rho\right)_{\alpha} - \left(I_{(hkl)\alpha}/I^{0}_{(hkl)\alpha}\right)\left[\left(\mu/\rho\right)_{\alpha} - \left(\mu/\rho\right)_{\beta}\right]}$$

The Spiking Method

(Method of Standard Additions)

$$\frac{I_{(hkl)\alpha}}{I_{(hkl)'\beta}} = \left(\frac{K_{(hkl)\alpha}}{K_{(hkl)'\beta}}\right)\left(\frac{\rho_\beta}{\rho_\alpha}\right)\left(\frac{X_\alpha}{X_\beta}\right)$$

β not analyzed, and not even identified

$$\frac{I_{(hkl)\alpha}}{I_{(hkl)'\beta}} = \frac{K_{(hkl)\alpha}\rho_{\beta}\left(X_{\alpha} + Y_{\alpha}\right)}{K_{(hkl)'\beta}\rho_{\alpha}X_{\beta}}$$

X_{α} = the initial weight fraction of phase α

X_{β} = the initial weight fraction of phase β

Y_{α} = the number of grams of pure phase α added per gram of the original sample

$$\frac{I_{(hkl)\alpha}}{I_{(hkl)'\beta}} = K\left(X_{\alpha} + Y_{\alpha}\right)$$

Spiking of Micronised MFI/Quartz Blend 21031-98-1

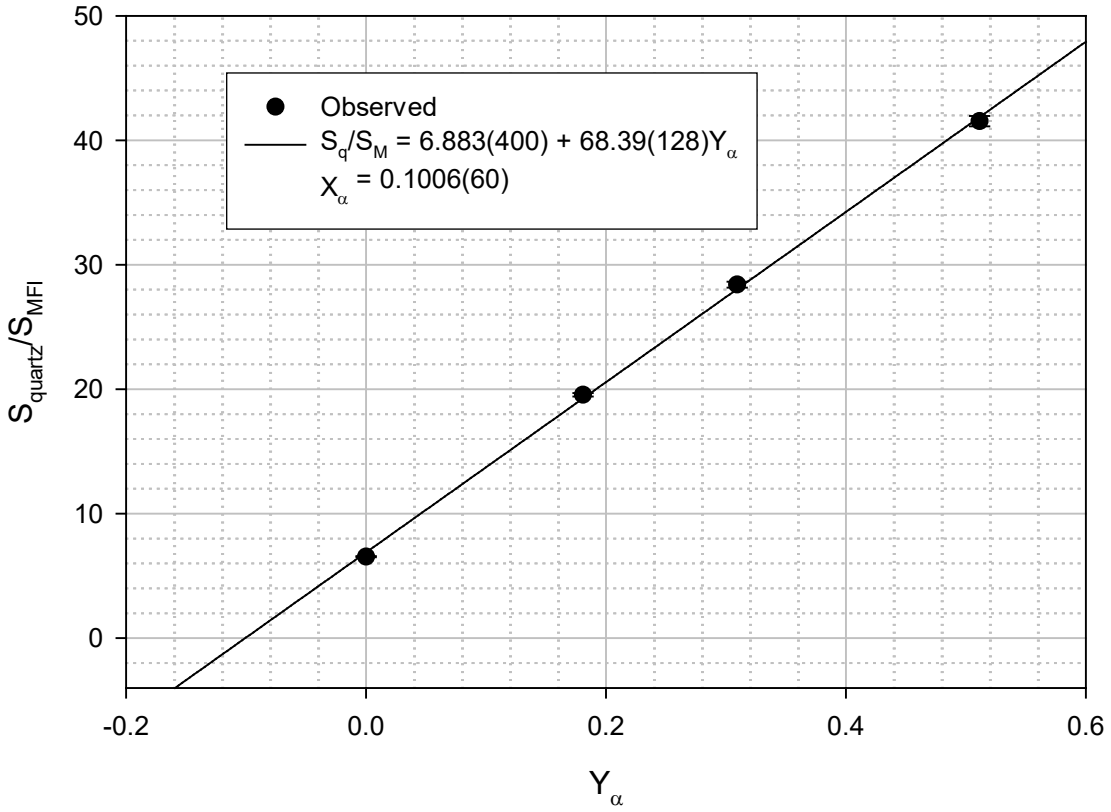

The Internal Standard Method

$$I_{(hkl)\alpha} = \frac{K_e K_{(hkl)\alpha} X_\alpha}{\rho_\alpha \left(\mu/\rho\right)_s}$$

$$\frac{I_{(hkl)\alpha}}{I_{(hkl)'\beta}} = k \frac{X_\alpha}{X_\beta}$$

A plot of

$$X_{\beta}\left(\frac{I_{(hkl)\alpha}}{I_{(hkl)'\beta}}\right) \quad vs \quad X_{\alpha}$$

is thus linear with a slope *k*. Therefore *k* is a measure of the inherent diffracted intensities of the two phases. If β is corundum in a 50:50 weight mixture with phase α, and we use the *hkl*s of the most-intense lines, we obtain the material constant of α called $I/I_{corundum}$, or I/I_c.
(peak or integrated intensity)

Generalize the Reference Intensity Ratio:

$$RIR_{\alpha,\beta} = \left(\frac{I_{(hkl)\alpha}}{I_{(hkl)'\beta}} \right) \left(\frac{I^{rel}_{(hkl)'\beta}}{I^{rel}_{(hkl)\alpha}} \right) \left(\frac{X_{\beta}}{X_{\alpha}} \right)$$

Quantitative Analysis with RIRs

$$X_{\alpha} = \left(\frac{I_{(hkl)\alpha}}{I_{(hkl)'\beta}} \right) \left(\frac{I^{rel}_{(hkl)'\beta}}{I^{rel}_{(hkl)\alpha}} \right) \left(\frac{X_{\beta}}{RIR_{\alpha,\beta}} \right)$$

How do I obtain the RIR?

- (PDF)
- Careful calibration (1-point)
- Slope of the internal standard plot
- Derivation from other RIRs:

$$RIR_{\alpha,\beta} = \frac{RIR_{\alpha,\gamma}}{RIR_{\beta,\gamma}}$$

- Calculation

$$X_\alpha = \left(\frac{I_{(hkl)\alpha}}{I_{(hkl)'\beta}} \right) \left(\frac{I^{rel}_{(hkl)'\beta}}{I^{rel}_{(hkl)\alpha}} \right) \left(\frac{RIR_{\beta,c}}{RIR_{\alpha,c}} \right) X_\beta$$

This equation is completely general, and is valid for mixtures containing unidentified phases, amorphous phases, or identified phases with unknown RIRs. If the four required constants are taken from the literature, however, the results should be considered only semiquantitative!

The Normalized RIR Method (Chung's matrix flushing) (adiabatic principle)

$$\left(\frac{X_\alpha}{X_\beta}\right) = \left(\frac{I_{(hkl)\alpha}}{I_{(hkl)'\beta}}\right)\left(\frac{I^{rel}_{(hkl)'\beta}}{I^{rel}_{(hkl)\alpha}}\right)\left(\frac{RIR_{\beta,c}}{RIR_{\alpha,c}}\right)$$

If no amorphous material is present,

$$\sum_{j=1}^{n} X_j = 1$$

$$X_\alpha = \frac{I_{(hkl)\alpha}}{RIR_\alpha I^{rel}_{(hkl)\alpha}} \left[\frac{1}{\sum_{j=1}^{n} \left(I_{(hkl)'j} \Big/ RIR_j I^{rel}_{(hkl)'j} \right)} \right]$$

Total Pattern Methods

- Structureless
- Rietveld

Structureless Full Patterns

- Generate a library of full patterns – experimental, calculated, amorphous, …
- (background)
- Full-pattern search/match, then least squares; use the scale factors to calculate quantitative phase analysis (bulk chemistry)
- GMQUANT: D. K. Smith, G. G. Johnson Jr., A. Scheible, A. N. Wims, J. L. Johnson, and G. Ullman, *Powder Diffr.*, **2**, 73-77 (1987).
- SNAP-1D (Bruker AXS/University of Glasgow)
- “infrared spectra”
- *FULLPAT*: S. J. Chipera and D. L. Bish, *J. Appl. Cryst.*, **35**(6), 744-749(2002).

The Rietveld Method

- Utilize the full profile, reducing systematic errors of preferred orientation, extinction, and instrument configuration
- More efficient treatment of overlapping peaks – handle greater complexity and/or broader peaks
- Refine the crystal structures and peak profiles – providing quantitative analysis on a microscopic scale, and eliminating the distorting effects of structural changes on the relative intensities
- Fit the background over the whole pattern, leading to better definition of peak intensities
- Compensate for preferred orientation
- Correct propagation of errors
- With an internal standard, quantify amorphous phase(s)

The “SMZ” Method

- R. J. Hill, *Powder Diffr.*, **6**, 74-77 (1991)
- J. A. Kaduk, “X-ray Diffraction in the Petroleum and Petrochemical Industry”, in *Industrial Applications of X-ray Diffraction*, F. K. Chung and D. K. Smith, eds., pp. 207-256, Marcel Dekker (2000).

The “SMZ” Method

- *S* (the phase fraction) is a quantity proportional to the number of unit cells of a phase present in the specimen (variable definitions – GSAS and FullProf use this one)
- *M* is the formula weight
- *Z* is the number of formula weights per unit cell
- *SMZ* is proportional to the mass of unit cells, and thus the concentration of the phase

Vanadium Phosphate Catalyst Precursor

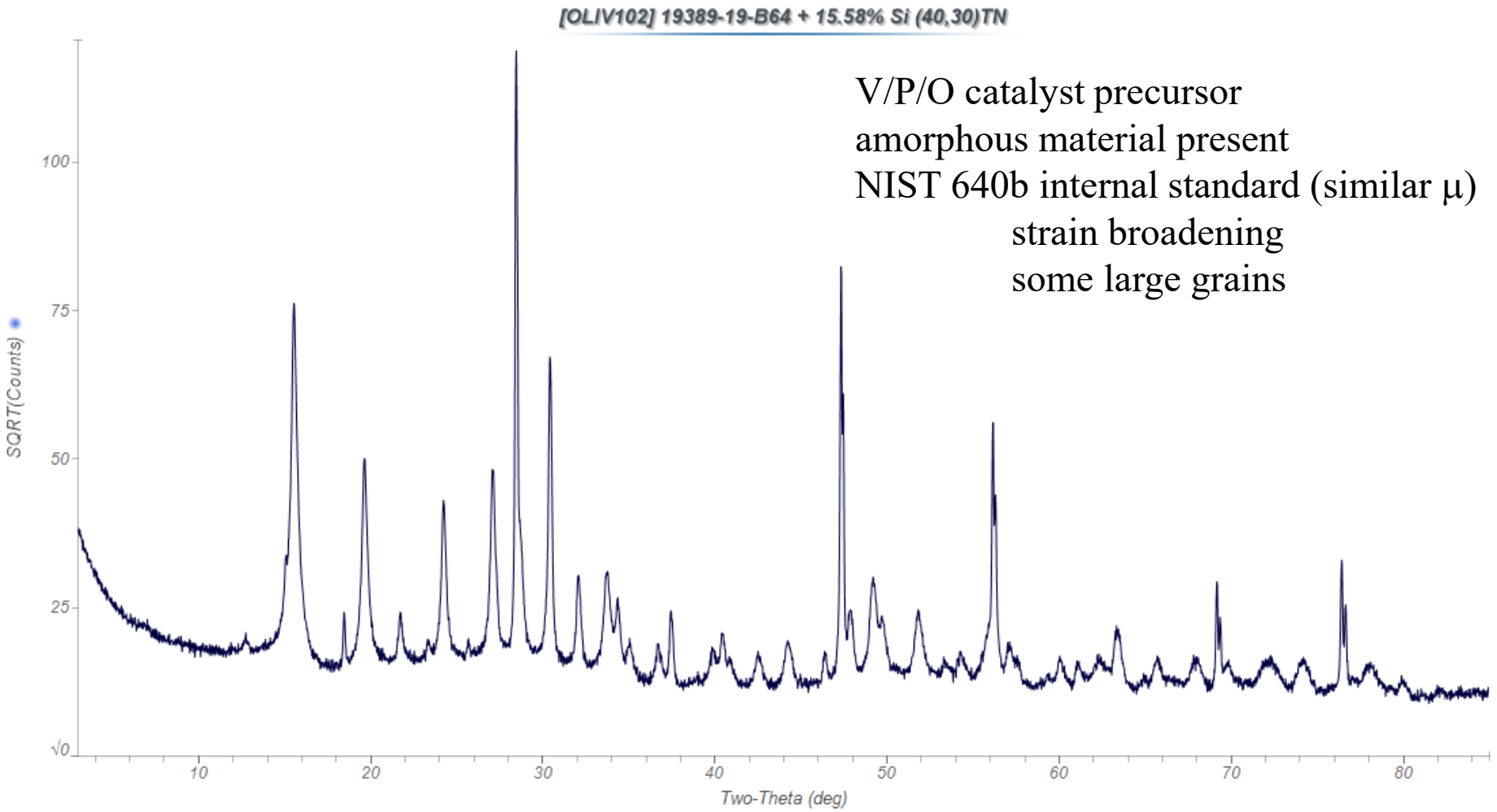

V/P/O catalyst precursor
amorphous material present
NIST 640b internal standard (similar μ)
strain broadening
some large grains

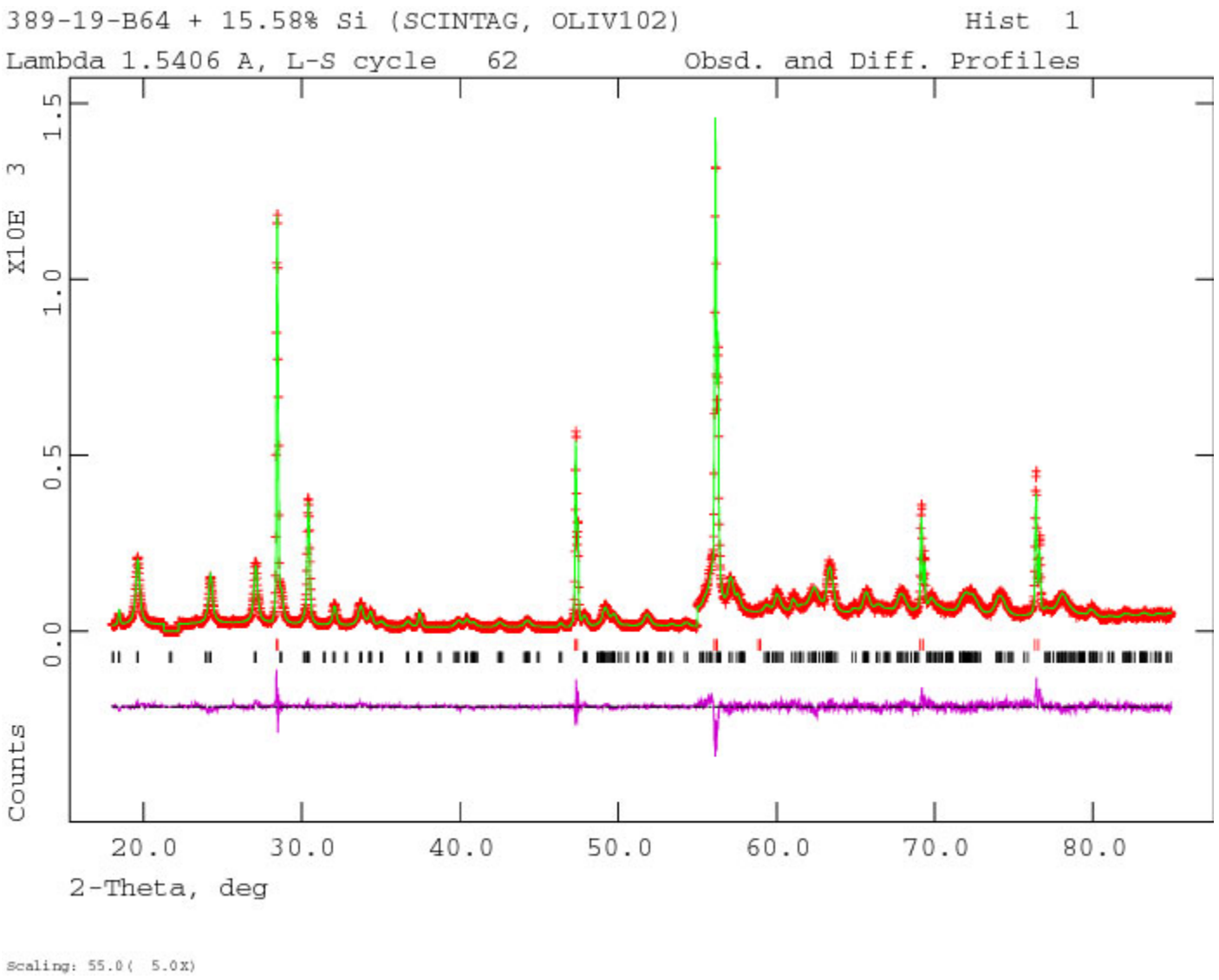
389-19-B64 + 15.58% Si (SCINTAG, OLIV102) Hist 1
Lambda 1.5406 A, L-S cycle 62 Obsd. and Diff. Profiles
X10E 3
1.5
1.0
0.5
0.0
Counts
20.0
30.0
40.0
50.0
60.0
70.0
80.0
2-Theta, deg
Scaling: 55.0(5.0X)

A Rietveld QPA Example, with Amorphous Material

Phase	S	M	Z	SMZ	Wt%	True wt%	Si-free wt%
$VO(HPO_4)(H_2O)_{0.5}$	5.82(3)	171.91	4	4002	66.0	30.3	35.9(2)
Si	9.17(7)	28.086	8	2060	33.9	15.58	-
Amorphous					0	54.1	64.1(2)
Sum				6062	99.9	100	100

15.58/33.9 = 0.459
1.0000 – 0.1558 = 0.8442

How do I choose the internal standard?

- Simple diffraction pattern / minimal overlap
- μ similar to sample / minimize microabsorption
- Minimal sample-related aberrations
  - Fine grained
  - No preferred orientation
  - 100% (or known) crystallinity
- Stable and unreactive
- Corundum, rutile, zincite, eskolaite, hematite, cerianite, fluorite, diamond
- Organic standard??

How much internal standard do I add?

T. Westphal, T. Füllmann, and H. Pöllmann, "Rietveld quantification of amorphous portions with an internal standard – Mathematical consequences of the experimental approach", *Powder Diffraction*, **24**(3), 239-243 (2009).

$$A = \frac{100\%}{100\% - R} \cdot 100\% \cdot \left[1 - \frac{R}{R_R} \right]$$

$$R = 100\% \cdot \frac{100\% - A}{2 \cdot 100\% - A}$$

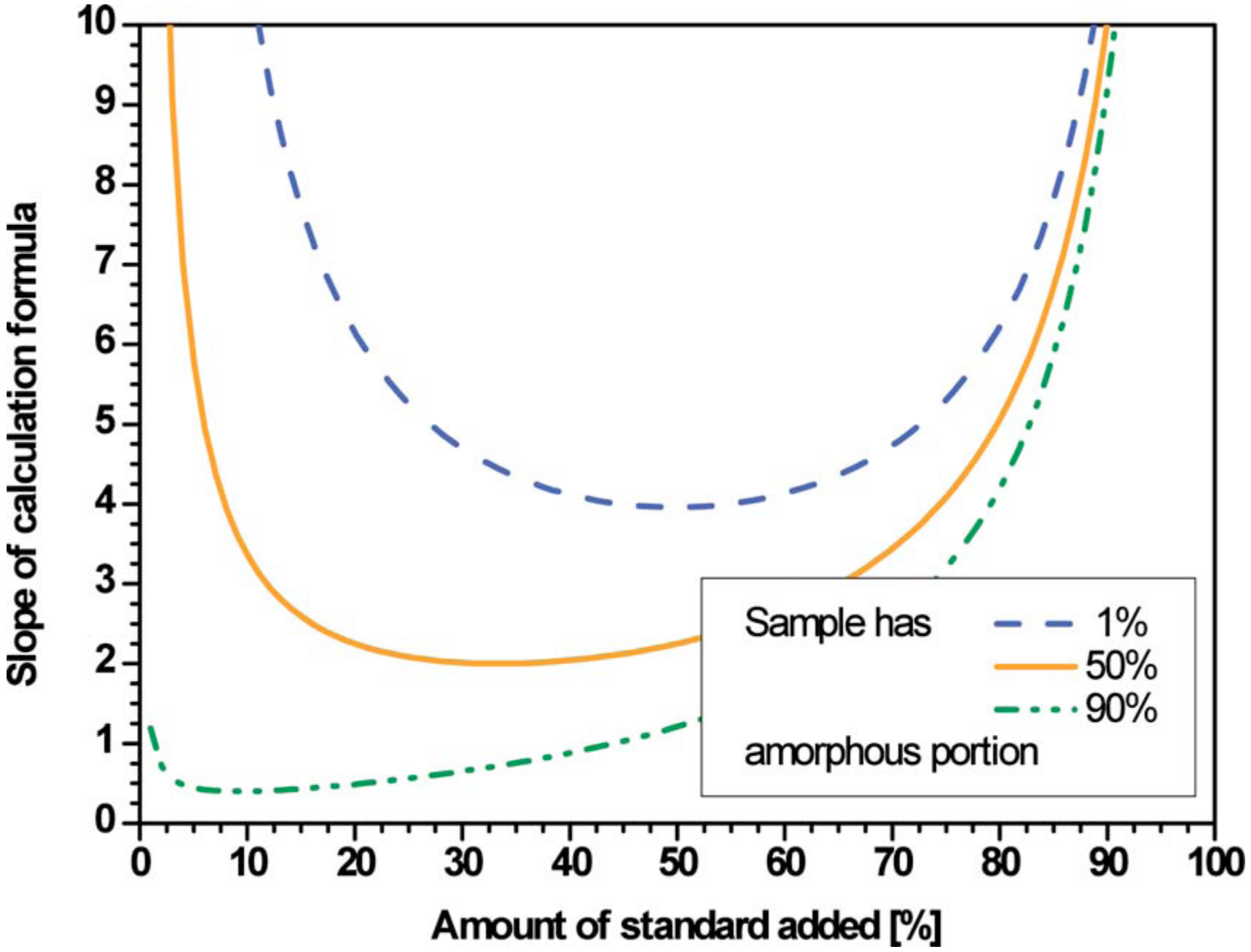
Slope of calculation formula
Amount of standard added [%]
0
1
2
3
4
5
6
7
8
9
10
0
10
20
30
40
50
60
70
80
90
100
Sample has
1%
50%
90%
amorphous portion

Partial or No Known Crystal Structure (PONKCS)

- hkl_phase
- peaks_phase (also for amorphous)
- Supercells
- Full pattern references / Debye functions
- Model the disorder
  - NEWMOD+, WILDFIRE, DIFFAX+, FAULTS

"Effect of microabsorption on the determination of amorphous content *via* powder X-ray diffraction", N. V. Y. Scarlett and I. C. Madsen, *Powder Diffraction* **33**(1), 26-37 (2018).

"Comparison of Rietveld-compatible structureless fitting analysis methods for accurate quantification of carbon dioxide fixation in ultramafic mine tailings", C. C. Turvey, J. L. Hamilton, and S. A. Wilson, *American Mineralogist*, **103**, 1649-1662 (2018).

A new method for quantitative phase analysis using X-ray powder diffraction: direct derivation of weight fractions from observed integrated intensities and chemical compositions of individual phases, H. Toraya, *J. Appl. Cryst.* **49**, 1058-1516 (2016).

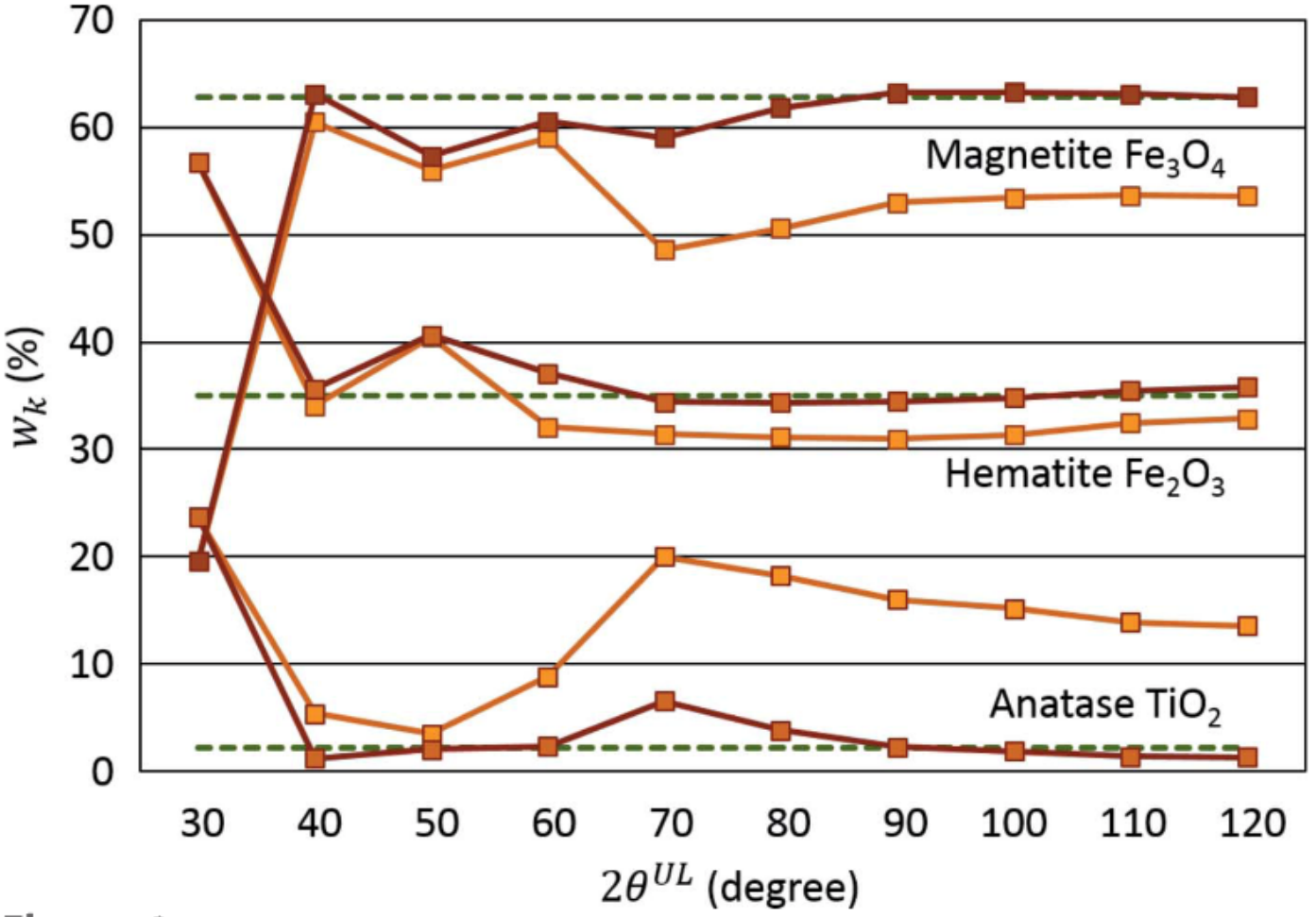

Figure 6

Variations of w_k as a function of $2\theta^{\mathrm{UL}}$ for individual components of S3-4. Red and yellow lines represent the w_k values obtained by applying VPP and EqP, respectively, for unresolved, overlapped diffraction lines. Dashed lines represent weight fractions as weighed for the three components.

Direct derivation (DD) of weight fractions of individual crystalline phases from observed intensities and chemical composition data: incorporation of the DD method into the whole-powder-pattern fitting procedure, H. Toraya, *J. Appl. Cryst*., **51**, 446-455 (2018)

Journal of Applied Crystallography

home archive editors for authors for readers submit subscribe open access

research papers

JOURNAL OF APPLIED CRYSTALLOGRAPHY

ISSN: 1600-5767

Volume 52 | **Part 3** | June 2019 | Pages 520-531
https://doi.org/10.1107/S1600576719003406
Viewed by 142

A practical approach to the direct-derivation method for QPA: use of observed powder patterns of individual components without background subtraction in whole-powder-pattern fitting

Hideo Toraya[a]*

[a]Rigaku Corporation, 3-9-12, Matsubara, Akishima, Tokyo 196-8666, Japan
*Correspondence e-mail: toraya@rigaku.co.jp

Edited by S. Sasaki, Tokyo Institute of Technology, Yokohama, Japan (Received 23 January 2019; accepted 10 March 2019; online 18 April 2019)

The direct-derivation (DD) method for quantitative phase analysis (QPA) can be used to derive weight fractions of individual phases in a mixture from the sums of observed intensities along with the chemical composition data [Toraya (2016). *J. Appl. Cryst.* **49**, 1508–1516]. The whole-powder-pattern fitting (WPPF) technique can be used as one of the tools for deriving the observed intensities of individual phases. In WPPF, the observed powder pattern of a single-phase sample after background (BG) subtraction can be used as the fitting function in combination with the fitting functions widely used in Pawley and Rietveld refinements. The direct fitting of the observed pattern is a very useful technique when the target component is a low-crystallinity or amorphous material [Toraya (2018). *J. Appl. Cryst.* **51**, 446–455]. Technical problems in utilizing the BG-subtracted pattern are the uncertainty associated with the determination of BG height and the parameter interaction between the BG function (BGF) and the BG-subtracted pattern in the least-squares fit. In this study, a practical approach in which single-phase observed patterns are used for the direct fitting without subtracting their BG intensities is proposed. In QPA, the contribution of BG intensities can be neutralized by converting the sum of BG-included intensities into the sum of BG-subtracted intensities by multiplying by a conversion factor. When the magnitudes of the conversion factors are almost identical for all components, they can be canceled out under the normalization condition in deriving weight fractions, and they are not required in QPA. The magnitude of the conversion factor for each component can be determined by one of two experimental techniques: using a single-phase powder of the target component or a mixture containing the target component in a known weight ratio. The theoretical basis of the present procedure is given, and the procedure is experimentally verified. In this procedure, the interaction between the BGF and the BG-included observed pattern is negligibly small. Least-squares fitting with a few adjustable parameters is very fast and stable. Accurate QPA could be conducted, as indicated by the average deviation of 0.05% from weighed values in QPA of α-Al_2O_3 + γ-Al_2O_3 mixtures with five different weight ratios and 0.4% in QPA of an α-SiO_2 + SiO_2 glass mixture

Keywords: **X-ray powder diffraction**; **quantitative phase analysis**; **direct-derivation method**; **intensity–composition formula**; **background subtraction**; **low-crystallinity materials**; **amorphous**

Journal of Applied Crystallography

IUCr IT WDC

search IUCr Journals

home archive editors for authors for readers submit subscribe open access

research papers

JOURNAL OF APPLIED CRYSTALLOGRAPHY

ISSN: 1600-5767

Volume 53 | Part 5 | October 2020 | Pages 1225-1235
https://doi.org/10.1107/S1600576720010225
Viewed by 93

Accurate and time-saving quantification of a component present in a very small amount in a mixture by the direct derivation method

Hideo Toraya[a]*

[a]Rigaku Corporation, 3-9-12 Matsubara, Akishima, Tokyo 196-8666, Japan
*Correspondence e-mail: toraya@rigaku.co.jp

Edited by K. Chapman, Stony Brook University, USA (Received 5 May 2020; accepted 23 July 2020; online 20 August 2020)

In quantitative phase analysis (QPA) using the direct derivation (DD) method, total sums of diffracted/scattered intensities for individual components are used as observed quantities. Fluctuation in their relative intensity ratios induces errors in derived weight fractions, and it ought to be suppressed for improving the accuracy in QPA, in particular, of a component that is present in a small amount. The fluctuation is primarily caused by the termination in summing/integrating diffracted/scattered intensities on the high-angle side. It is usually associated with changing the 2θ range in whole-powder-pattern fitting (WPPF) used to decompose the mixture pattern into individual component patterns. In this study, calculated patterns for individual components, fitted in WPPF, are normalized so as to give the unit area when they are separately integrated over their definition ranges in 2θ. The termination effect could effectively be reduced by extending the definition range to a certain high-angle limit. Scale parameters for adjusting the calculated patterns become non-fluctuating against the change of the 2θ range in WPPF. Thus, the time spent for intensity data collection of mixture patterns can be reduced by shortening the scan range. The present procedure has been tested with binary mixtures containing small amounts of crystalline phases of 0.02–0.4 wt%. QPA could be conducted with errors of 0.01–0.03 wt% for both inorganic materials chosen as ideal samples and pharmaceutical materials as practical ones. QPA of an amorphous component present in a small amount is also discussed.

Keywords: **X-ray powder diffraction**; **quantitative phase analysis**; **direct-derivation method**; **intensity–composition formula**; **normalization of fitting function**; **very small/trace amounts**.

Similar articles **PowerPoint slides**

Intensity Errors in Quantitative Analysis

- Instrument aberrations (Cline *et al*.)
- Beam spillover at low angles
- Absorption
- Variable sampling volume
- Surface roughness
- Particle statistics
- Microabsorption
- Signal/noise
- Change of the sample during specimen preparation
- Preferred orientation

Absorption

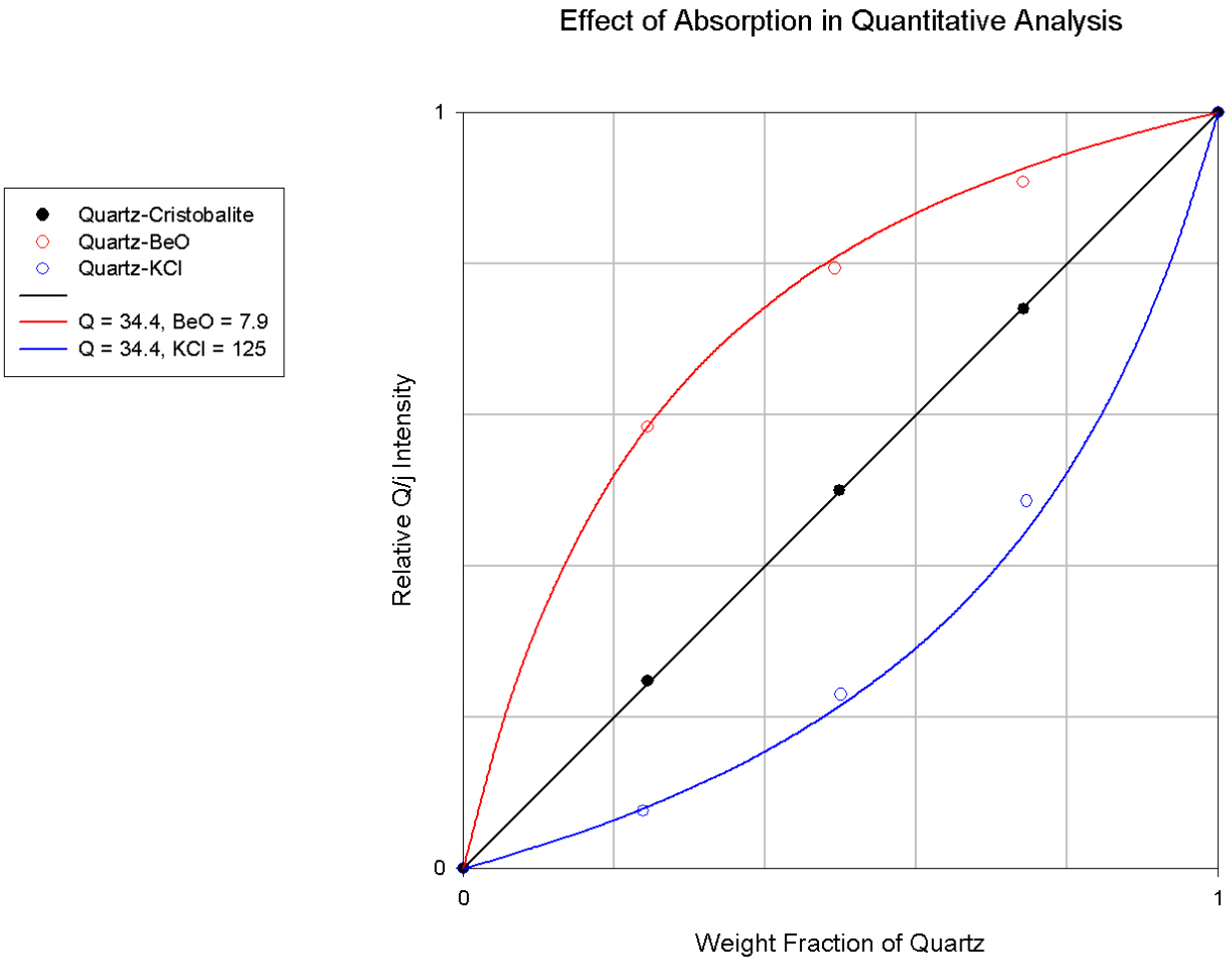

Data from H. P. Klug & L. E. Alexander,
X-ray Diffraction Procedures, Second Edition (1974).

Bulk Absorption

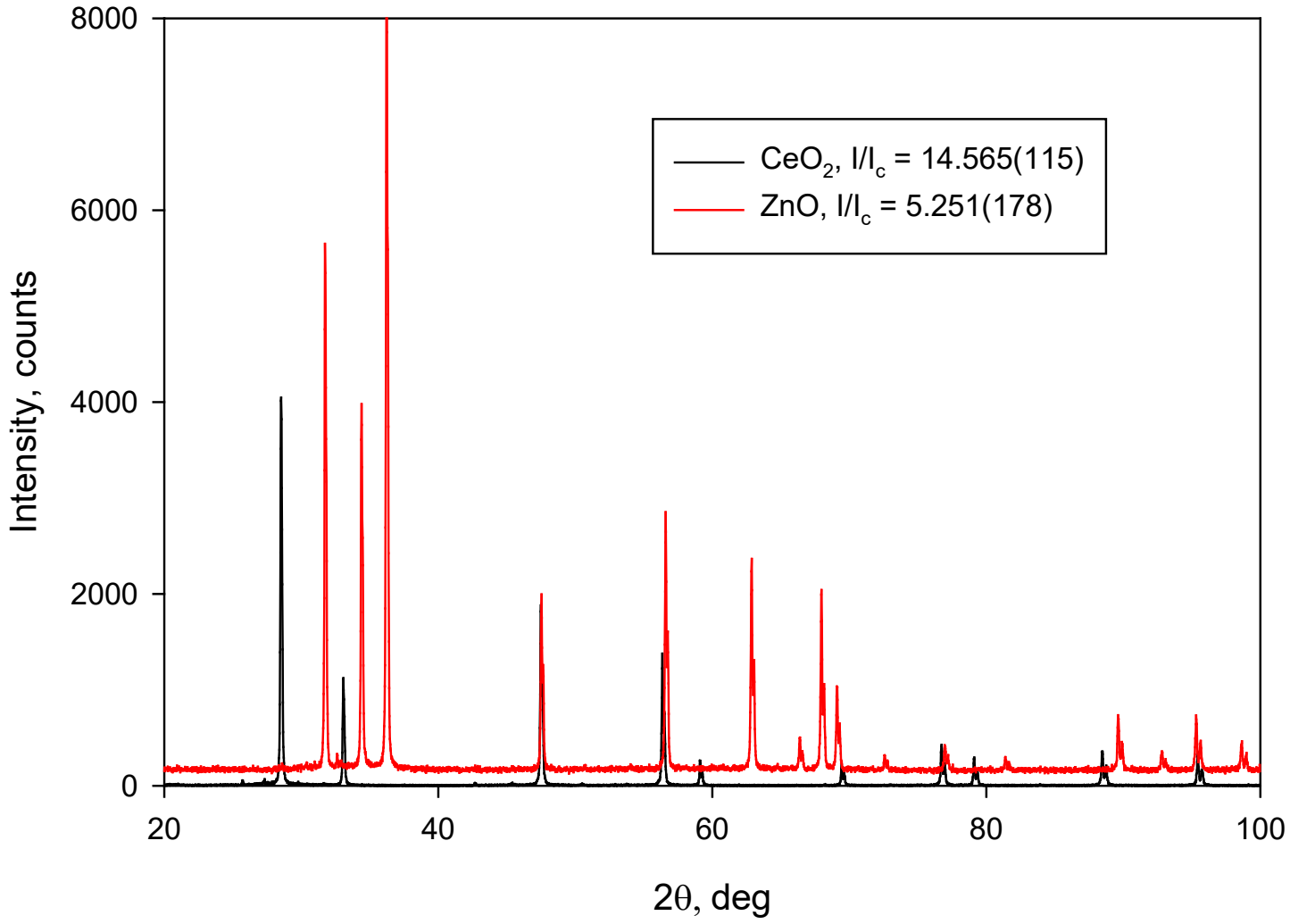

Effective Specimen Thickness

$$t = \frac{3.2}{\mu}\frac{\rho}{\rho'}\sin\theta$$

H. P. Klug & L. E. Alexander,
X-ray Diffraction Procedures, Second Edition, p. 486 (1974)

Effective Specimen Thickness

Compound	μ, cm^{-1}	*t*, μm
ZnO	277	50
CeO_2	2176	6

$$\frac{I_{Ce}}{I_{Zn}} = \frac{14.565}{5.251} \times \frac{6}{50} = 0.33$$

Variable Sampling Volume

$$t = \frac{3.2}{\mu}\frac{\rho}{\rho'}\sin\theta$$

10% RuO_2/SiO_2 Catalyst

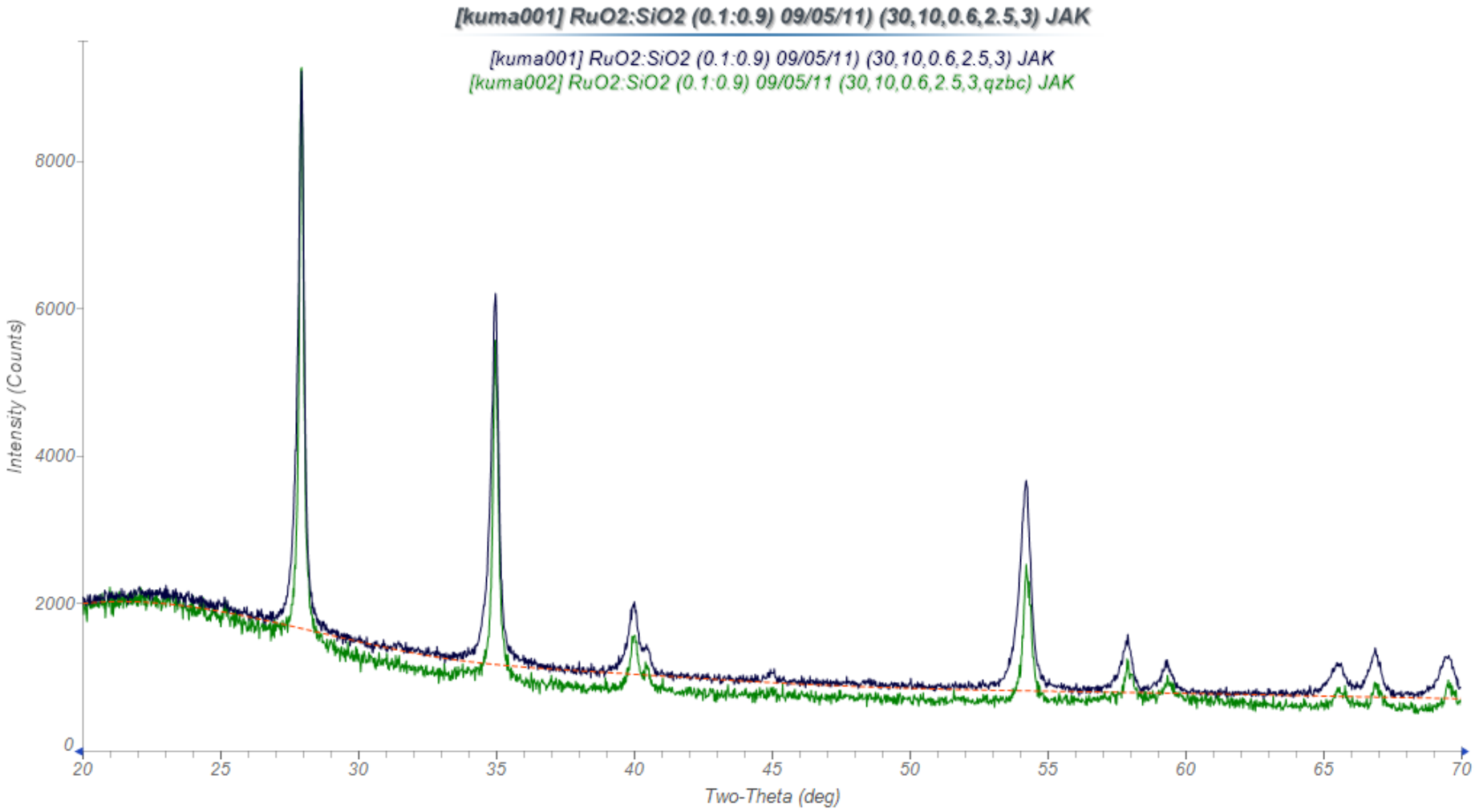

Penetration Depth, μm

2θ, °	**28**	**130**
Pure RuO_2	22	70
10% RuO_2/90% SiO_2	100	340

Mario Birkholz, *Thin Film Analysis by X-ray Scattering*, Wiley-VCH (2006).

International Tables for Crystallography, Volume H, Chapter 5.4, pp. 581-600 (2019)

Surface Roughness

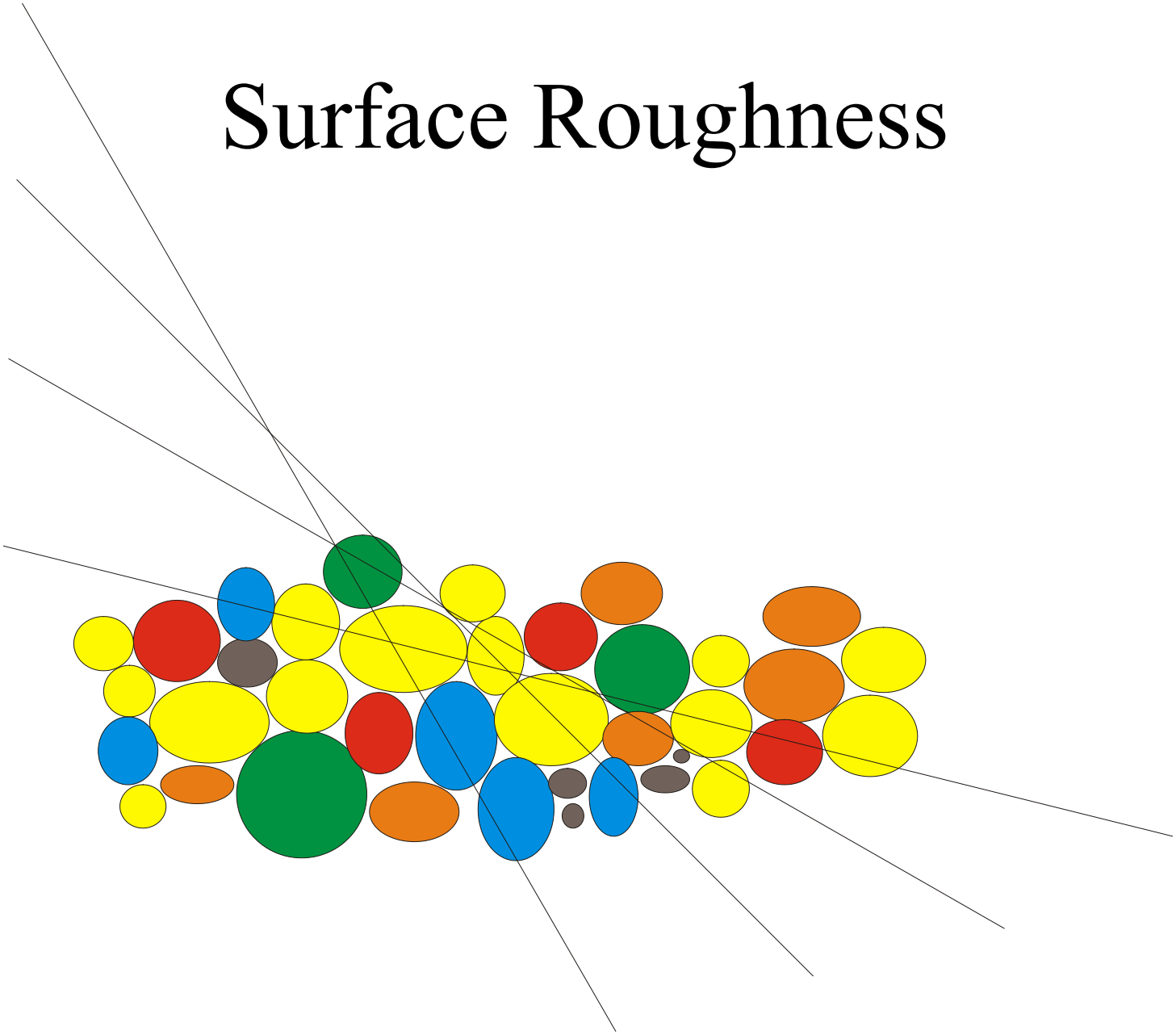

Surface Roughness

R. J. Harrison and A. Paskin, *Acta Cryst.*, **17**, 325 (1964).

P. Suortti, *J. Appl. Cryst.*, **5**, 325-331 (1972).

$$I = I_1 + I_2 =$$

$$\frac{I_0}{2\mu} + \frac{I_0 \cos\theta}{x_B - x_A} \int_0^{\infty} dL \int_{x_A + L\cos\theta}^{x_B + L\cos\theta} \frac{1}{2} e^{\left[-\mu\left(L_a + L_a^*\right)\right]} \left[\frac{\partial (L_a - L_a^*)}{\partial x}\right] dx$$

Surface Roughness

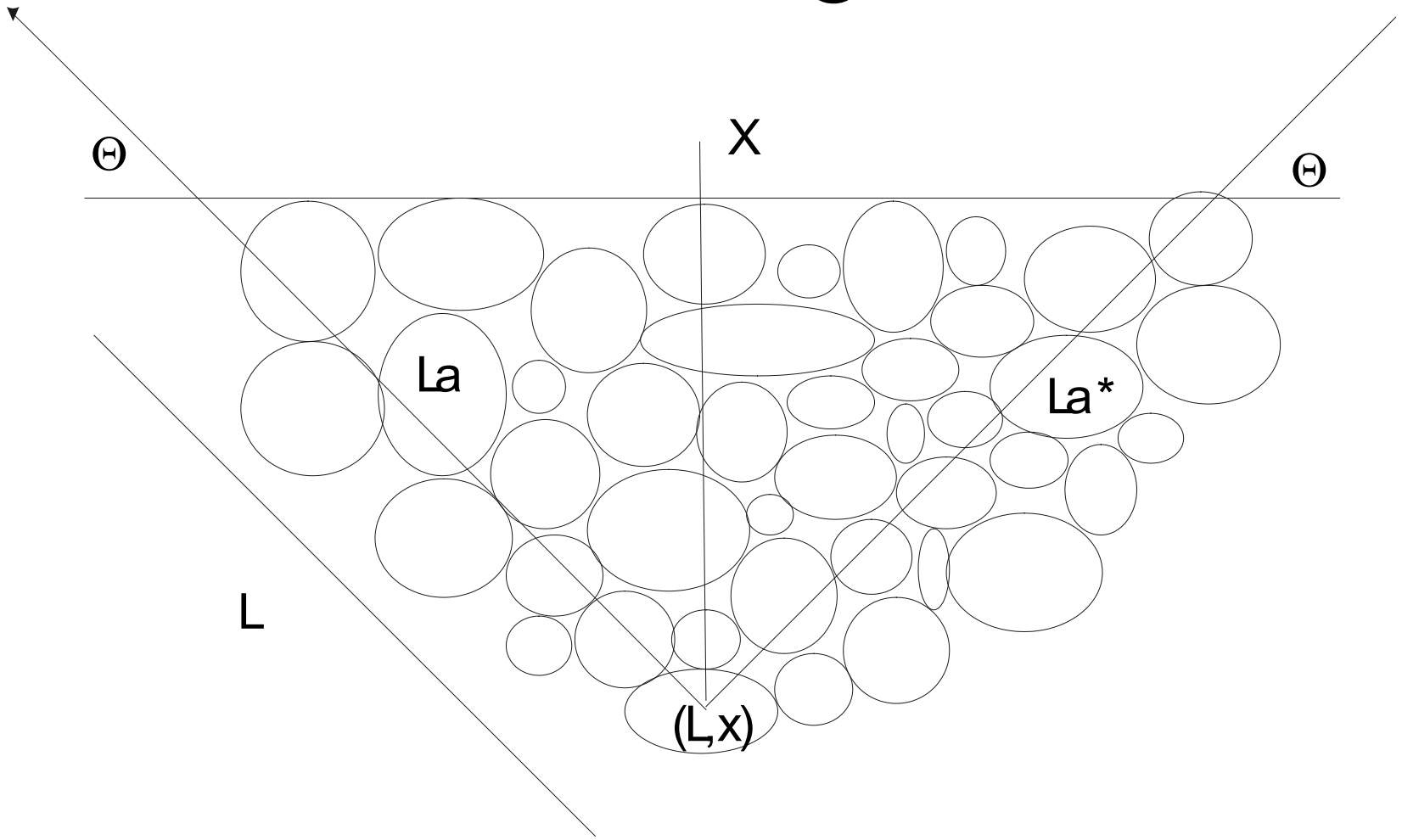

Surface Roughness Effects in Cu

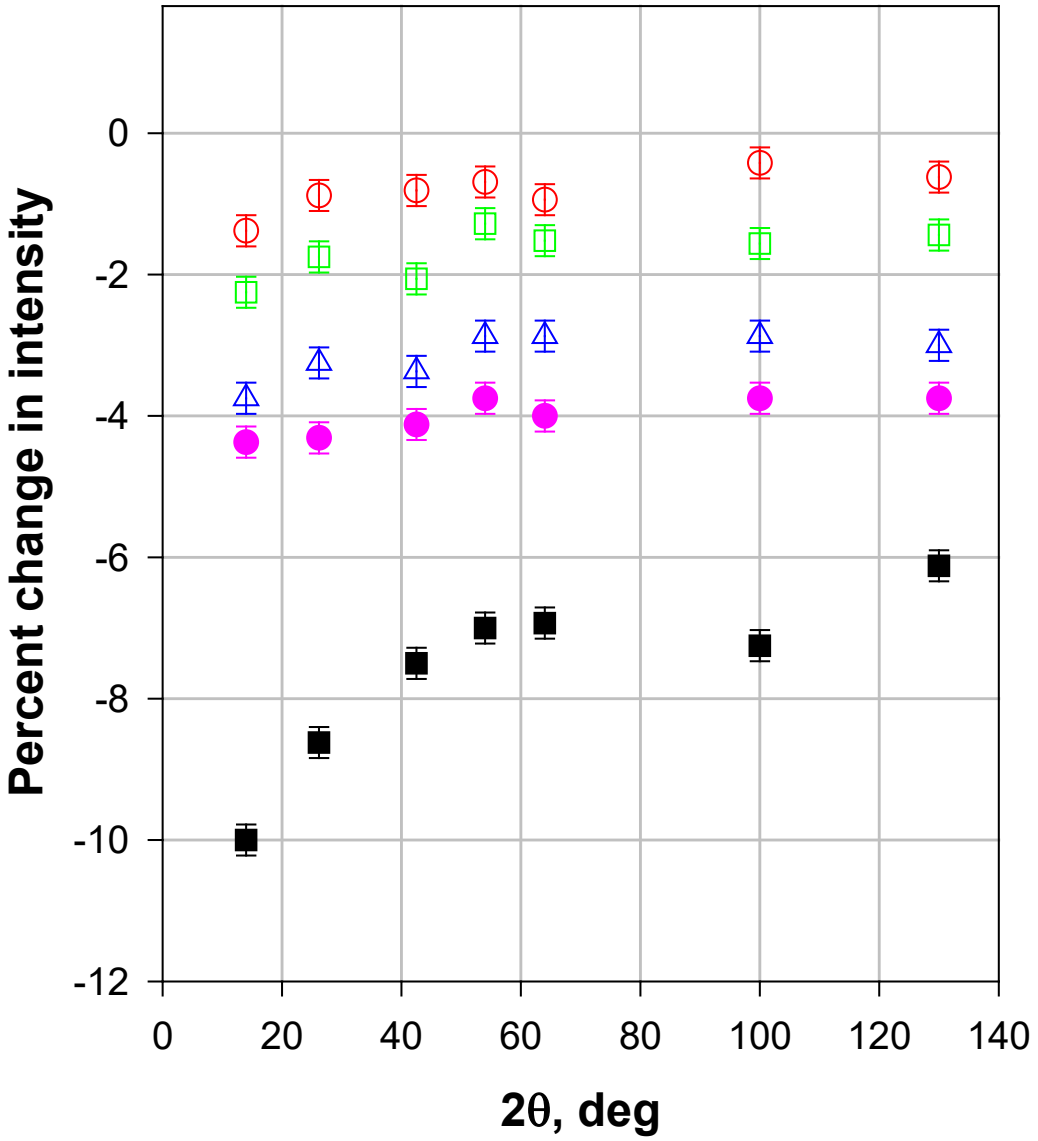

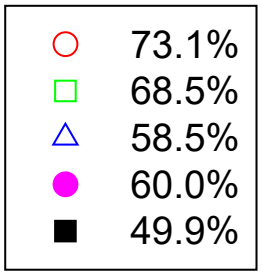

bulk packing density

"A phase diagram for jammed matter", C. Song, P. Wang, and H. A. Makse, *Nature*, **453**, 629-632 (2008).

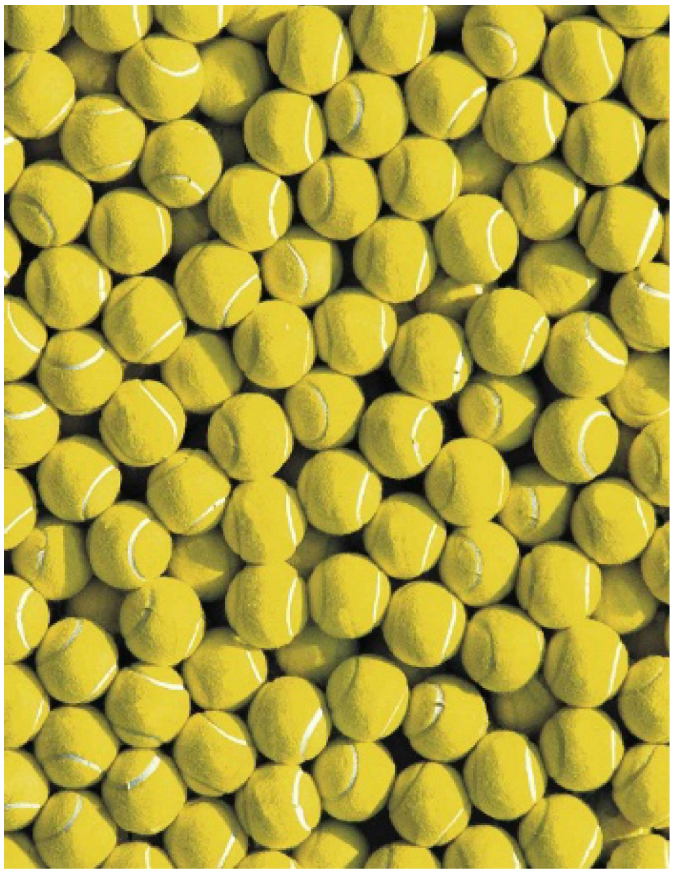

Random Close Packing
= 63.4%

Random Loose Packing
= 53.6%

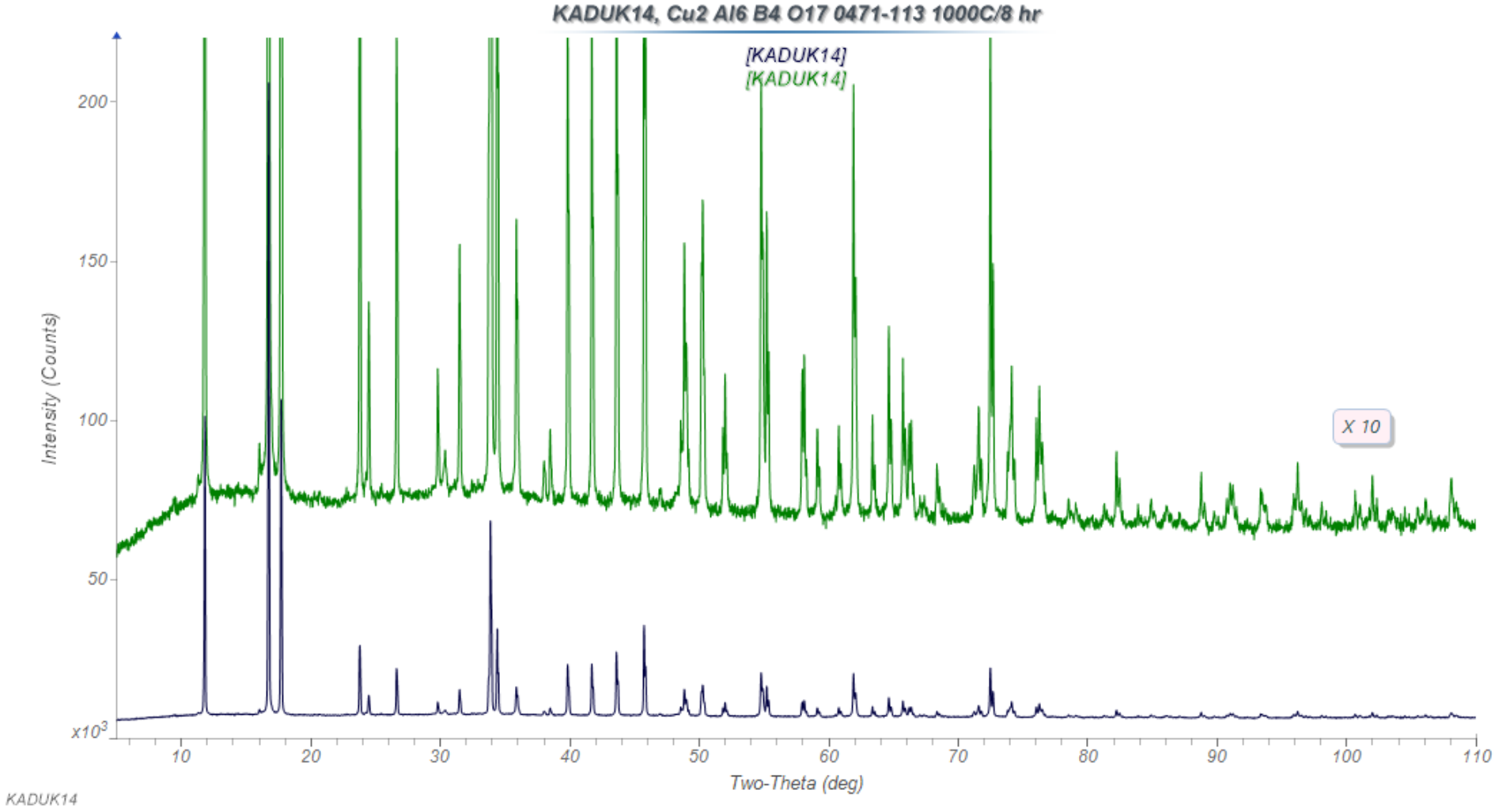
KADUK14, Cu2 Al6 B4 O17 0471-113 1000C/8 hr
[KADUK14]
[KADUK14]
X 10
Intensity (Counts)
x10^3
200
150
100
50
10
20
30
40
50
60
70
80
90
100
110
Two-Theta (deg)
KADUK14

An Extreme Example of Surface Roughness

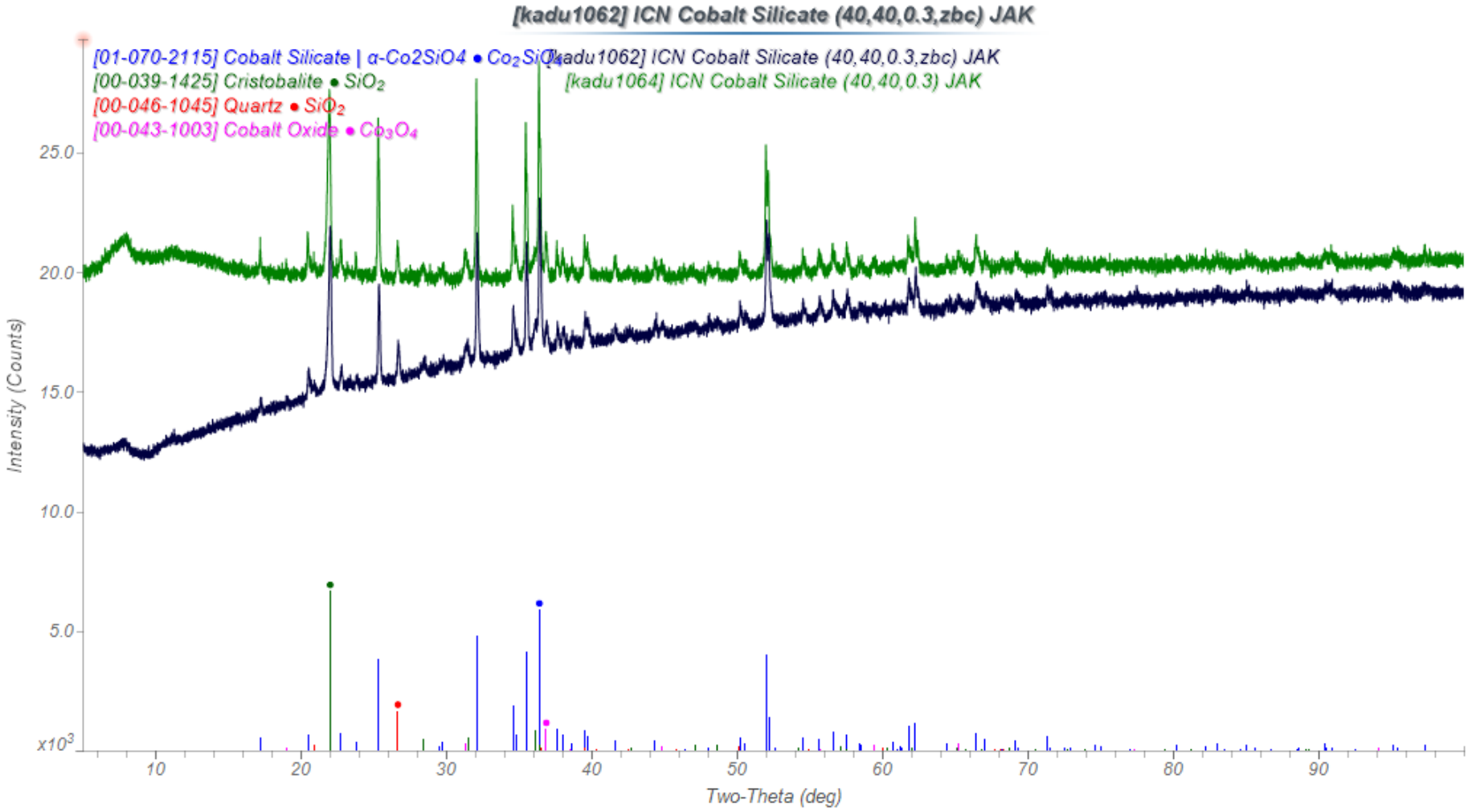

Effect of Surface Roughness

Mounting	Packed Powder	Slurry	Slurry
Correction	None	None	Suortti 0.34/0.70
Co U_{iso}, Å^2	0.0125(8)	-0.0042(11)	0.0142(8)
Si U_{iso}, Å^2	0.0117(19)	-0.0049(22)	0.0135(21)
O U_{iso}, Å^2	0.003(2)	-0.013(2)	0.009(2)

Particle Statistics

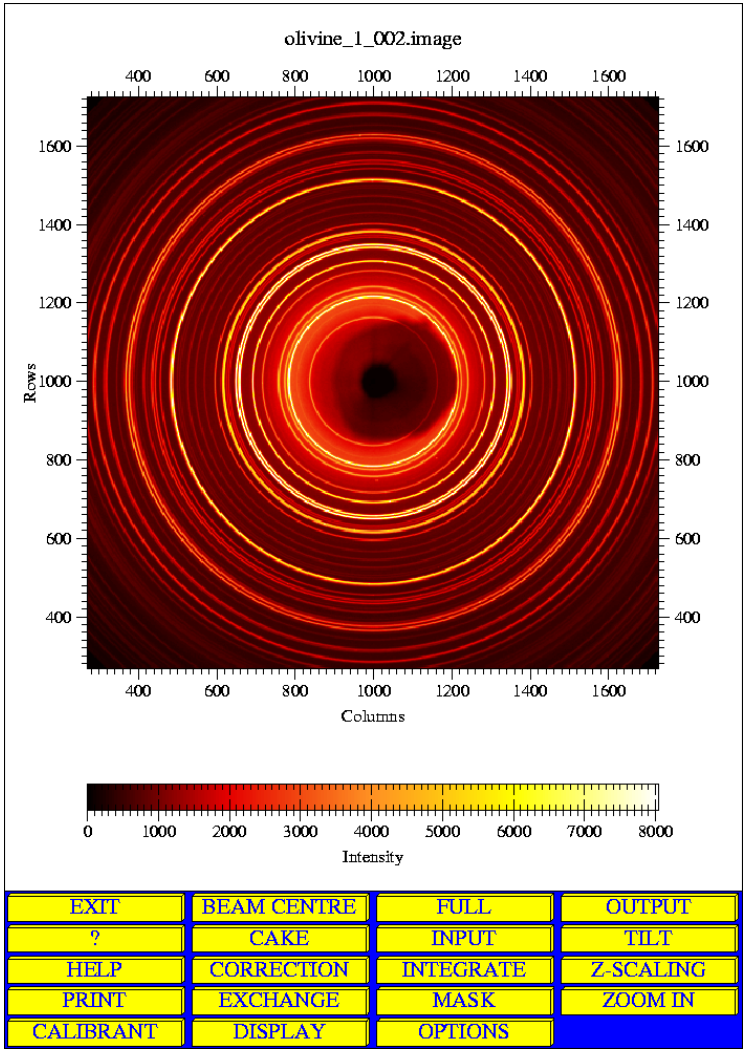

Intensity Measurements on Different Size Fractions of < 325-Mesh Quartz Powder

Specimen #	15-50 μ fraction	5-50 μ fraction	5-15 μ fraction	< 5 μ fraction
1	7612	8688	10841	11055
2	8373	9040	11336	11040
3	8255	10232	11046	11386
4	9333	9333	11597	11212
5	4823	8530	11541	11460
6	11123	8617	11336	11260
7	11051	11598	11686	11241
8	5773	7818	11288	11428
9	8527	8021	11126	11406
10	10255	10190	10878	11444
Mean area	8513	9227	11268	11293
Mean deviation	1545	929	236	132
Mean % dev.	18.2	10.1	2.1	1.2

Klug and Alexander, *X-ray Diffraction Procedures* (1974), p. 366.

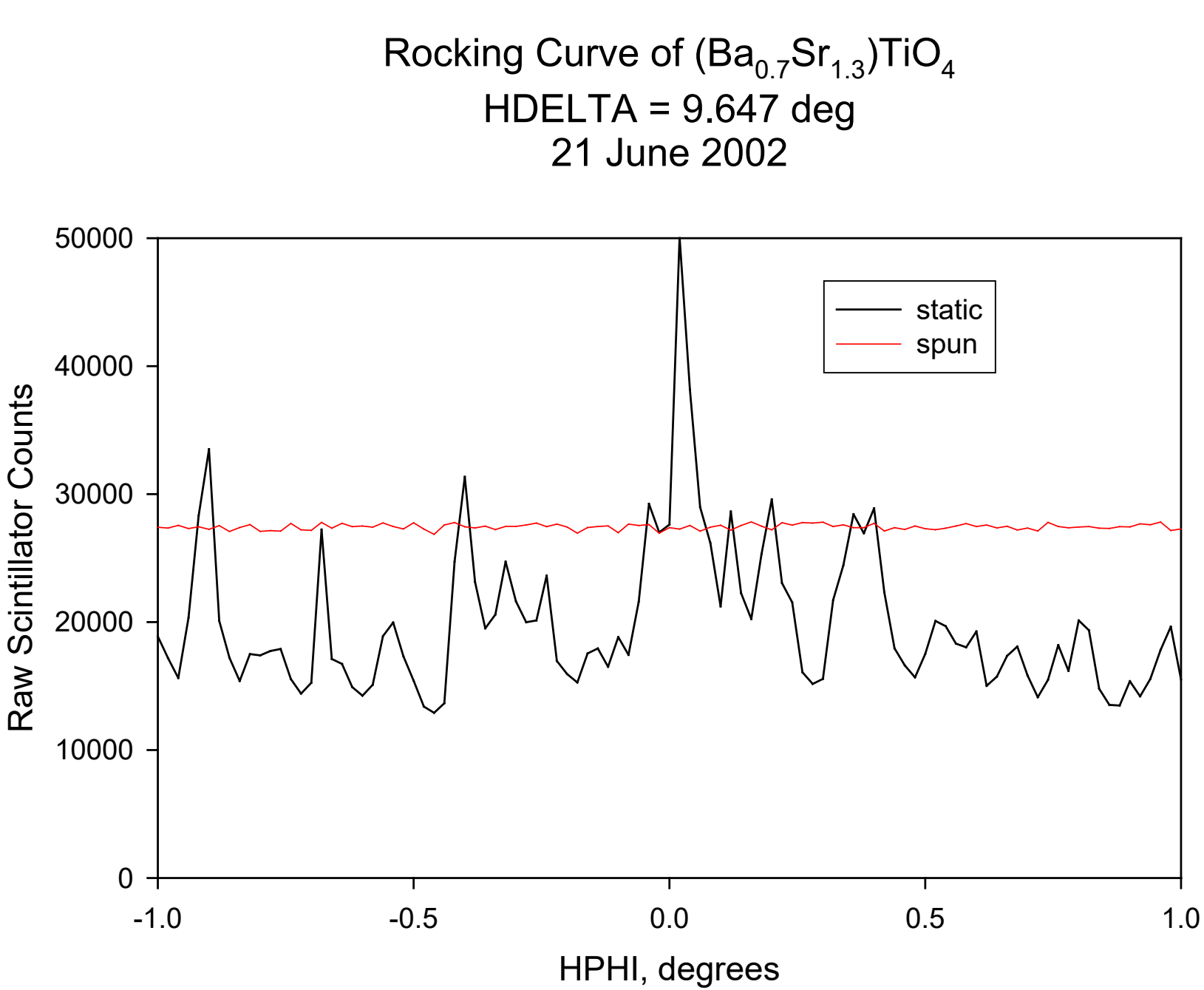
Rocking Curve of $(Ba_{0.7}Sr_{1.3})TiO_4$
HDELTA = 9.647 deg
21 June 2002
Raw Scintillator Counts
50000
40000
30000
20000
10000
0
-1.0
-0.5
0.0
0.5
1.0
HPHI, degrees
static
spun

Particle Statistics

- How many grains are necessary to obtain a random pattern?
  - Describe orientation analytically
    - Represent all Bragg planes of a given set (*hkl*) by a perpendicular vector (reciprocal lattice vector)

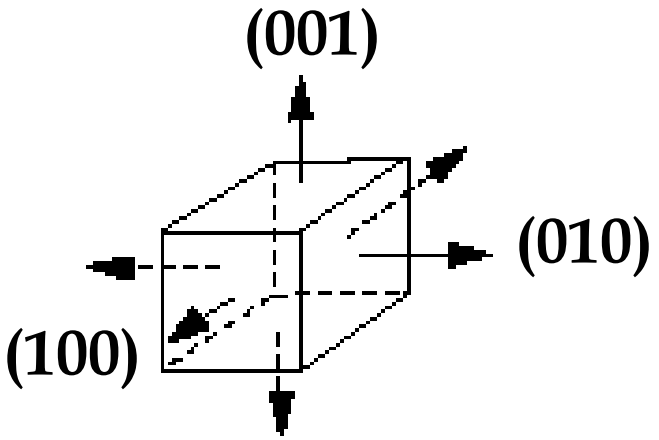

D. K. Smith, *Powd. Diffr.*, **16**, 186-191 (2001).

Particle Statistics

- Randomness requires that the distribution of these vectors be uniform over space.

- Number of vectors per crystallite is multiplicity

Stereographic Projection

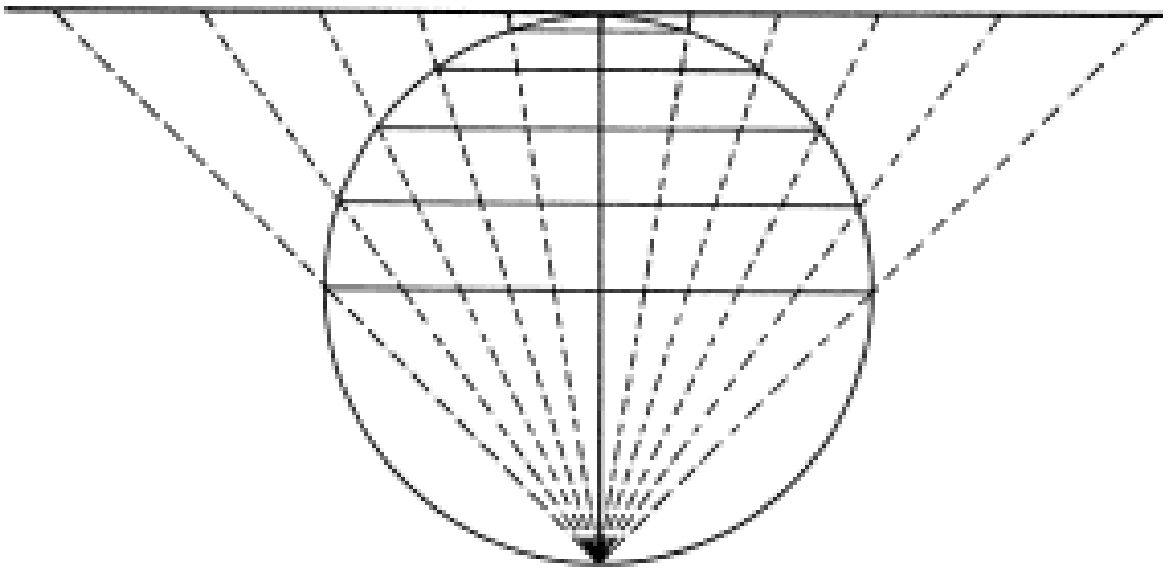

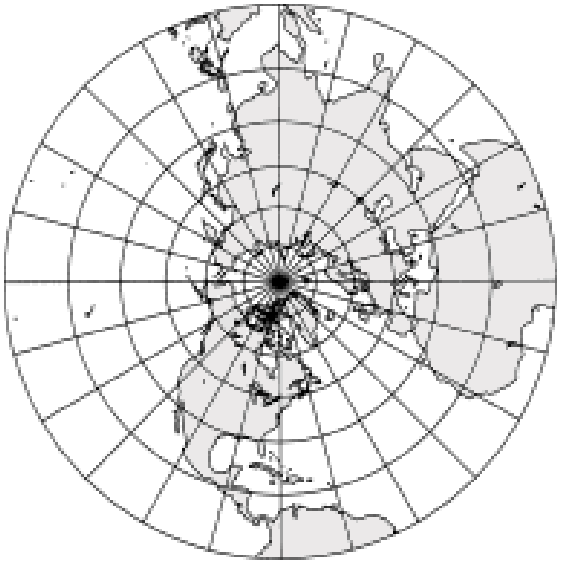

http://www.3dsoftware.com/Cartography/USGS/MapProjections/Azimuthal/Stereographic

Particle Statistics

- Circumscribe unit sphere around specimen
  - Distribution of vectors on sphere is uniform if random

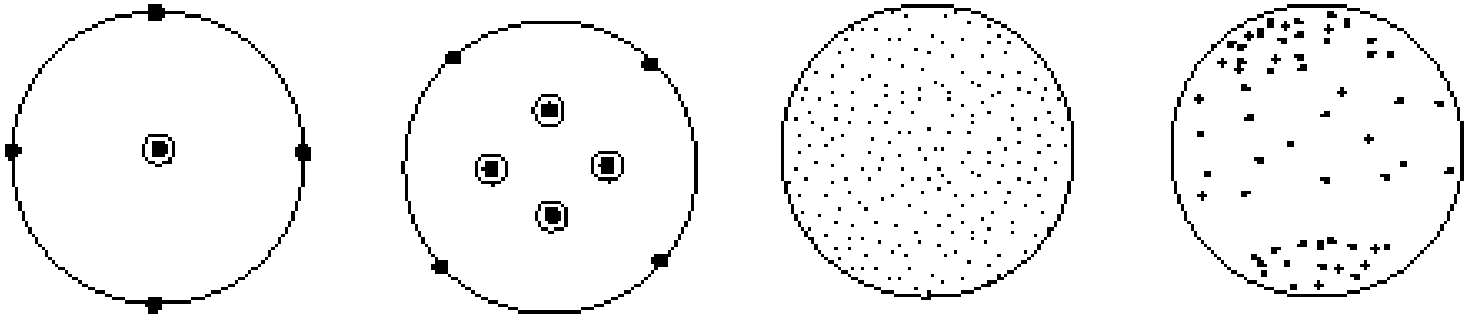

6 pts **12 pts** **n pts** **oriented**

Non-uniform if oriented

Particle Statistics

- Estimate volume of specimen in the beam
- V = area × (3×half-depth)
- Assume area ~ 1 cm × 1 cm = 100 mm^2
- $I/I_0 = e^{-\mu t} \rightarrow t_{1/2} = 0.693/\mu$
- $\mu(SiO_2)$ = 9.76 mm^{-1} $\rightarrow$ $3t_{1/2}$ ~ 0.2 mm
- $\therefore V \sim 20$ mm^3

Particle Statistics

number of particles in irradiated volume

Diameter	40 μm	10 μ	1 μ
V/grain	3.35×10^{-5} mm^3	5.24×10^{-7}	5.24×10^{-10}
grains/mm^3	2.98×10^{4}	1.91×10^{6}	1.91×10^{9}
grains/ 20 mm^3	5.97×10^{5}	3.82×10^{7}	3.82×10^{10}

How many particles are sufficient to observe a random powder pattern?

Particle Statistics

area of sphere = 4π steradians

diameter	40 μm	10 μm	1 μm
area/pole $A_p = 4\pi/N$	2.11×10^{-5}	3.29×10^{-7}	3.29×10^{-10}
interpole angle = $\arcsin[2(A_p)^{1/2}/\pi]$	0.297°	0.037°	0.005°

Particle Statistics

To determine how many particles will actually diffract, the angular range of diffraction is necessary.

Because the particle is small compared to the sample, the divergence is limited by the size of the X-ray target and the particle size.

Particle Statistics

Conditions of diffraction for a single particle

R = radius of diffractometer = 170-215 mm
F = 0.1-0.4 mm
S = 0.001-0.040 mm
$\alpha = \sin^{-1}[(F+S)/R]$
$\approx \sin^{-1} F/R$

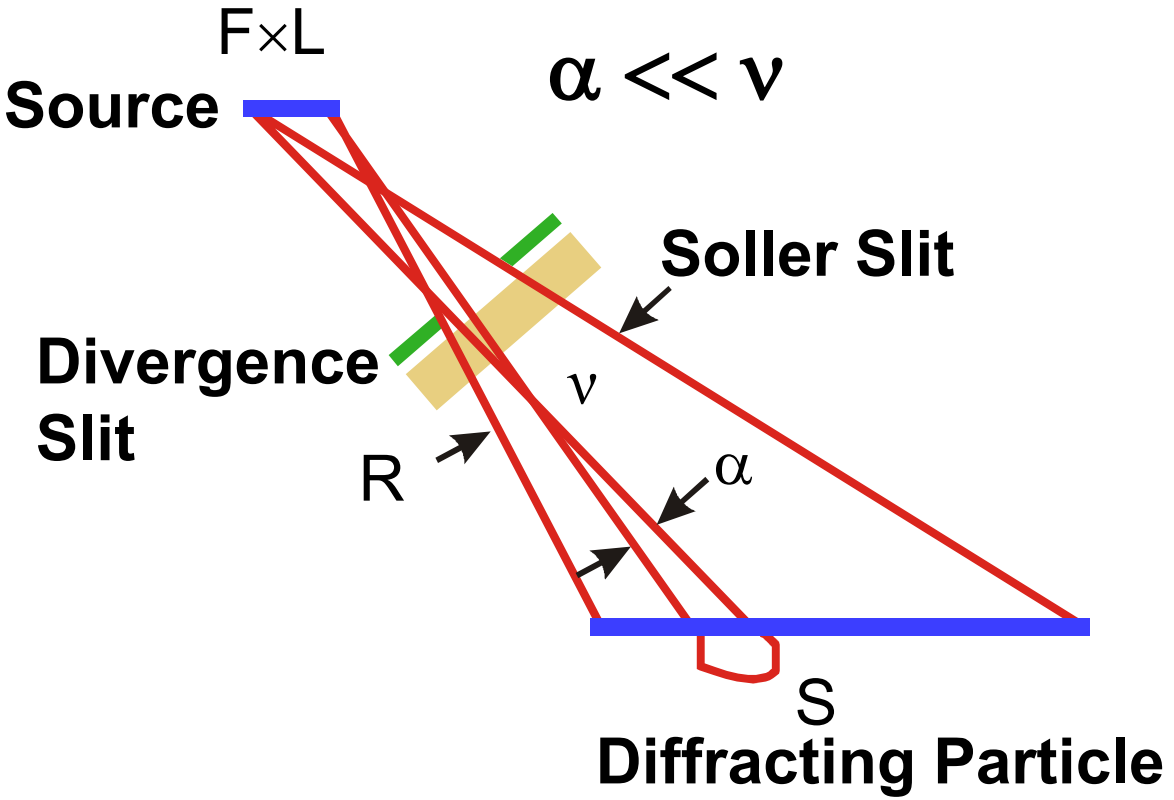

Particle Statistics

- Effect of Soller slit is to limit the length of the source visible to sample particle

$$L = 0.5 \text{ mm}$$

Particle Statistics

- N_p = number of particles which may diffract

  = (area on unit sphere corresponding to divergence)/

  area on unit sphere per particle

  = A_D/A_P

To determine A_D requires relating effective source area, F×L, to area on a unit sphere

$$A_D = \frac{FL}{R} = \frac{(0.1)\ (0.5)}{200}$$

$$= 2.5 \times 10^{-4}$$

Particle Statistics

diameter	40 μm	10 μm	1 μm
N_p	12	760	3800

The standard uncertainty in Poisson statistics is proportional to $n^{1/2}$, where n is the number of particles. If we'd like a relative error < 1%, we need $2.3\sigma = 2.3n^{1/2}/n < 1\%$.
This means that
$n > 52900$ particles!

Particle Statistics

- Even 1 μm particles do not yield a sufficiently-uniform distribution of crystallites to achieve 1% accuracy in intensities!
  - Other factors affecting analysis:
    - Concentration
    - Reflection multiplicity
    - Specimen thickness
    - Peak width (crystallite size)
    - Specimen rotation/rocking

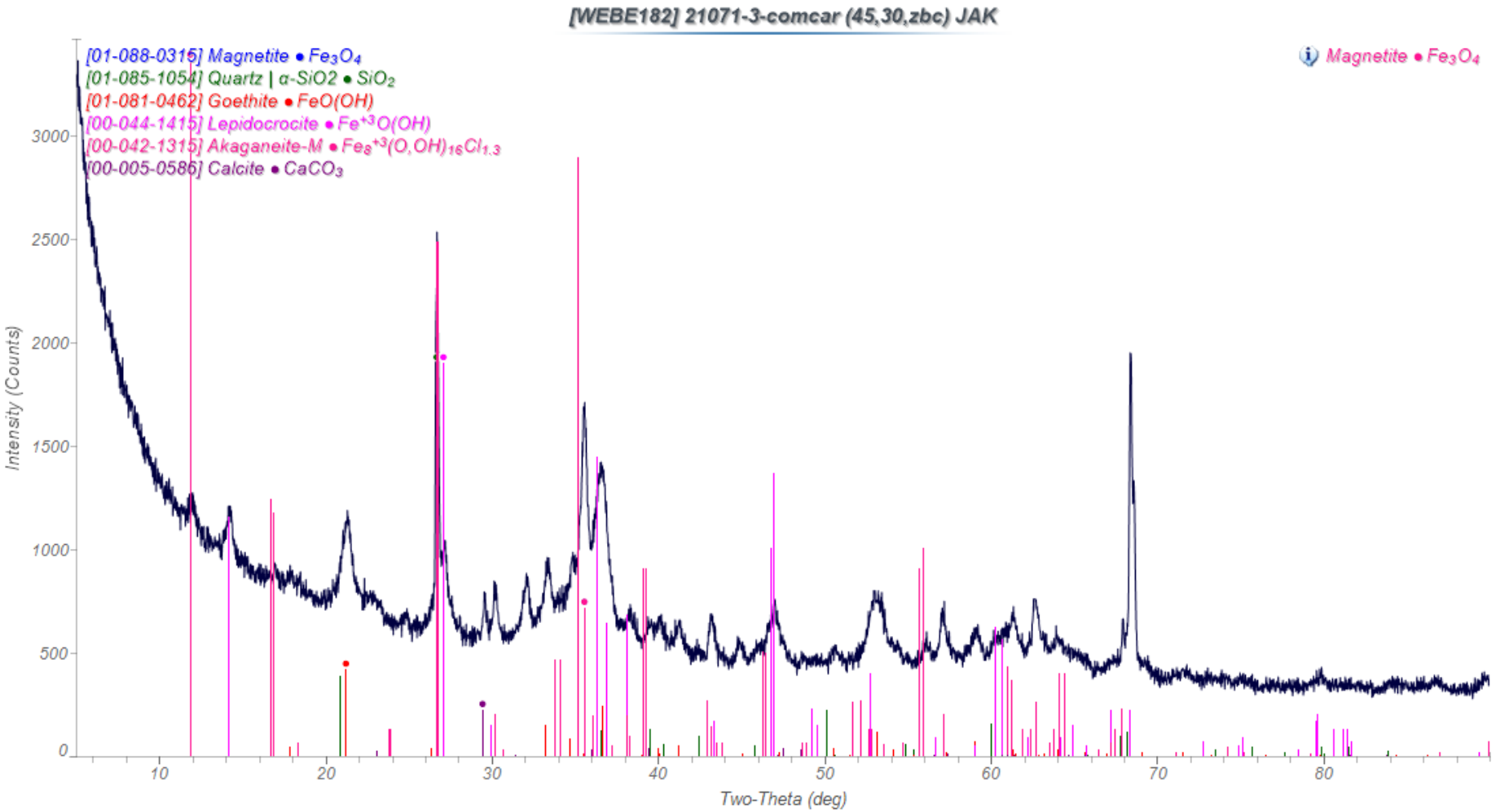
[WEBE182] 21071-3-comcar (45,30,zbc) JAK
[01-088-0315] Magnetite • Fe3O4
[01-085-1054] Quartz | α-SiO2 • SiO2
[01-081-0462] Goethite • FeO(OH)
[00-044-1415] Lepidocrocite • Fe+3O(OH)
[00-042-1315] Akaganeite-M • Fe8+3(O,OH)16Cl1.3
[00-005-0586] Calcite • CaCO3
Magnetite • Fe3O4
Intensity (Counts)
0
500
1000
1500
2000
2500
3000
10
20
30
40
50
60
70
80
Two-Theta (deg)

Scott's Moss Control Granules

0-0-16 (N-P-K oxides)
double sulfate of K and Mg
17.5% $FeSO_4(H_2O)$

K_2O	16%
Mg	8%
S	20%
Fe	5%

Grind in a mortar and pestle, and measure from a static specimen

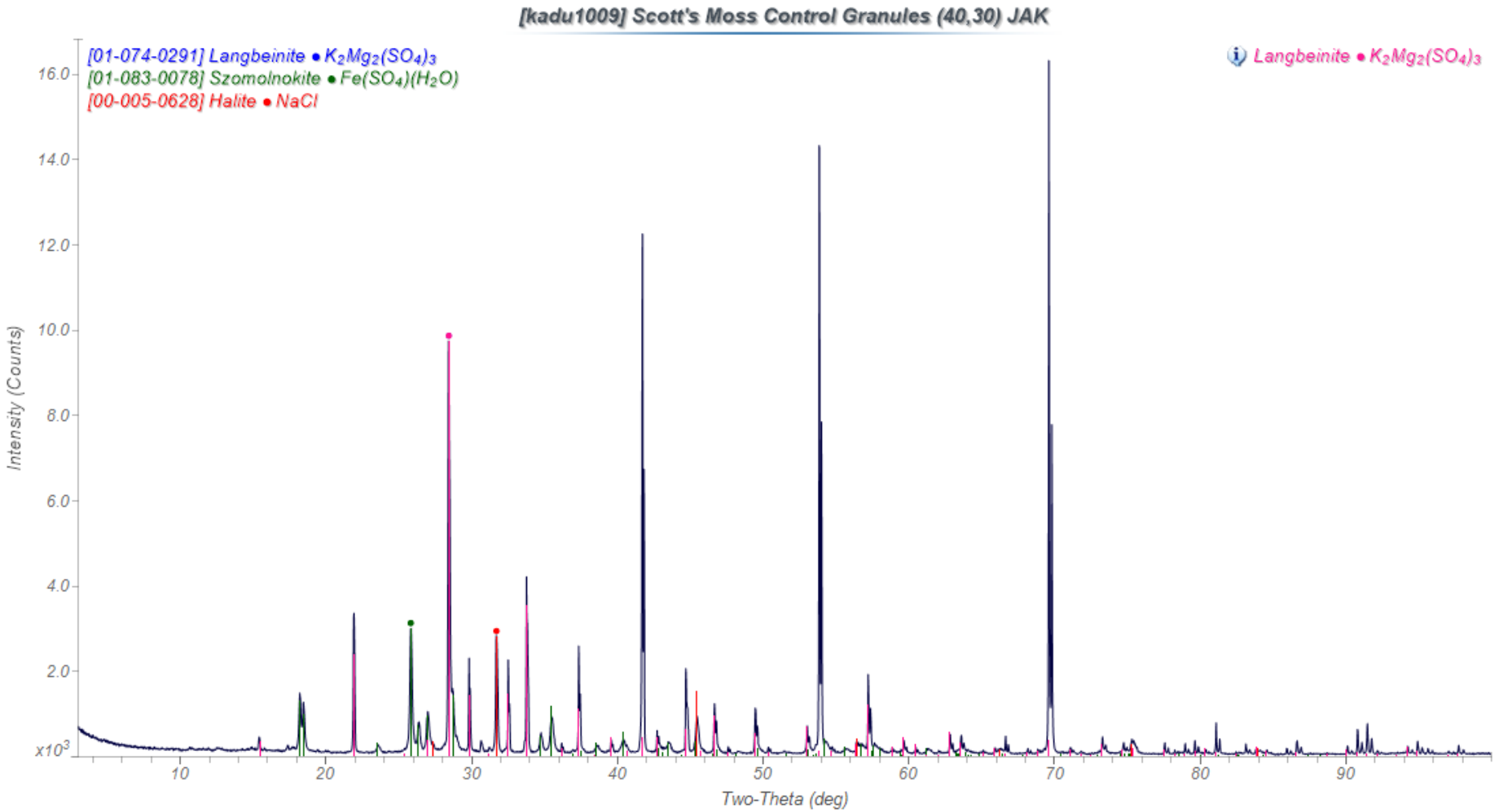
[kadu1009] Scott's Moss Control Granules (40,30) JAK
[01-074-0291] Langbeinite • K2Mg2(SO4)3
[01-083-0078] Szomolnokite • Fe(SO4)(H2O)
[00-005-0628] Halite • NaCl
Langbeinite • K2Mg2(SO4)3
Intensity (Counts)
x10^3
16.0
14.0
12.0
10.0
8.0
6.0
4.0
2.0
10
20
30
40
50
60
70
80
90
Two-Theta (deg)

Micronize (corundum/hexane) and re-measure a rotating specimen

Pictures of the specimen surfaces

Hand Ground

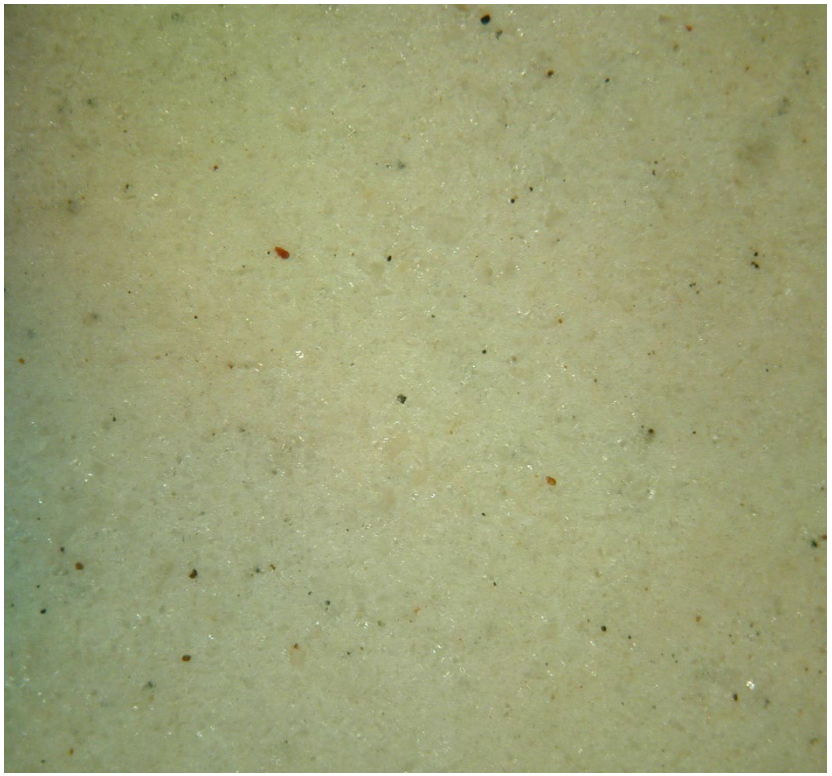

Micronised

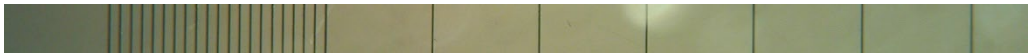

100 μm

Pictures by B. J. Huggins, BP Analytical

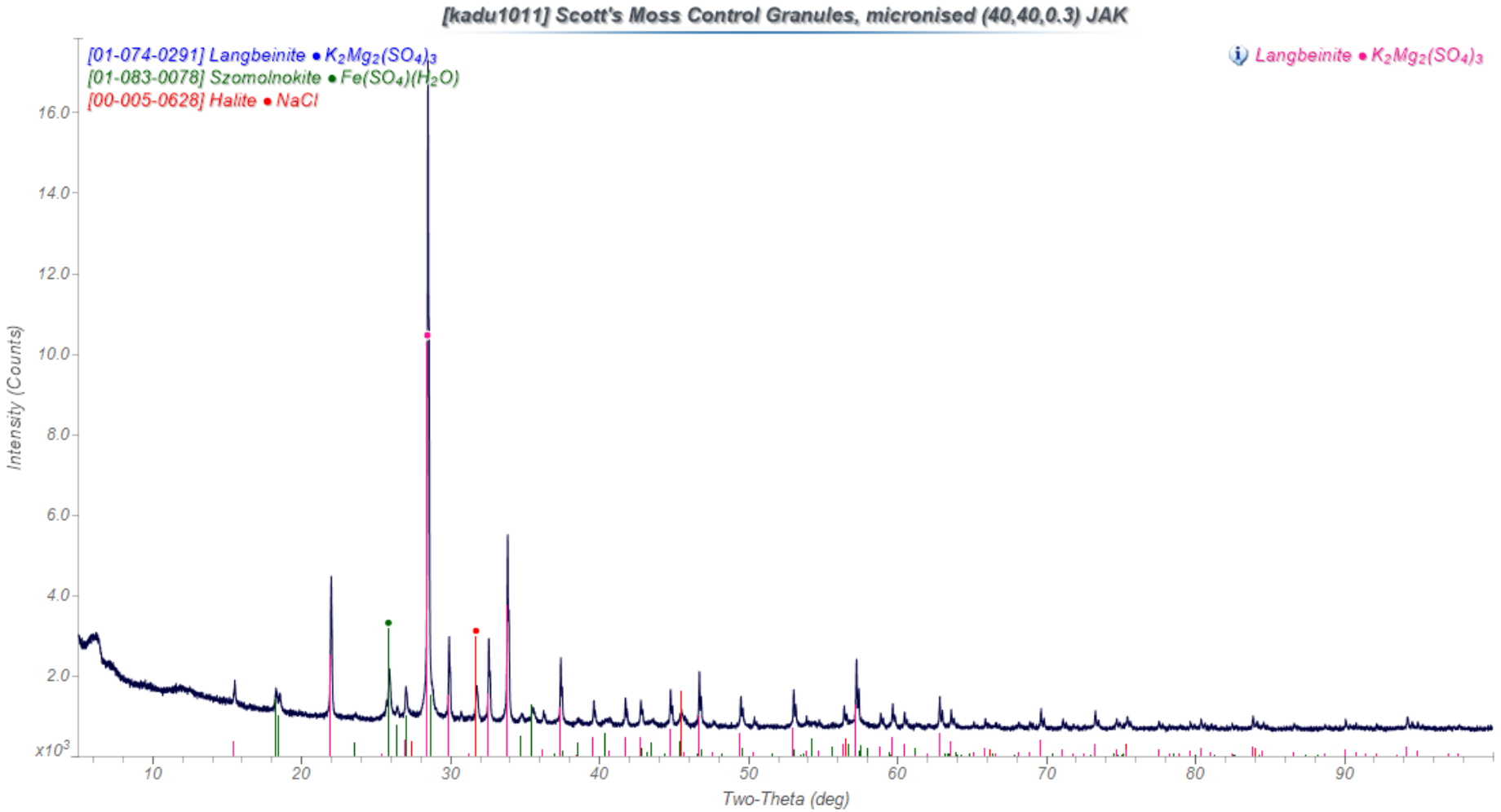
[kadu1011] Scott's Moss Control Granules, micronised (40,40,0.3) JAK
[01-074-0291] Langbeinite • K2Mg2(SO4)3
[01-083-0078] Szomolnokite • Fe(SO4)(H2O)
[00-005-0628] Halite • NaCl
Langbeinite • K2Mg2(SO4)3
Intensity (Counts)
x10^3
16.0
14.0
12.0
10.0
8.0
6.0
4.0
2.0
10
20
30
40
50
60
70
80
90
Two-Theta (deg)

Look up the structures and carry out a Rietveld refinement

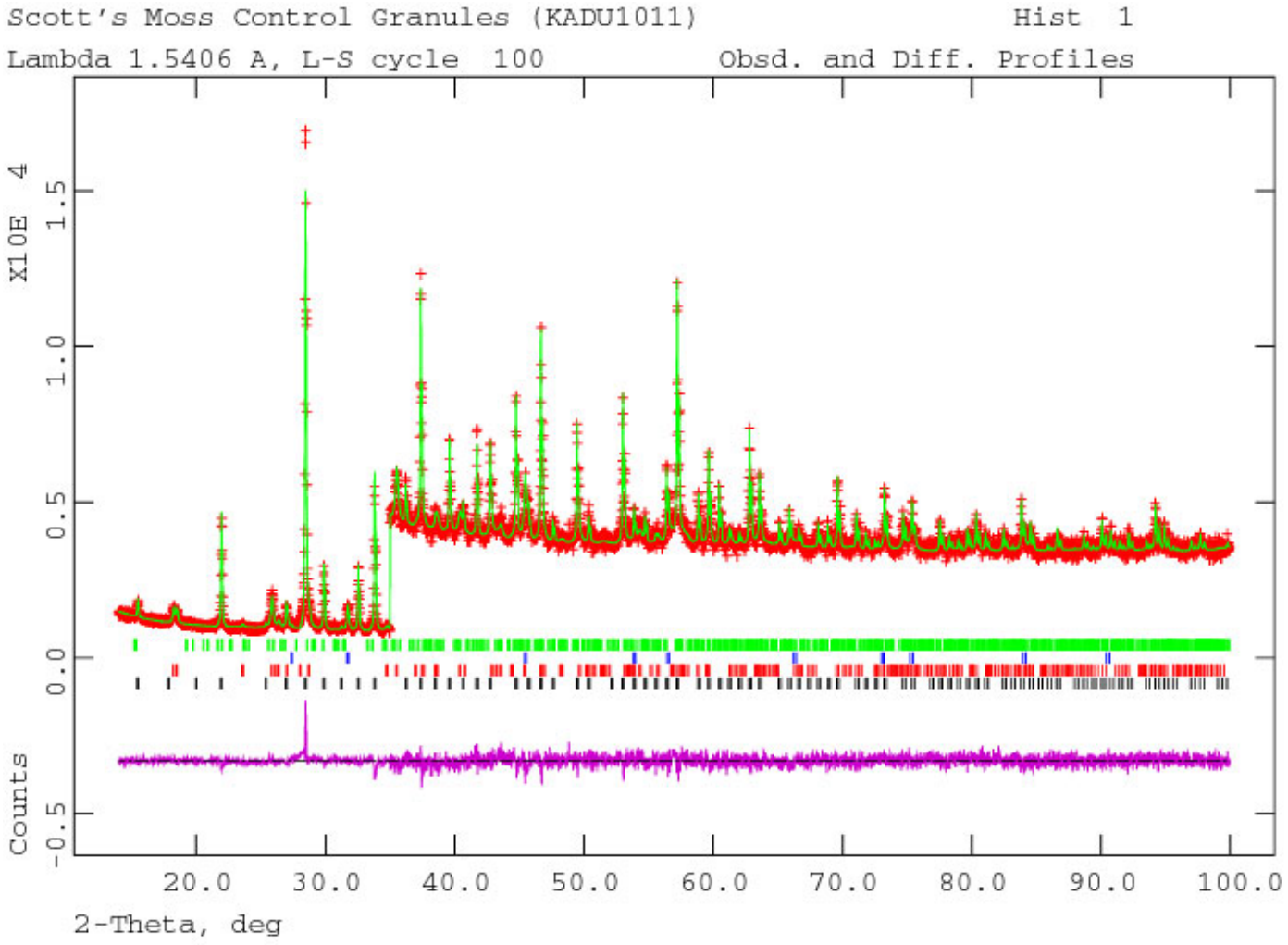

Quantitative Phase Analysis

Langbeinite	$K_2Mg_2(SO_4)_3$	80.49(4) wt%
Szomolnokite	$FeSO_4(H_2O)$	15.6(1) wt%
Halite	NaCl	3.74(6) wt%
Vanthoffite??	$Na_6Mg(SO_4)_4$	0.2(2) wt%

Observed and Expected Composition

	Observed, wt%	Bag, wt%
$FeSO_4(H_2O)$	15.6(1)	17.5
Fe	5.1	5
K_2O	18.2	16
Mg	9.4	8
S	21.5	20

"Particle statistics in quantitative X-ray diffractometry",
N. J. Elton and P. D. Salt,
Powder Diffraction, **11**(3),
218-229 (1996).

Microabsorption

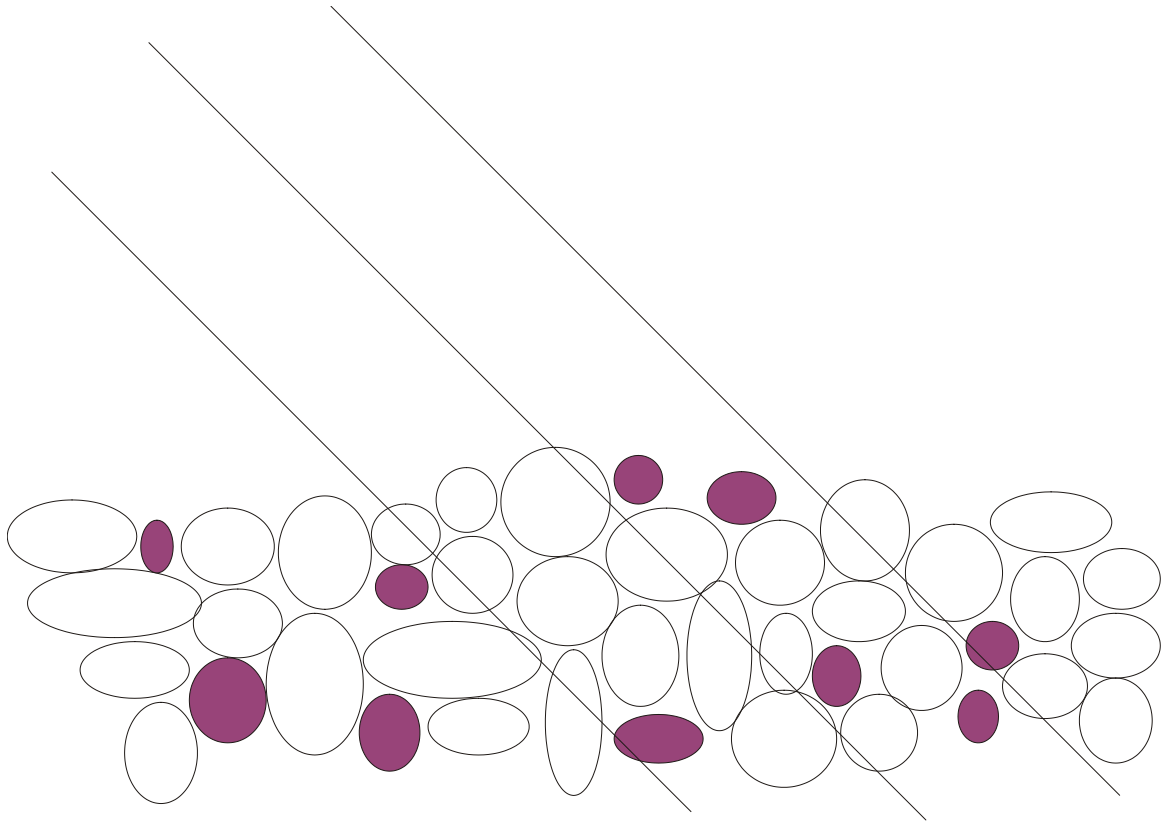

Microabsorption

G. W. Brindley, *Phil. Mag.*, **36**(7), 347 (1945)

The ideal ratio $I_{(hkl)\alpha}/I_{(hkl)'\beta}$ is multiplied by a factor:

$$K = \frac{\tau_\alpha}{\tau_\beta} = \frac{V_\beta \int_0^{V_\alpha} e^{-\left(\mu_\alpha - \bar{\mu}\right)x} dx}{V_\alpha \int_0^{V_\beta} e^{-\left(\mu_\beta - \bar{\mu}\right)x} dx}$$

Microabsorption
assumed: R_β = 2 microns, μbar = 0.5*(μ_α+μ_β)

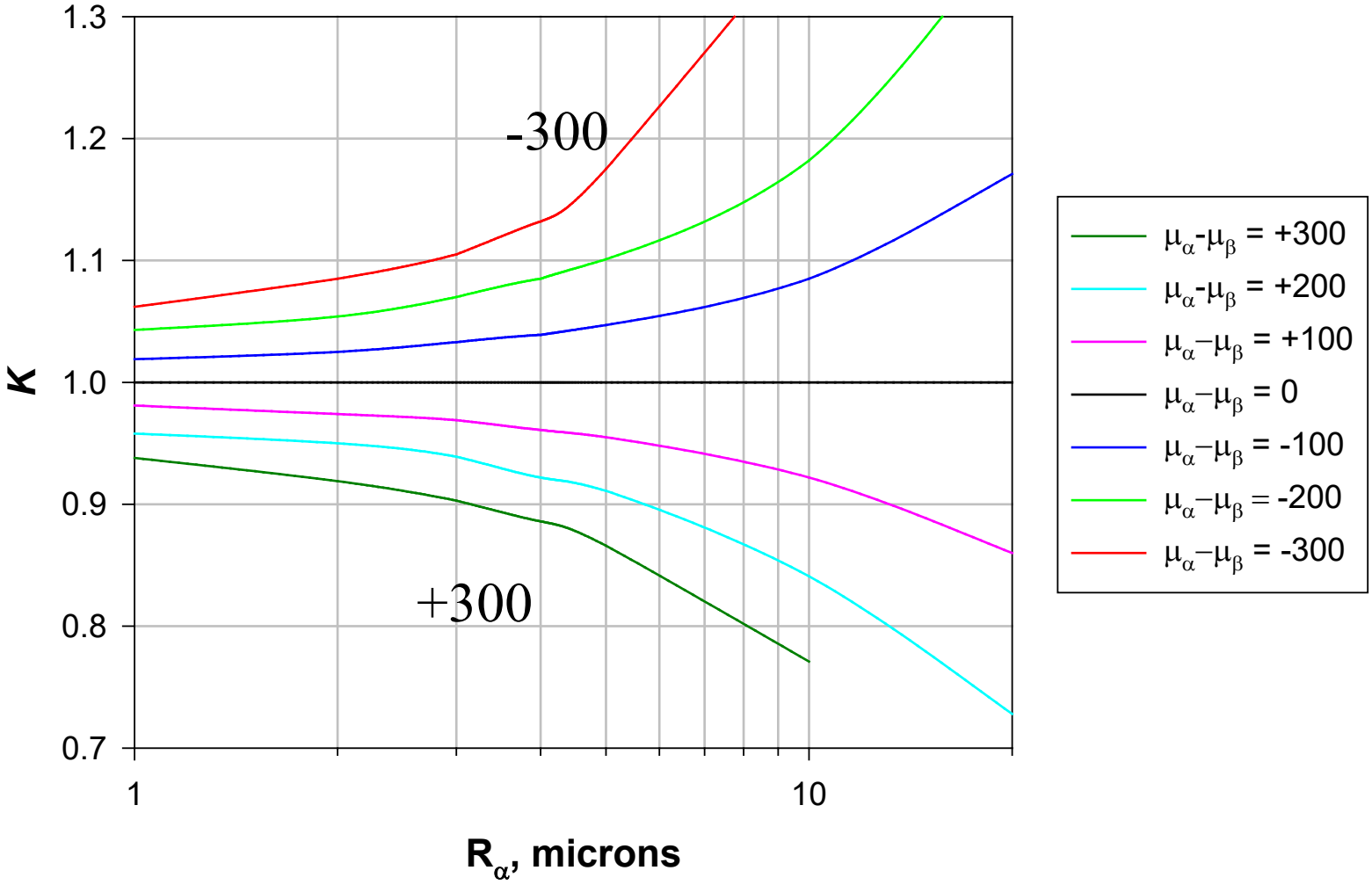

Anatase/Rutile Mixtures

Quantitative Phase Analysis

$$\left(\frac{X_\alpha}{X_\beta}\right) = \left(\frac{I_{(hkl)\alpha}}{I_{(hkl)'\beta}}\right)\left(\frac{I^{rel}_{(hkl)'\beta}}{I^{rel}_{(hkl)\alpha}}\right)\left(\frac{RIR_{\beta,c}}{RIR_{\alpha,c}}\right)$$

$$\left(\frac{X_r}{X_a}\right) = \left(\frac{I_{(110)r}}{I_{(101)a}}\right)\left(\frac{100}{100}\right)\left(\frac{I/I_{c,a}}{I/I_{c,r}}\right)$$

What are the I/I_c for anatase and rutile? Search the PDF-4+:

Rutile from PDF-4+ 2019

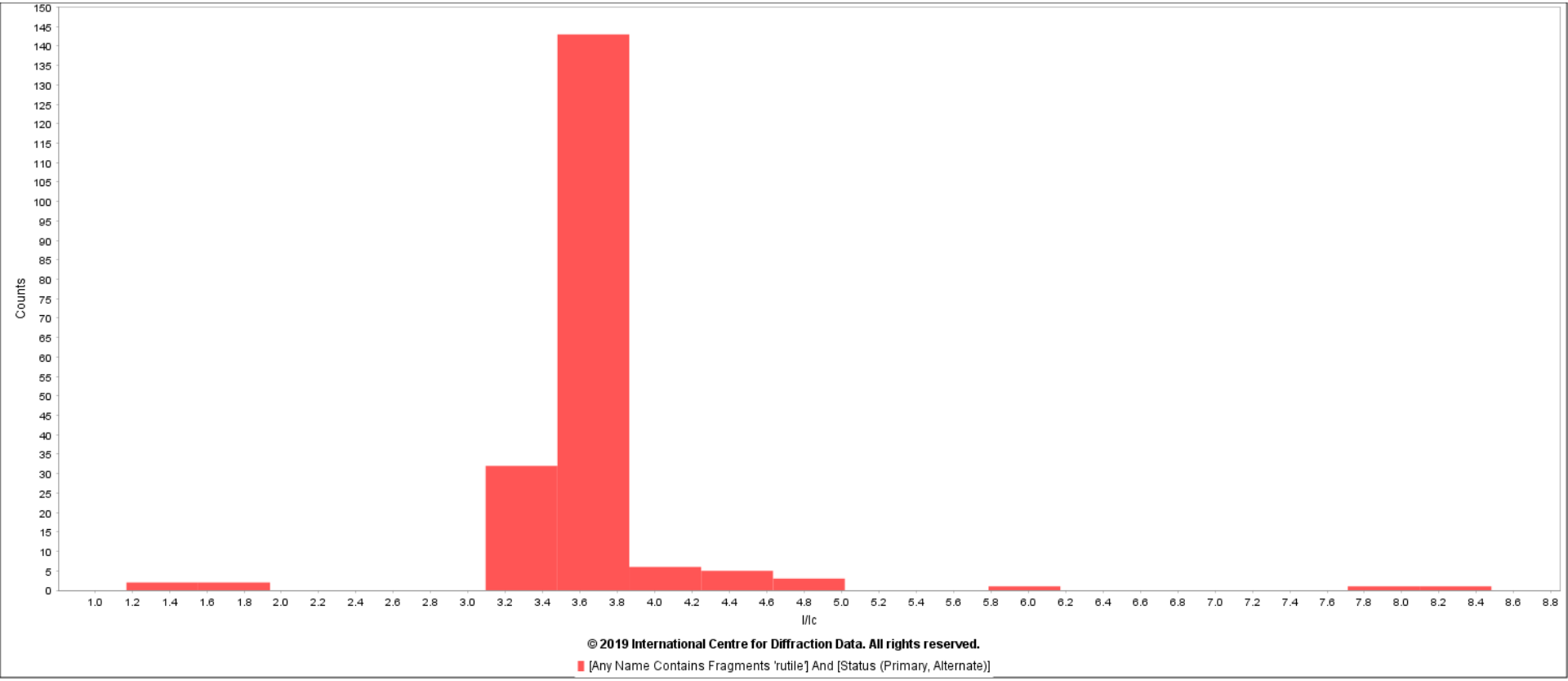

One of the High Ones

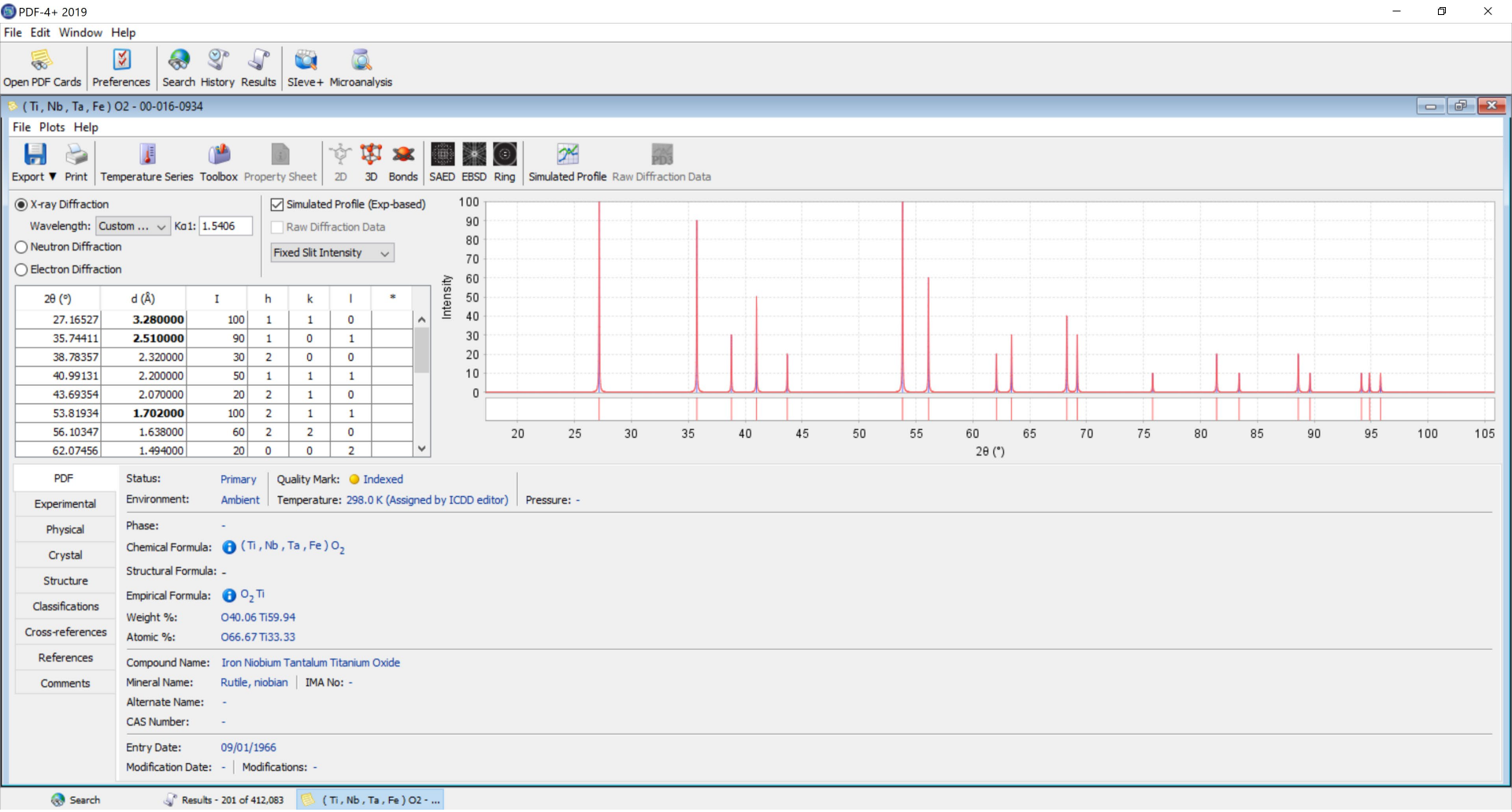

Ti and O only, Star, $P4_2/mnm$

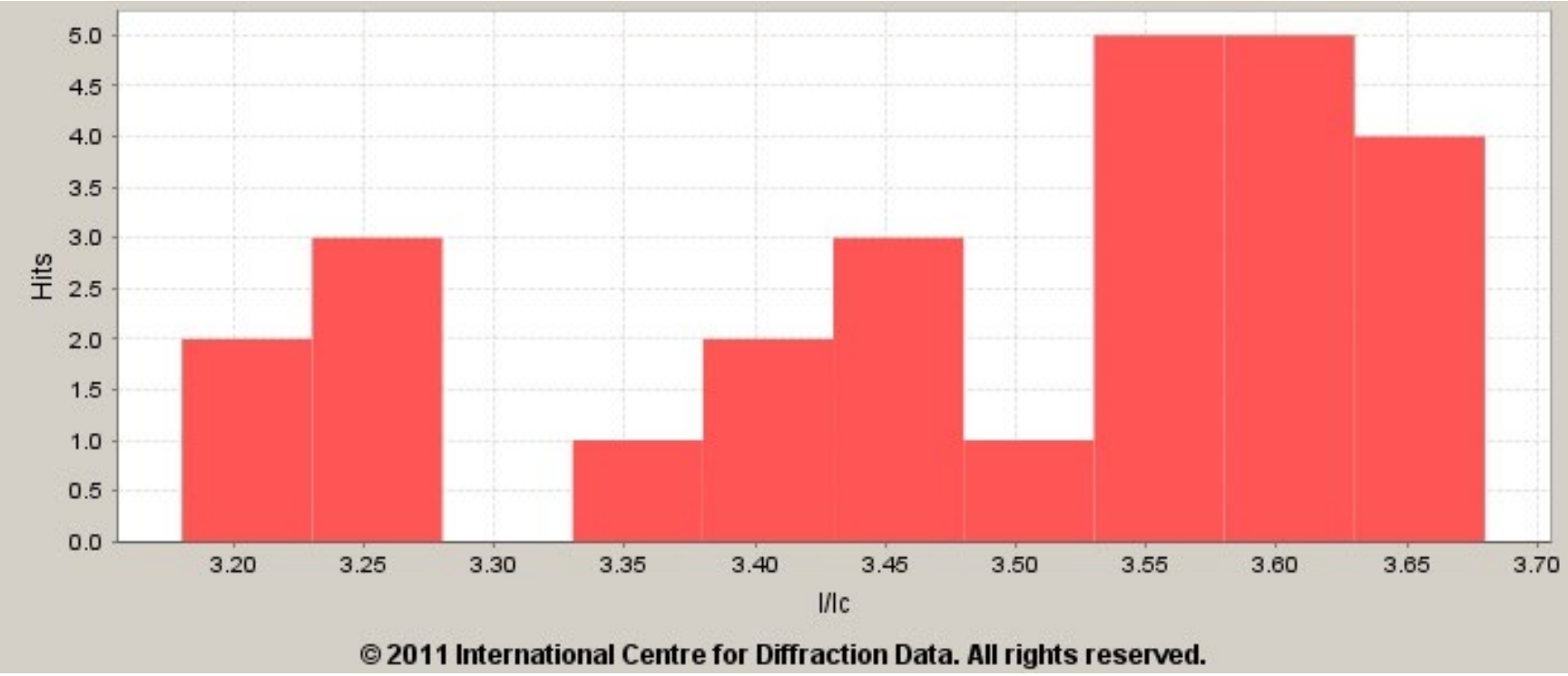

00-021-1276 = 3.4!

Add ambient

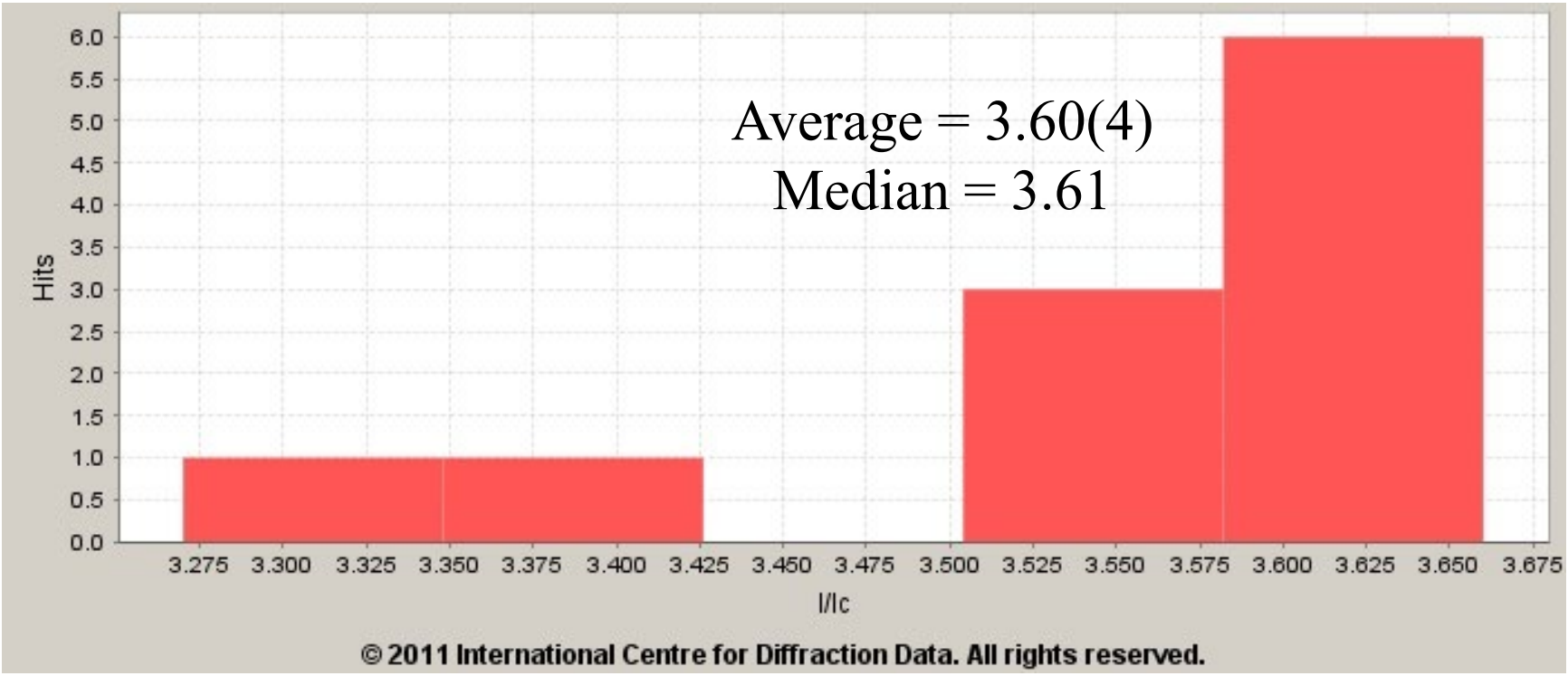
Average = 3.60(4)
Median = 3.61
Hits
I/Ic
6.0
5.5
5.0
4.5
4.0
3.5
3.0
2.5
2.0
1.5
1.0
0.5
0.0
3.275 3.300 3.325 3.350 3.375 3.400 3.425 3.450 3.475 3.500 3.525 3.550 3.575 3.600 3.625 3.650 3.675
© 2011 International Centre for Diffraction Data. All rights reserved.

Ti and O only, Star, ambient $I4_1/amd$

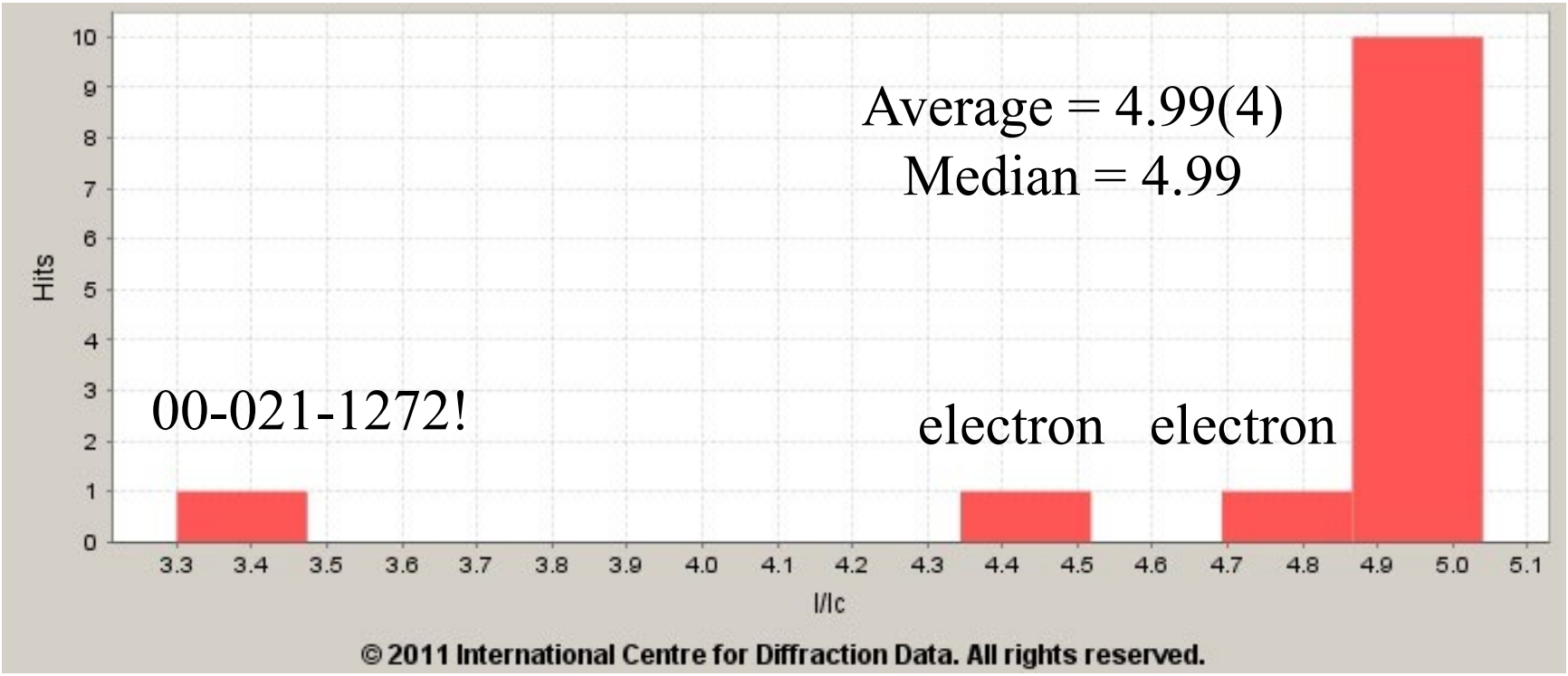

The support vendor and BP disagreed on the anatase concentrations…

The I/I_c Values

Phase	Vendor	BP GSAS	Average Fit
Anatase	5 (71-1166)	5.04	4.74(69) 5.11(169)
Rutile	3.4 (21-1276)	3.65	3.52(16) 3.605(1)

The equations are thus:

Vendor	BP
$\frac{X_r}{X_a} = 1.5\frac{I_r}{I_a}$	$\frac{X_r}{X_a} = 1.38\frac{I_r}{I_a}$

BP's method thus always yields anatase concentrations which are higher than the vendor's. Which (if either) of the methods is accurate?

Calcine some anatase to yield rutile. Make a series of mixtures.

Initial refinements yielded good fits, but anatase concentrations which were ~8% relative higher than expected. Refine the U_{iso}, but then the concentrations are too low. Manually vary to get the best fit to the concentrations:

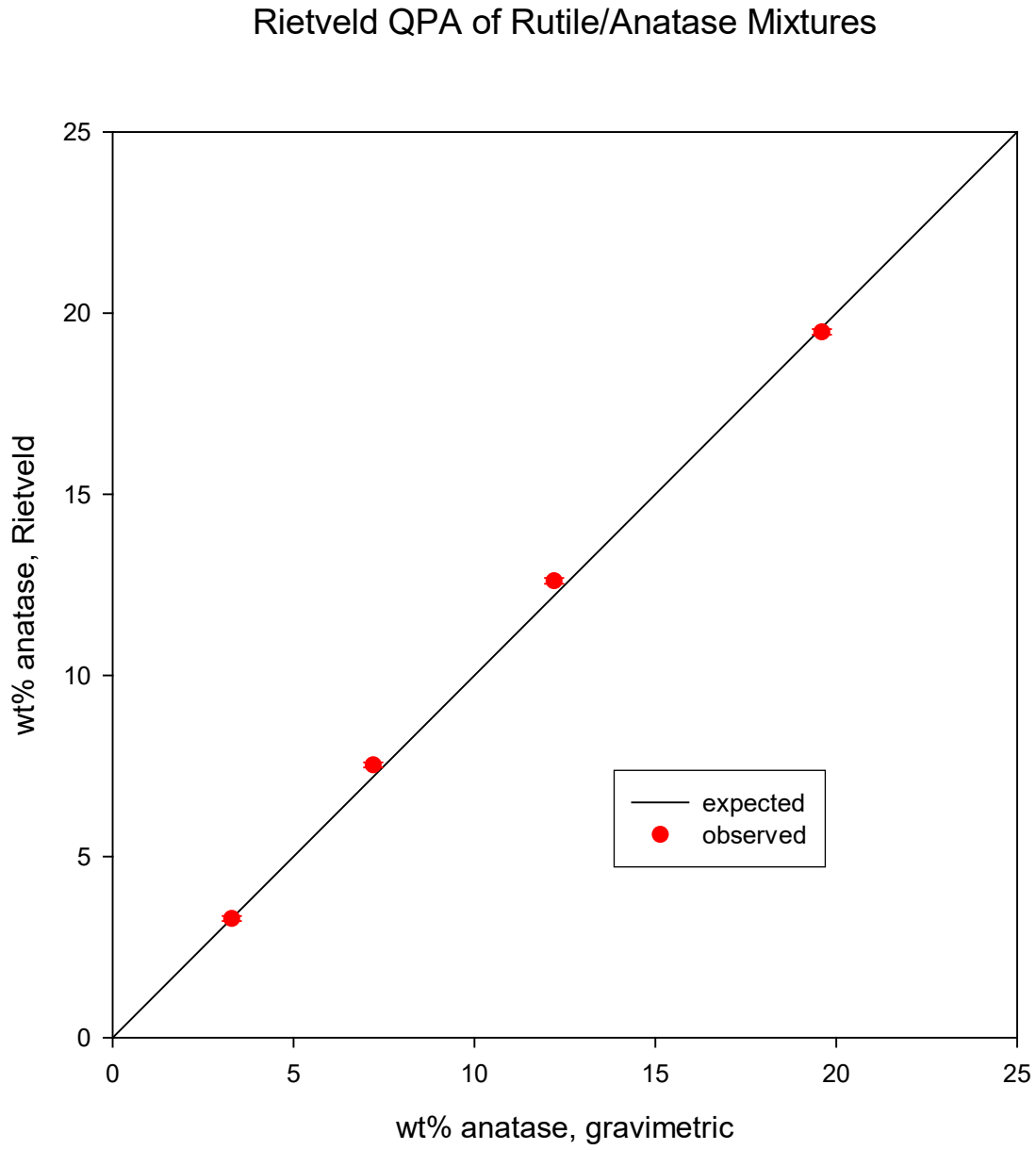
Rietveld QPA of Rutile/Anatase Mixtures
wt% anatase, Rietveld
wt% anatase, gravimetric
0
5
10
15
20
25
expected
observed

The new structural models correspond to I/I_c of 3.58 and 5.04 for rutile and anatase. If we both use these values, our anatase concentrations should agree…

Wt% Anatase in Lot 2004250526

Filename	04780263a	04780263g	04780263m	BHAT199	BHAT200	BHAT201
Location	Vendor	Vendor	Vendor	BP	BP	BP
Vendor Rietveld	10.1(1)	10.0(1)	9.8(1)	8.9(1)	8.8(1)	8.9(1)
BP Rietveld	9.89(12)	9.87(12)	9.70(12)	8.45(7)	8.62(8)	8.38(7)
Vendor RIR	9	8	8	8	11	10
BP RIR p-V	9.22(88)	10.08(95)	9.38(75)	8.02(59)	8.19(62)	8.00(57)
BP RIR SPVII	9.84(34)	10.08(35)	9.30(37)	8.71(14)	8.61(17)	8.07(17)

Interim Conclusions

- The Vendor RIR and BP Rietveld methods yield the same value (= insignificantly different).
- BP Rietveld and RIR methods applied to the same data yield the same concentrations.
- The largest source of error in the RIR method is the error of the anatase (101) peak area.
- There is a subtle difference between the Vendor and BP Rietveld methods.
- There is a difference between the diffractometers (and sample preparations), which is yet to be explained.

Which (if any) analysis is correct?

The explanation?

Calcine some anatase at 1180°C to yield pure rutile. Make a new series of mixtures.

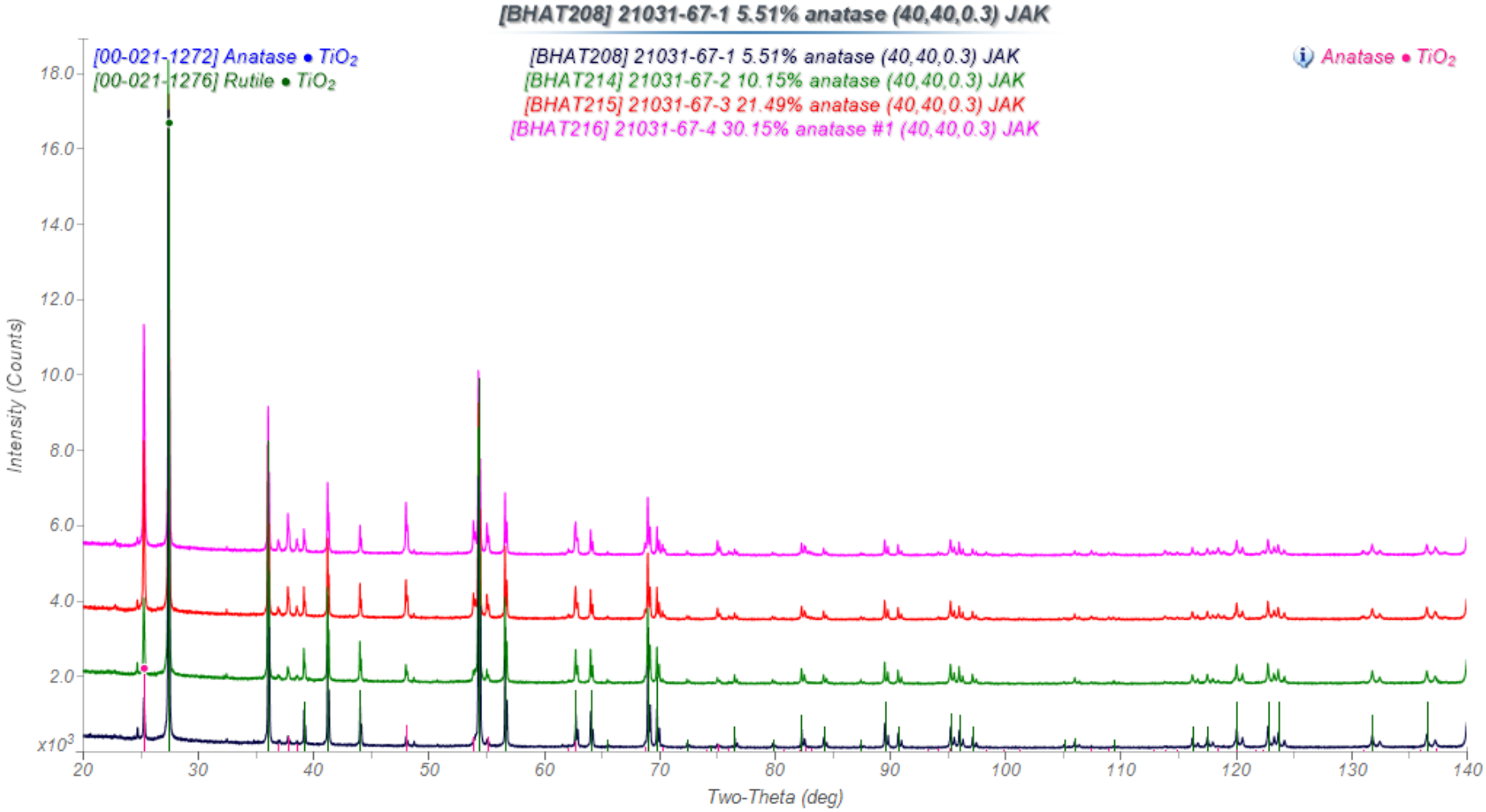
[BHAT208] 21031-67-1 5.51% anatase (40,40,0.3) JAK
[00-021-1272] Anatase • TiO2
[00-021-1276] Rutile • TiO2
[BHAT208] 21031-67-1 5.51% anatase (40,40,0.3) JAK
[BHAT214] 21031-67-2 10.15% anatase (40,40,0.3) JAK
[BHAT215] 21031-67-3 21.49% anatase (40,40,0.3) JAK
[BHAT216] 21031-67-4 30.15% anatase #1 (40,40,0.3) JAK
Anatase • TiO2
Intensity (Counts)
x10^3
18.0
16.0
14.0
12.0
10.0
8.0
6.0
4.0
2.0
20
30
40
50
60
70
80
90
100
110
120
130
140
Two-Theta (deg)

QPA of As-Prepared Anatase/Rutile Mixtures

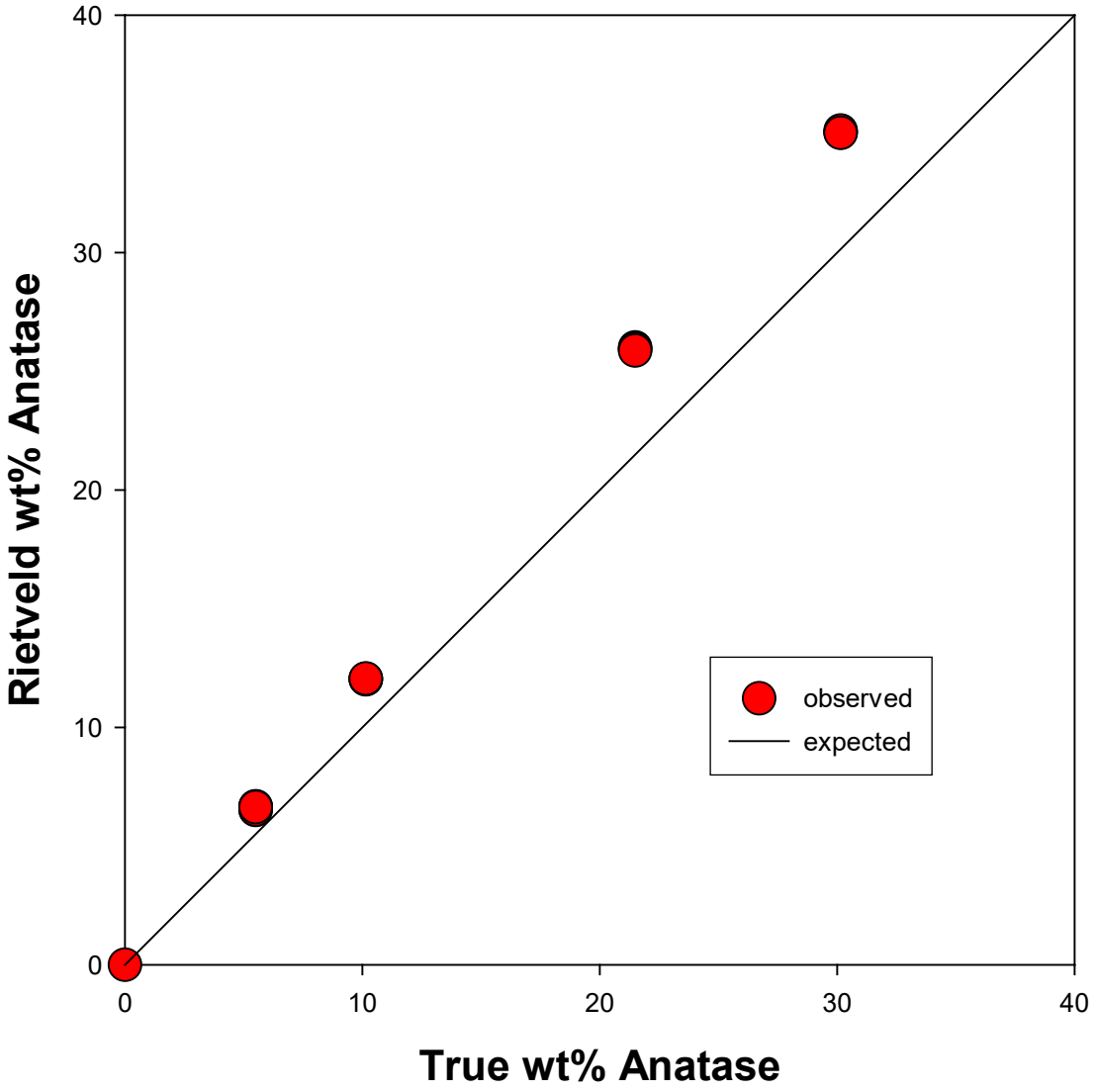

What's wrong?
Microabsorption??

Microabsorption

G. W. Brindley, *Phil. Mag.*, **36**(7), 347-369 (1945)

The ideal ratio $I_{(hkl)\alpha}/I_{(hkl)'\beta}$ is multiplied by a factor:

$$K = \frac{\tau_\alpha}{\tau_\beta} = \frac{V_\beta \int_0^{V_\alpha} e^{-\left(\mu_\alpha - \bar{\mu}\right)x} dx}{V_\alpha \int_0^{V_\beta} e^{-\left(\mu_\beta - \bar{\mu}\right)x} dx}$$

Particle Size Distributions

Anatase

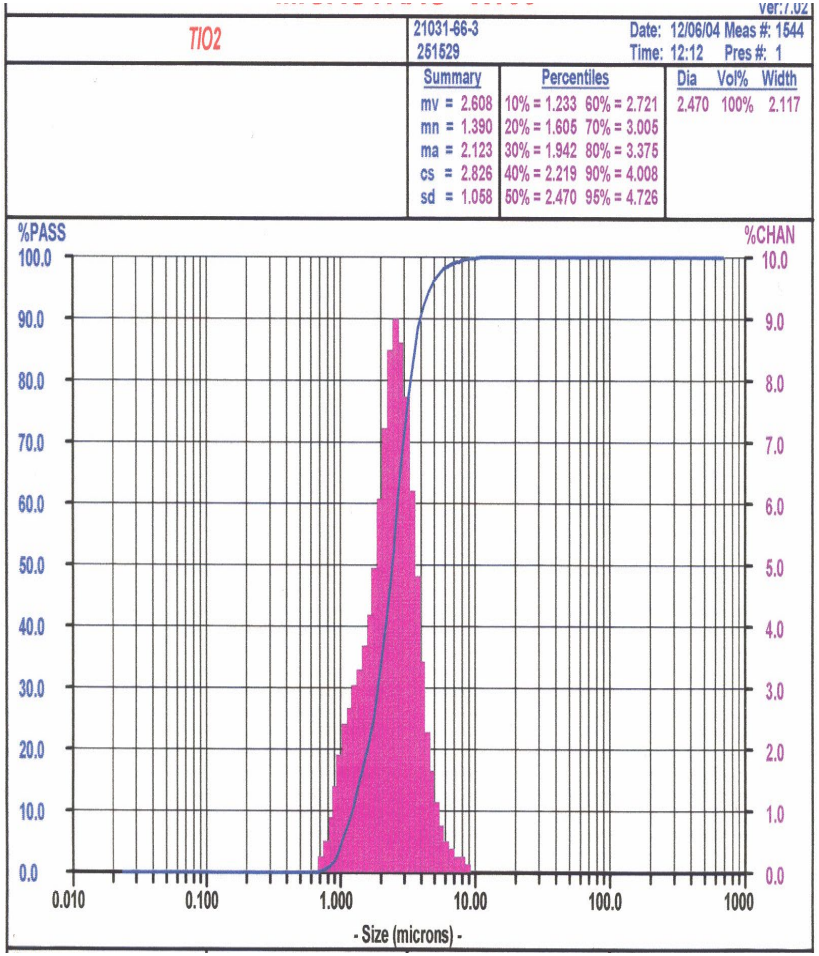

Rutile

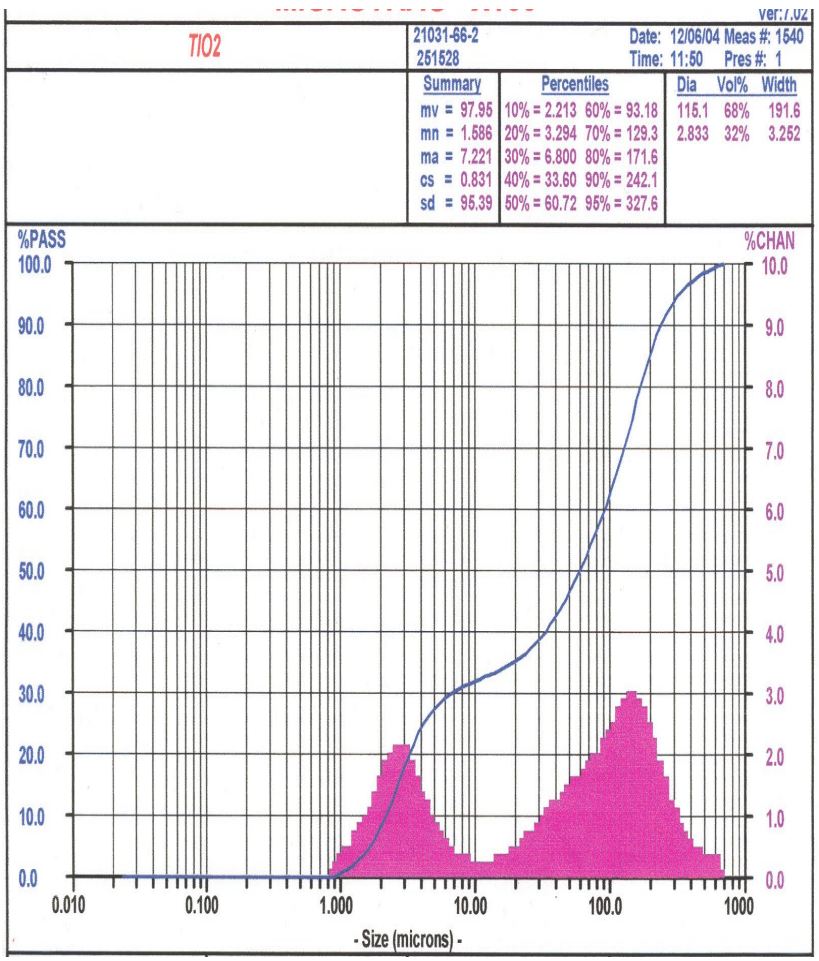

How big might the effect be? Consider the 30.15/69.85 wt% anatase/rutile mixture ($\mu = 520.6\ cm^{-1}$).

Phase	Anatase	Rutile
μ/ρ, cm^2/g	125.7	125.7
ρ, g/cm^3	3.893	4.250
μ, cm^{-1}	489.4	534.2
$\mu - \mu_{avg}$, cm^{-1}	-31.2	+13.6
D, μm	3	150
μD	0.147	8.01
Size	Coarse powder	Very coarse powder!

The correction factor is

$$\frac{\tau_A}{\tau_R} = \frac{1.014}{0.75} = 1.35$$

so the anatase concentrations should be 35% too high. But only 2/3 of the rutile is “large”, so they should be only 23% too high.

Correct the problem by micronising the mixtures:

QPA of Anatase/Rutile Mixtures

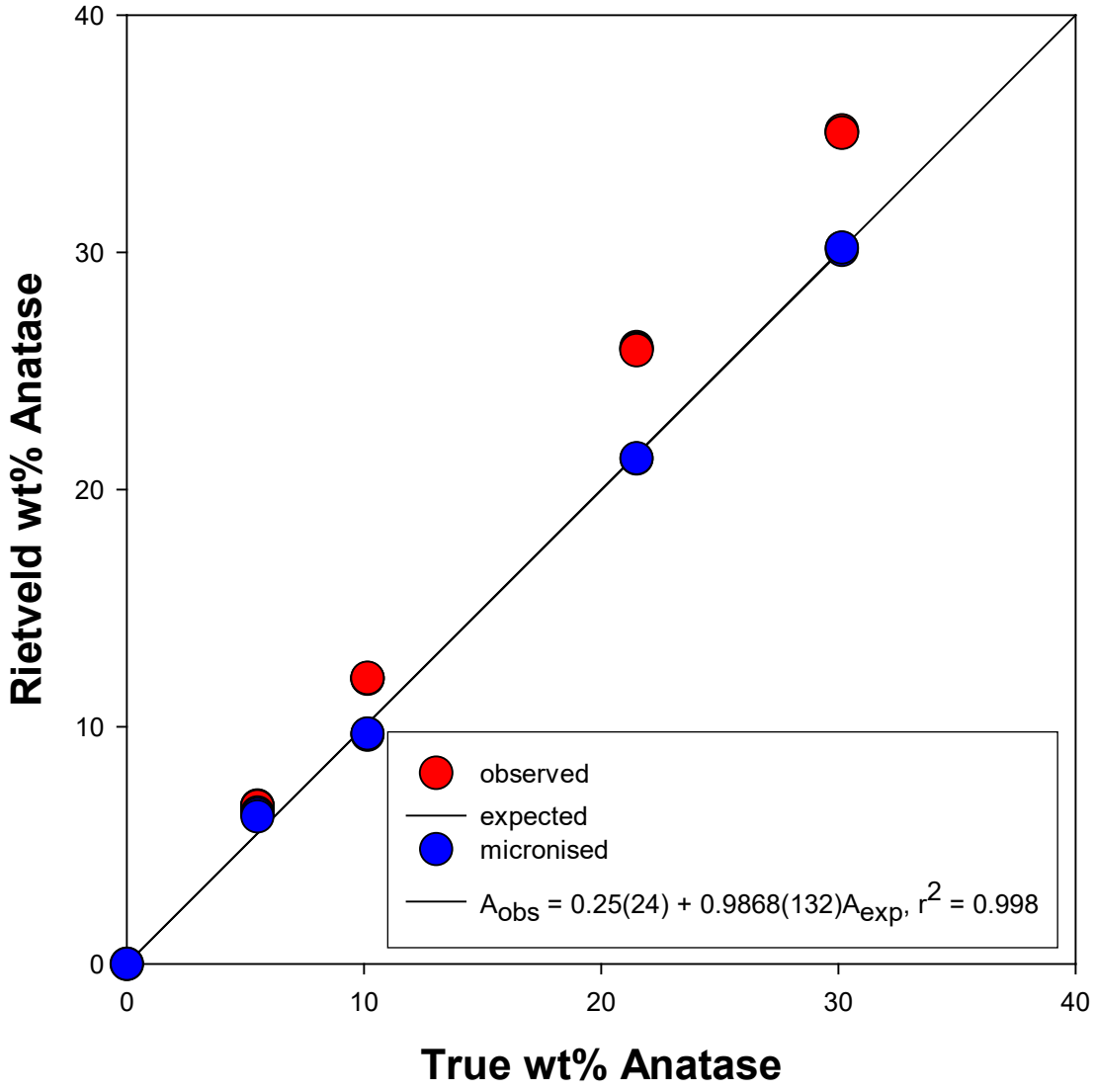

Quantitative Analysis of Micronised Anatase/Rutile Mixtures

Sample #	True wt% anatase	Filename	anatase, wt%	average wt% anatase	accuracy abs. wt%
21031-67-1	5.51	BHAT232 BHAT233 BHAT234	6.38(7) 6.31(7) 6.21(7)	6.30(8)	+0.79
21067-67-2	10.15	BHAT229 BHAT230 BHAT231	9.70(6) 9.65(6) 9.71(6)	9.69(3)	-0.46
21067-67-3	21.49	BHAT226 BHAT227	21.30(6) 21.32(7)	21.31(1)	-0.18
21067-67-4	30.15	BHAT223 BHAT224 BHAT225	30.19(6) 30.09(6) 30.20(6)	30.16(6)	0.01

Microabsorption Effects in Real Catalysts

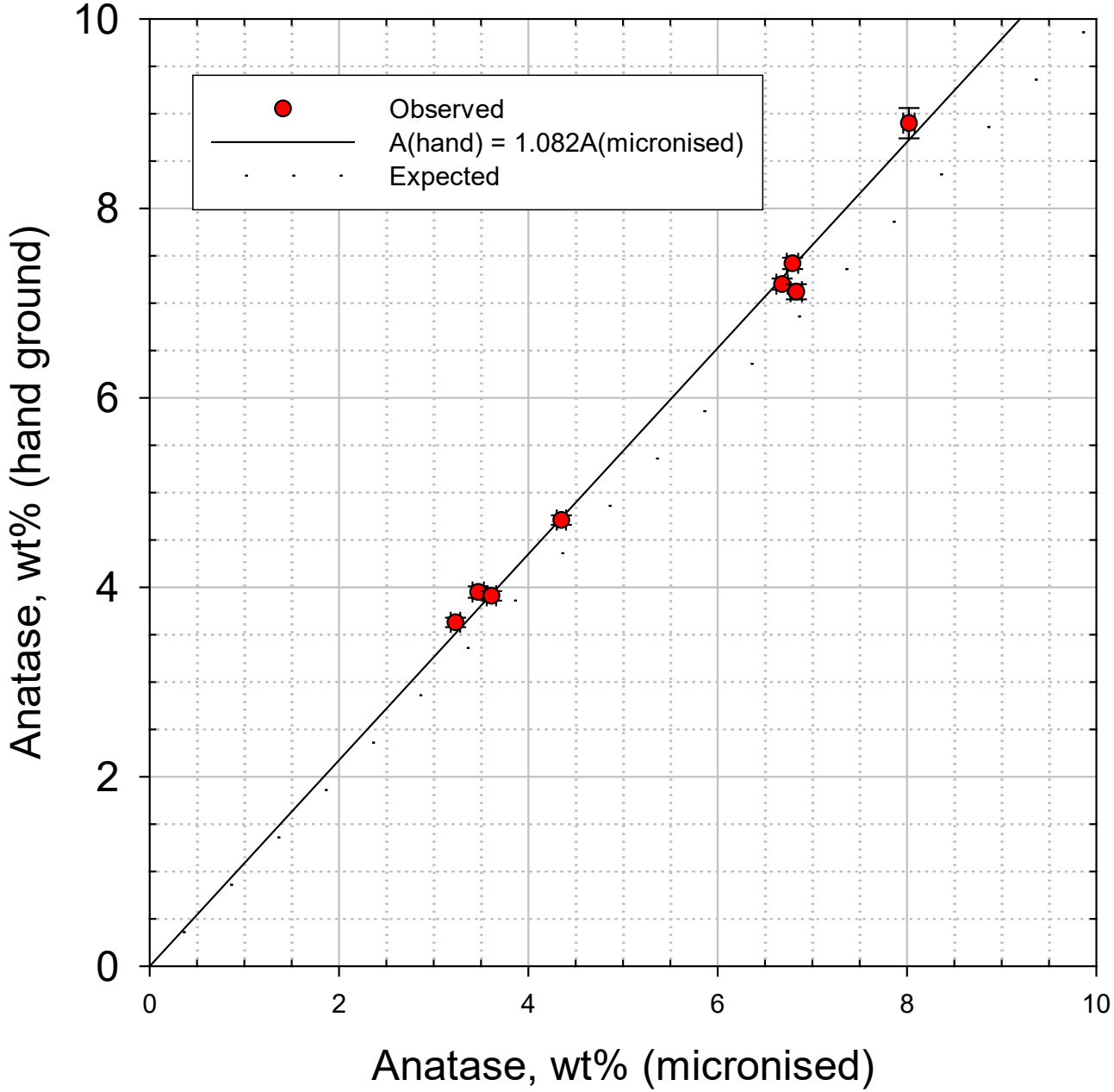

The Effect of Signal/Noise on Quantitative Analysis

Fairfield County Fuel Deposit

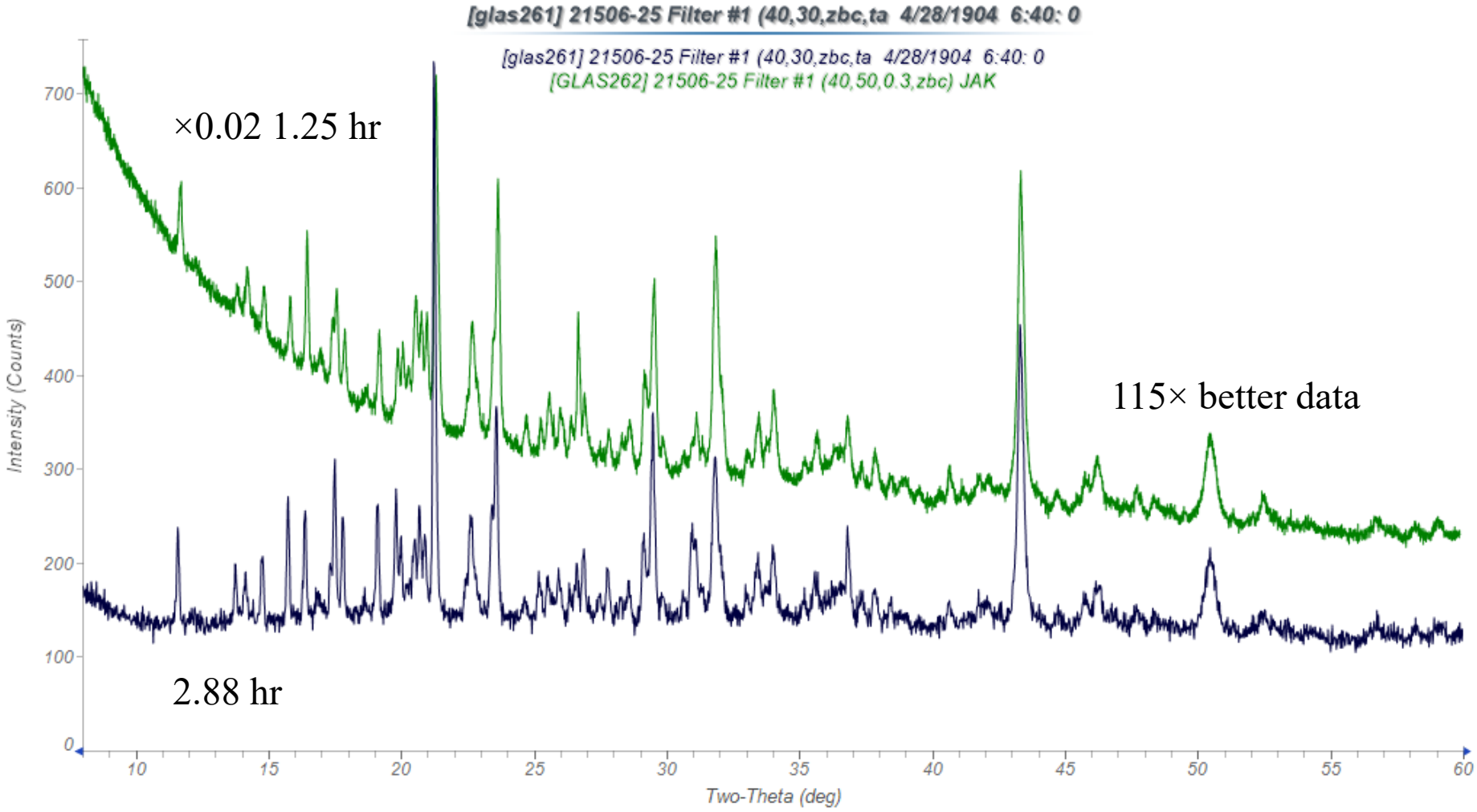

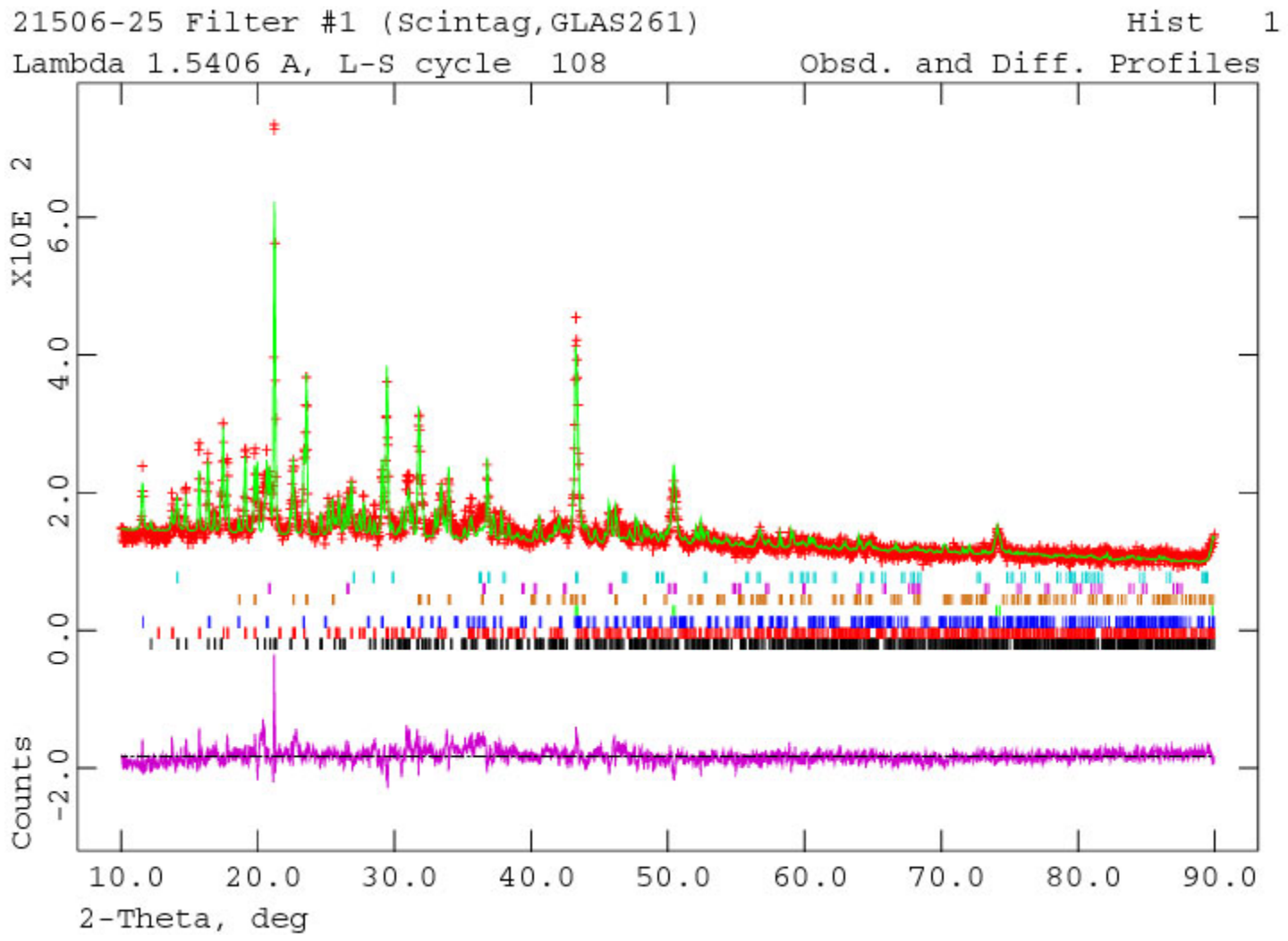
21506-25 Filter #1 (Scintag,GLAS261)
Hist 1
Lambda 1.5406 A, L-S cycle 108
Obsd. and Diff. Profiles
X10E 2
6.0
4.0
2.0
0.0
-2.0
Counts
10.0
20.0
30.0
40.0
50.0
60.0
70.0
80.0
90.0
2-Theta, deg

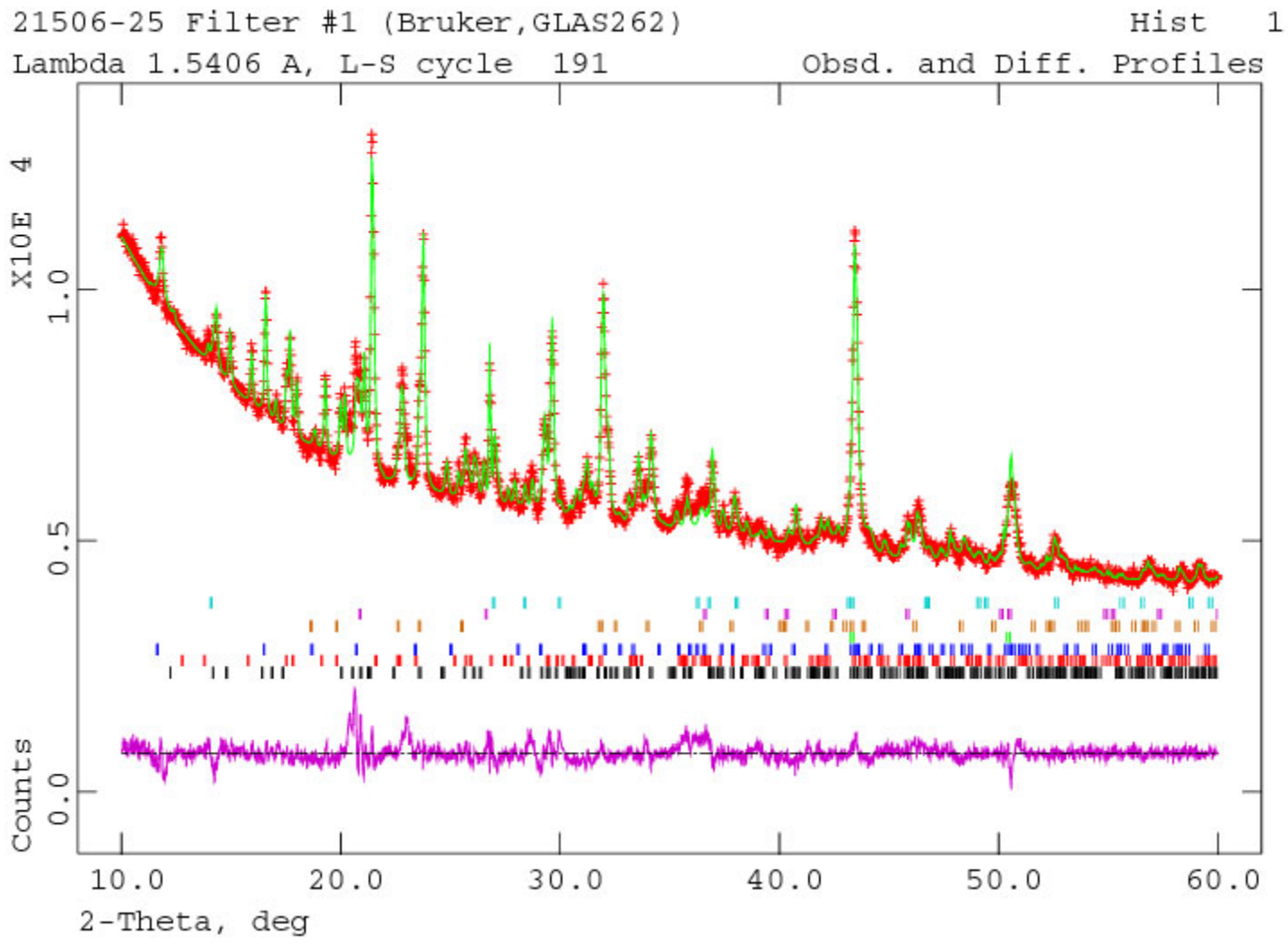
21506-25 Filter #1 (Bruker,GLAS262)
Hist 1
Lambda 1.5406 A, L-S cycle 191
Obsd. and Diff. Profiles
X10E 4
1.0
0.5
Counts
0.0
10.0
20.0
30.0
40.0
50.0
60.0
2-Theta, deg

Fairfield County Fuel Deposits

Sample #21506-25	Filter #1	Filter #2
Filename	GLAS262	GLAS263
mohrite, $(NH_4)_2Cu(SO_4)_2(H_2O)_6$, wt%	29.2(1)	24.1(3)
Na_2SO_4-III, wt%	21.1(2)	31.4(2)
lecontite, $(NH_4)NaSO_4(H_2O)_2$, wt%	18.9(2)	4.5(4)
mascagnite, $(NH_4)_2SO_4$, wt%	8.1(2)	19.0(2)
gypsum, $CaSO_4(H_2O)_2$, wt%	6.0(1)	-
copper, Cu, wt%	11.9(1)	13.1(1)
lepidocrocite, γ-FeOOH, wt%	2.3(1)	2.4(1)
quartz, SiO_2, wt%	2.5(1)	5.3(1)

Changes during Specimen Preparation

Plaster Scratch Coat

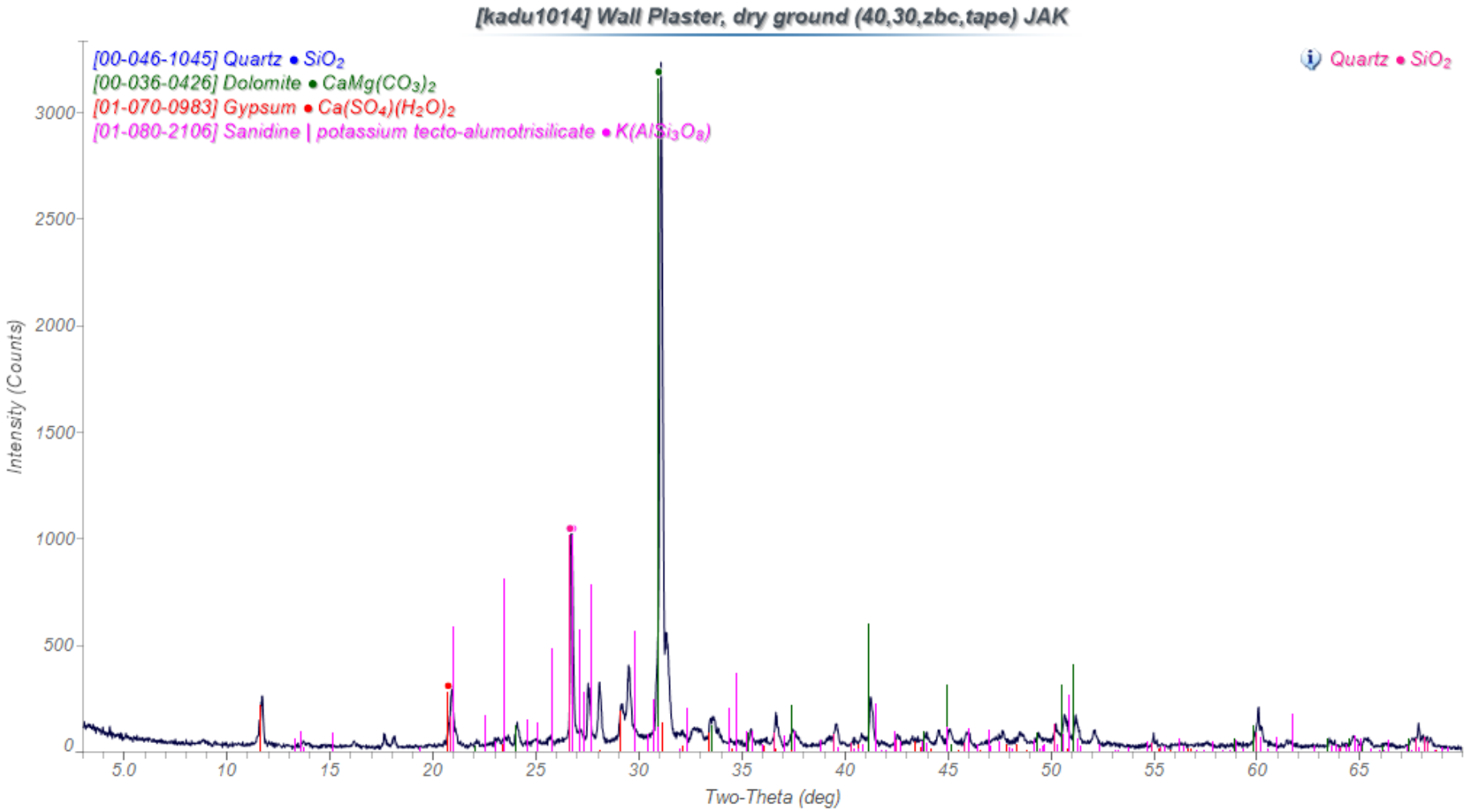
[kadu1014] Wall Plaster, dry ground (40,30,zbc,tape) JAK
[00-046-1045] Quartz • SiO2
[00-036-0426] Dolomite • CaMg(CO3)2
[01-070-0983] Gypsum • Ca(SO4)(H2O)2
[01-080-2106] Sanidine | potassium tecto-alumotrisilicate • K(AlSi3O8)
Quartz • SiO2
Intensity (Counts)
3000
2500
2000
1500
1000
500
0
5.0
10
15
20
25
30
35
40
45
50
55
60
65
Two-Theta (deg)

The data and sample look/feel granular, so micronise the sample…

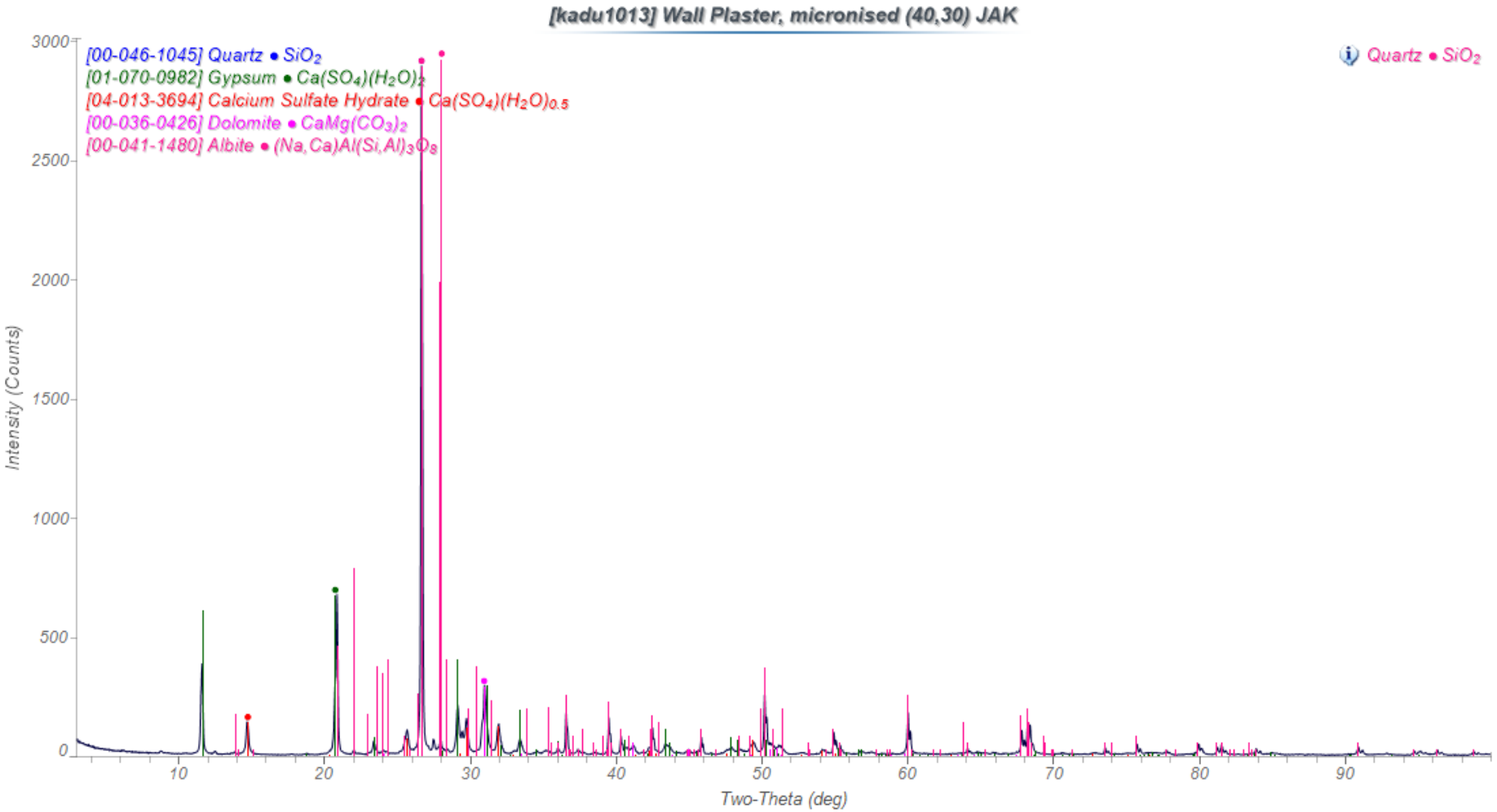
[kadu1013] Wall Plaster, micronised (40,30) JAK
[00-046-1045] Quartz • SiO2
[01-070-0982] Gypsum • Ca(SO4)(H2O)2
[04-013-3694] Calcium Sulfate Hydrate • Ca(SO4)(H2O)0.5
[00-036-0426] Dolomite • CaMg(CO3)2
[00-041-1480] Albite • (Na,Ca)Al(Si,Al)3O8
Quartz • SiO2
Intensity (Counts)
3000
2500
2000
1500
1000
500
0
10
20
30
40
50
60
70
80
90
Two-Theta (deg)

Carry out a Rietveld refinement

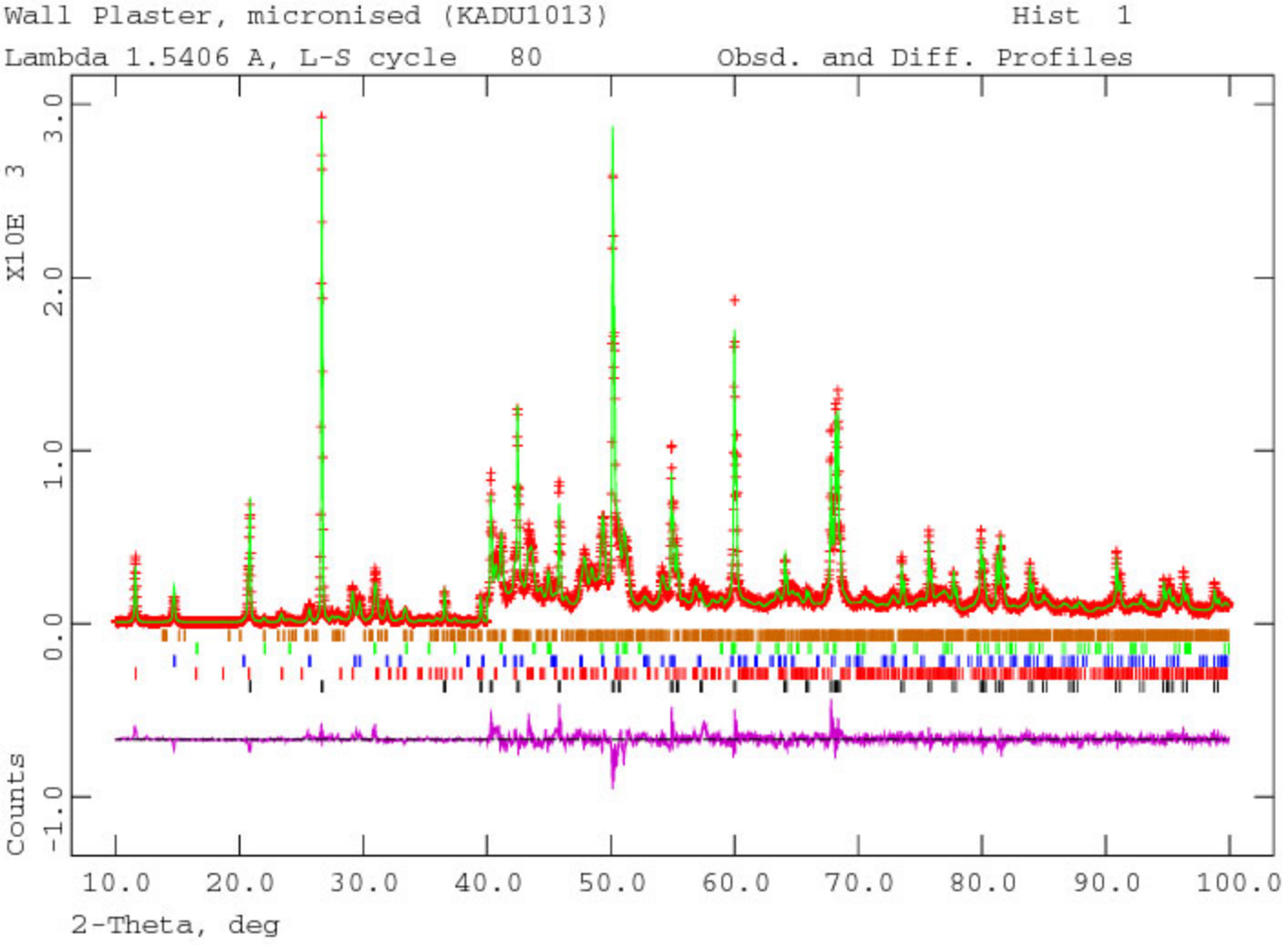

Quantitative Phase Analysis

Name	Formula	Concentration, wt%
Quartz	SiO_2	48.0(2)
Gypsum	$CaSO_4(H_2O)_2$	22.8(2)
Bassanite	$CaSO_4(H_2O)_{0.5}$	12.0(1)
Dolomite	$CaMg(CO_3)_2$	9.3(2)
Albite	$(Na,Ca)(Si,Al)_4O_8$	7.9(2)

But the bassanite was not present in the original sample!

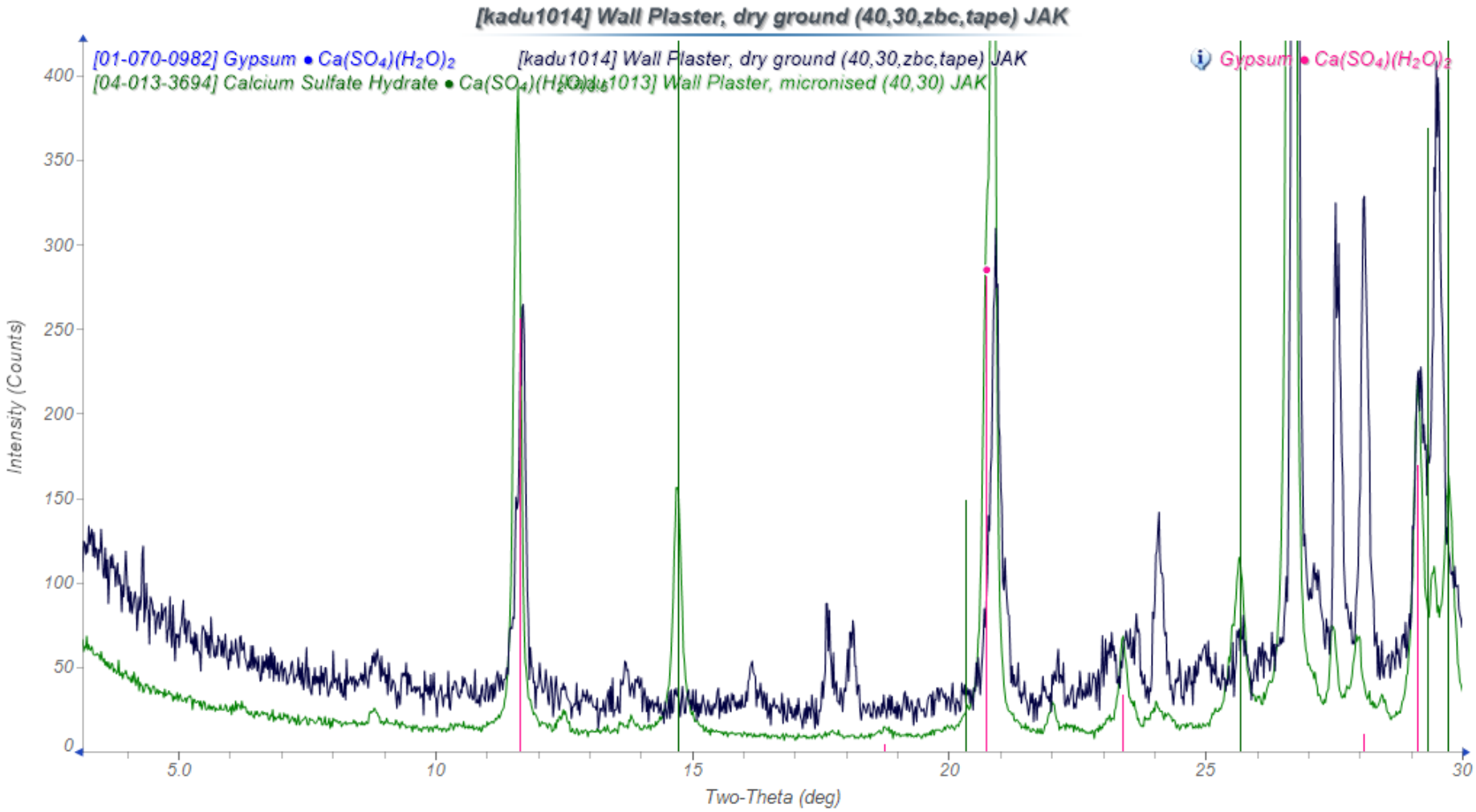
[kadu1014] Wall Plaster, dry ground (40,30,zbc,tape) JAK
[01-070-0982] Gypsum • Ca(SO4)(H2O)2
[04-013-3694] Calcium Sulfate Hydrate • Ca(SO4)(H2O)0.6
[kadu1014] Wall Plaster, dry ground (40,30,zbc,tape) JAK
[kadu1013] Wall Plaster, micronised (40,30) JAK
Gypsum • Ca(SO4)(H2O)2
Intensity (Counts)
Two-Theta (deg)
0
50
100
150
200
250
300
350
400
5.0
10
15
20
25
30

When heated in air, gypsum is converted slowly to the (metastable) hemihydrate at about 70°C or below, and rapidly at 90°C and above…

W. A. Deere, R. A. Howie, and J. Zussman,

An Introduction to the Rock-Forming Minerals,

2nd Edition (1992), p. 614.

3rd edition (2013)

Renormalize the concentrations:

Name	Formula	Concentration, wt%
Quartz	SiO_2	47.0(2)
Gypsum	$CaSO_4(H_2O)_2$	36.2(3)
Dolomite	$CaMg(CO_3)_2$	9.1(2)
Albite	$(Na,Ca)(Si,Al)_4O_8$	7.7(2)

The finish coat plaster is different

(dry the slurry at ambient conditions!)

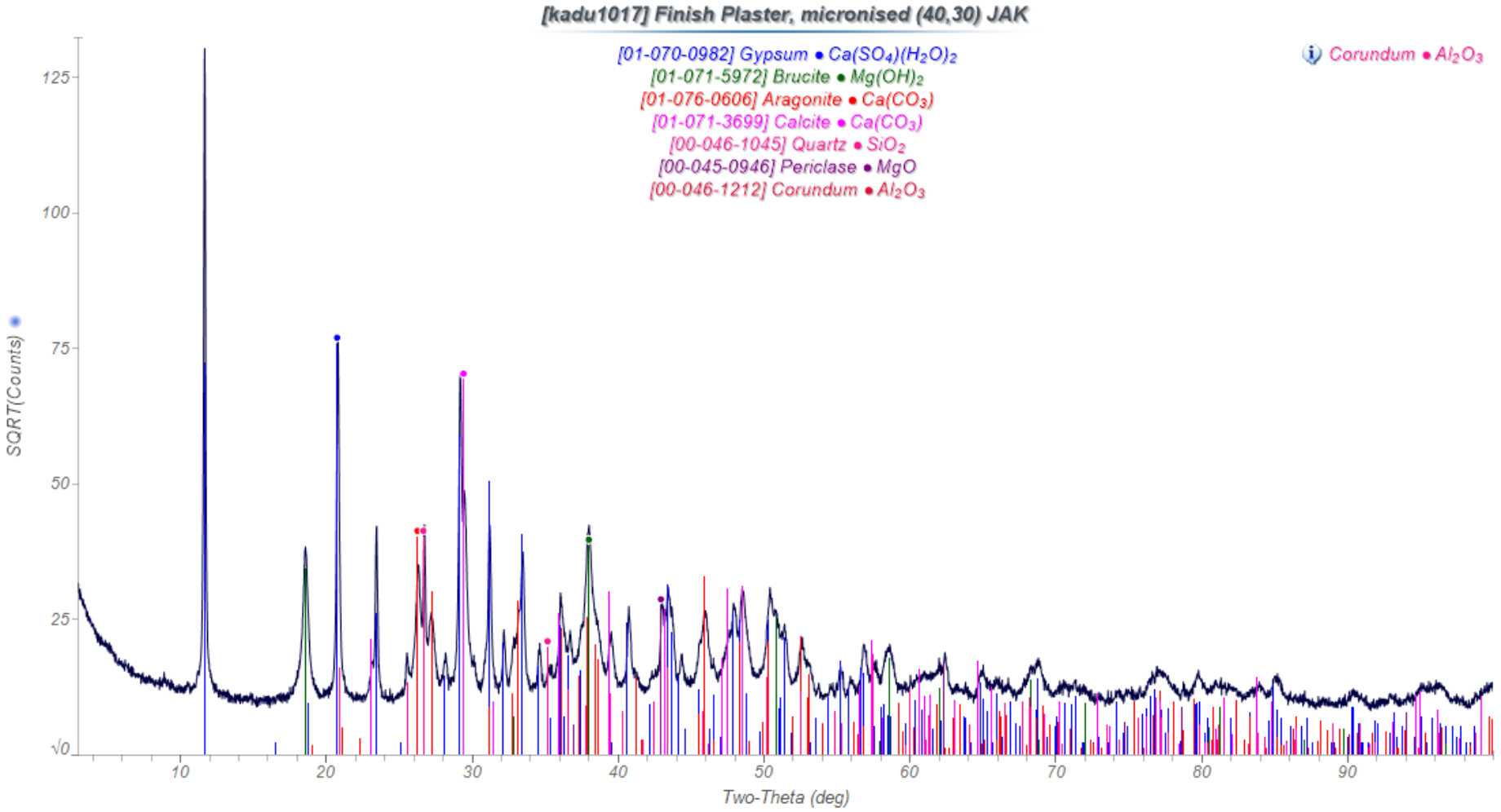

QPA of Finish Coat Plaster

Mineral	Formula	Concentration, wt%
Gypsum	$CaSO_4(H_2O)_2$	34.2(2)
Brucite	$Mg(OH)_2$	19.3(1)
Aragonite	$CaCO_3$	26.0(2)
Calcite	$CaCO_3$	13.0(1)
Quartz	SiO_2	3.09(6)
Periclase	MgO	2.12(8)
Corundum (!)	Al_2O_3	2.3(1)

Accuracy in Quantitative Phase Analysis

IUCr CPD QPA Round Robin

Sample	Data Source	Al_2O_3 wt%	CaF_2 wt%	ZnO wt%		Sample	Data Source	Al_2O_3 wt%	CaF_2 wt%	ZnO wt%
1A	Amoco	1.1(1)	95.0(3)	3.86(7)		1E	Amoco	56.2(3)	29.0(1)	14.8(1)
	CPD	1.3(2)	94.2(6)	4.5(1)			CPD	55.4(2)	29.7(1)	14.9(1)
	Weight	1.15	94.81	4.04			Weight	55.12	29.62	15.25
	XRF	1.22	94.11	4.12			XRF	55.79	29.39	15.34
1B	Amoco	94.0(4)	4.37(8)	1.58(4)		1F	Amoco	28.4(4)	18.0(2)	53.6(2)
	CPD	94.1(3)	4.37(6)	1.53(3)			CPD	27.6(2)	18.0(1)	54.3(2)
	Weight	94.31	4.33	1.36			Weight	27.06	17.72	55.22
	XRF	94.73	4.32	1.38			XRF	27.32	17.44	54.88
1C	Amoco	7.1(5)	1.5(2)	91.4(5)		1G	Amoco	32.9(3)	33.9(2)	33.2(2)
	CPD	6.1(3)	1.47(9)	92.5(3)			CPD	31.8(2)	34.5(2)	33.7(1)
	Weight	5.04	1.36	93.59			Weight	31.37	34.42	34.21
	XRF	5.12	1.33	93.15			XRF	31.70	33.86	34.01
1D	Amoco	14.1(2)	53.8(2)	32.1(2)		1H	Amoco	36.3(3)	34.3(2)	29.4(2)
	CPD	14.1(1)	53.5(2)	32.4(1)			CPD	35.2(2)	35.1(2)	29.7(1)
	Weight	13.53	53.58	32.89			Weight	35.12	34.69	30.19
	XRF	13.80	52.99	32.98			XRF	35.35	34.26	30.03

CPD Rietveld QPA Round Robin
Sample 1 Series
Amoco Results

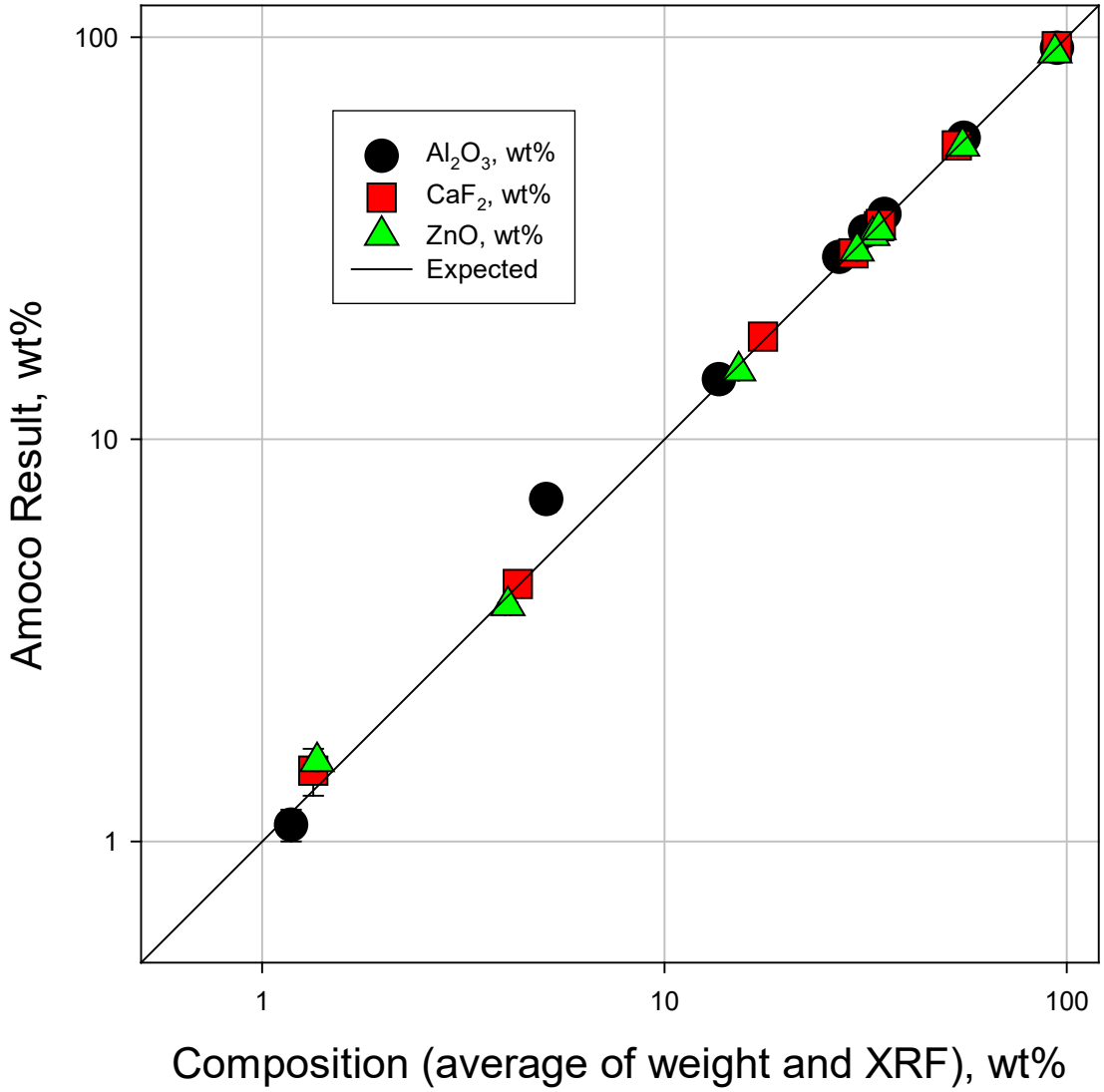

Errors in Concentrations

Absolute

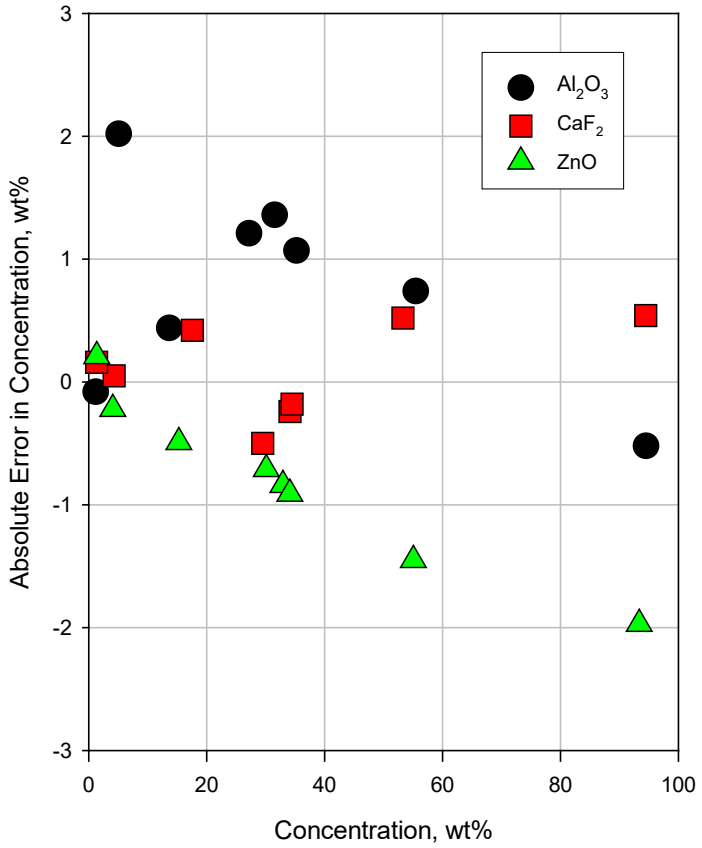

Relative

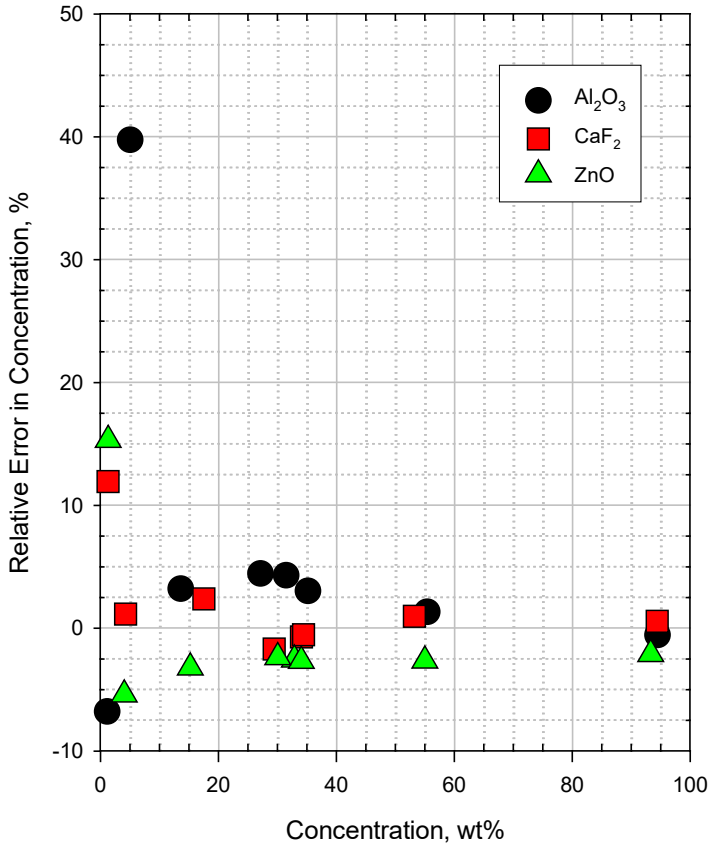

"Outcomes of the International Union of Crystallography Commission on Powder Diffraction Round Robin on Quantitative Phase Analysis: Samples 1a to 1h," I. C. Madsen, N. V. Y. Scarlett, L. M. D. Cranswick, and T. Lwin, *J. Applied Cryst.*, **34**, 409-426 (2001).

Sample 2 – Preferred Orientation

Phase	Corundum	Fluorite	Zincite	Brucite
Weight	21.27	22.53	19.94	36.26
All data	21.8(26)	22.1(28)	19.6(52)	36.5(73)
σ_{rel}, %	12	13	26	20
My results	23.2(2)	22.1(1)	19.4(1)	35.3(4)

AKLD = 0.019 (4^{th}-order spherical harmonics for brucite)
Absolute Kullback-Liebler Distance

$$KLD = 0.01 \times wt\%_{true} \times \ln\left(\frac{wt\%_{true}}{wt\%_{measured}}\right)$$

$$AKLD = \sum_{i-1}^{n} \left| KLD_i \right|$$

Sample 3 – Amorphous Content

Phase	Corundum	Fluorite	Zincite	Amorphous
Weight	30.79	20.06	19.68	29.47
All data	31.7(37)	19.9(45)	18.5(8)	30.6(21)
σ_{rel}, %	12	23	4	7
My results	29.6(2)	17.6(1)	17.1(1)	35.8

AKLD = 0.123 (added a quartz internal standard)

Sample 4 - Microabsorption

Phase	Corundum	Magnetite	Zircon
Weight	50.46	19.64	29.90
All data	63.6(155)	13.5(148)	22.9(100)
Neutron	51.7(15)	21.6(38)	26.7(47)
My results, raw	60.9(1)	13.6(7)	25.5(2)
My results, corrected	57.9(1)	15.8(7)	26.3(2)

AKLD = 0.149 (corrected)

Synthetic Bauxite

Phase	Anatase	Boehmite	Goethite	Hematite	Quartz	Gibbsite	Kaolinite
Weight	2.00	14.93	9.98	10.00	5.16	54.90	3.02
All data	3.0(4)	20.3(22)	13.9(33)	14.6(47)	7.0(12)	37.6(66)	3.9(20)
σ_{rel}, %	13	11	24	32	17	18	51
My results	2.6(1)	17.3(2)	11.2(1)	10.0(1)	5.2(1)	49.3(2)	4.5(3)

$AKLD = 0.110$

2nd-order spherical harmonic preferred orientation correction on for gibbsite

Natural Granodiorite

Phase	Quartz	ΣFeldspars	Biotite	Clinochlore	Hornblende	Zircon
All data	31(6)	56	9(4)	2(1)	1.6(13)	0.06(18)
My results	44	50	4	Trace	2	-

Pharmaceutical 1

Phase	β-D-mannitol	Sucrose	DL-valine	Nizatidine
Weight	45.9	35.0	10.0	10.0
"all data"	40.4(73)	32.6(26)	15.2(139)	11.6(93)
My results	38.4(4)	28.3(4)	17.8(6)	15.4(6)

A look at this sample under an optical microscope (good advice for any analyst – and advice which should probably be included in the paper!) was enough to scare anyone away from it. It contained large grains, and some really platy material. Even after micronising for 10 minutes using hexane as the milling liquid, preferred orientation was significant for mannitol and valine. The micronising added significant strain broadening to the profiles.

Pharmaceutical 2

Phase	β-D-mannitol	Sucrose	DL-valine	Nizatidine	Amorphous starch
Weight	20.0	15.0	20.0	15.0	30.0
Analysis #3	19.4	19.9	20.4	7.4	32.9
My results	27.0(4)	17.4(4)	20.7(6)	17.3(4)	17.6

This sample also had to be micronised – even after blending with the quartz internal standard. I collected the pattern relatively quickly, and a simple 3-term cosine Fourier series appeared to describe the background adequately. I suspect that better counting statistics would require the use of a real space pair correlation function, and would result in better quantification of the amorphous material. The ratios of the crystalline phases are actually not too bad.

IUCr CPD Round Robin on Quantitative Phase Analysis

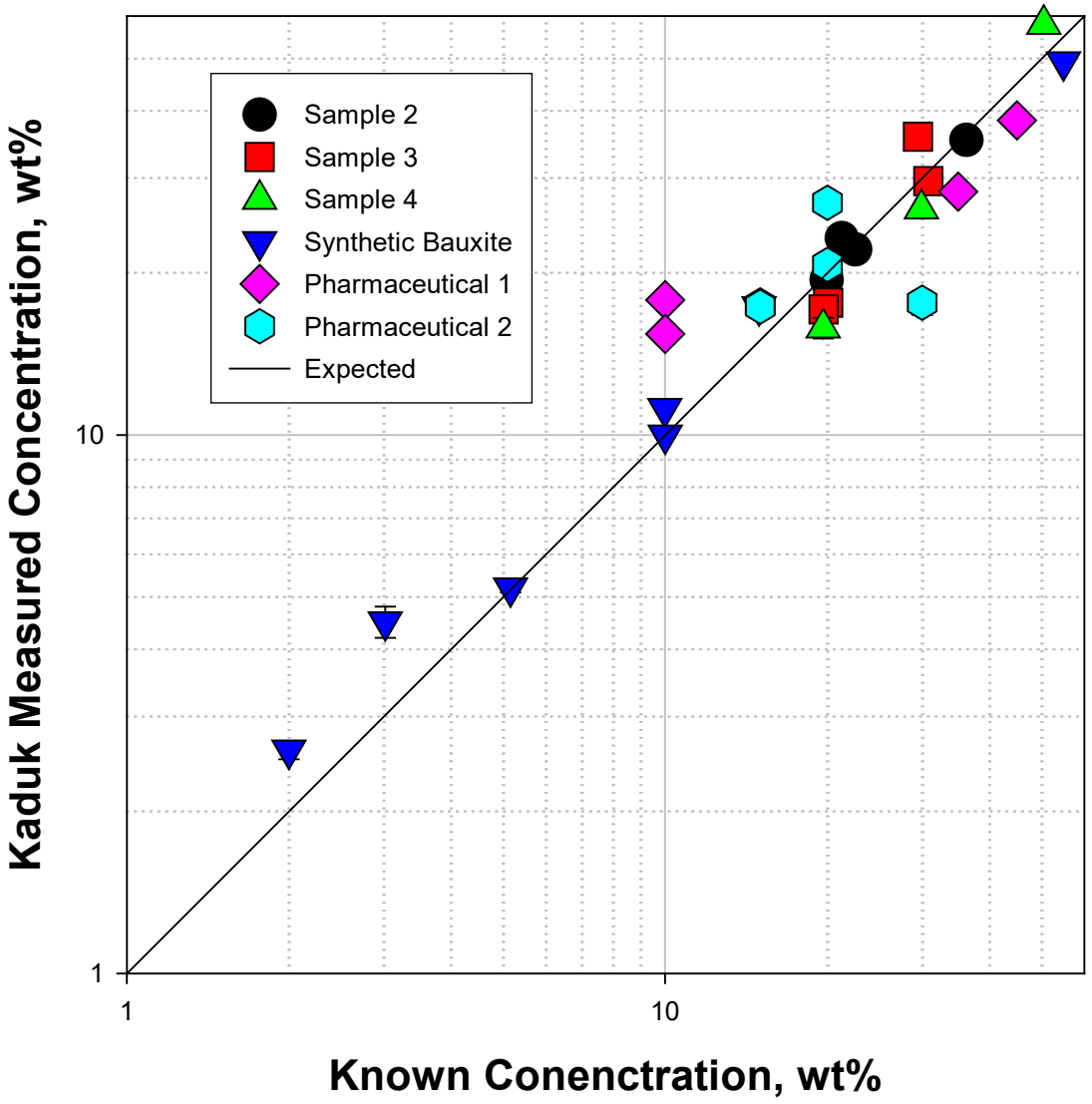

"Outcomes of the International Union of Crystallography Commission on Powder Diffraction Round Robin on Quantitative Phase Analysis: samples 2, 3, 4, synthetic bauxite, natural granodiorite and pharmaceuticals," N. V. Y. Scarlett, I. C. Madsen, L. M. D. Cranswick, T. Lwin, E. Groleau, G. Stephenson, M. Aylmore, and N. Agron-Olshina, *J. Applied Cryst.*, **35**, 383-400 (2002).

Accuracy in Rietveld quantitative phase analysis of Portland cements

G. De la Torre and M. A. G. Aranda,

J. Appl. Cryst., **36**(5), 1169-1176 (2003).

Concentration Errors in Synthetic Portland Cements

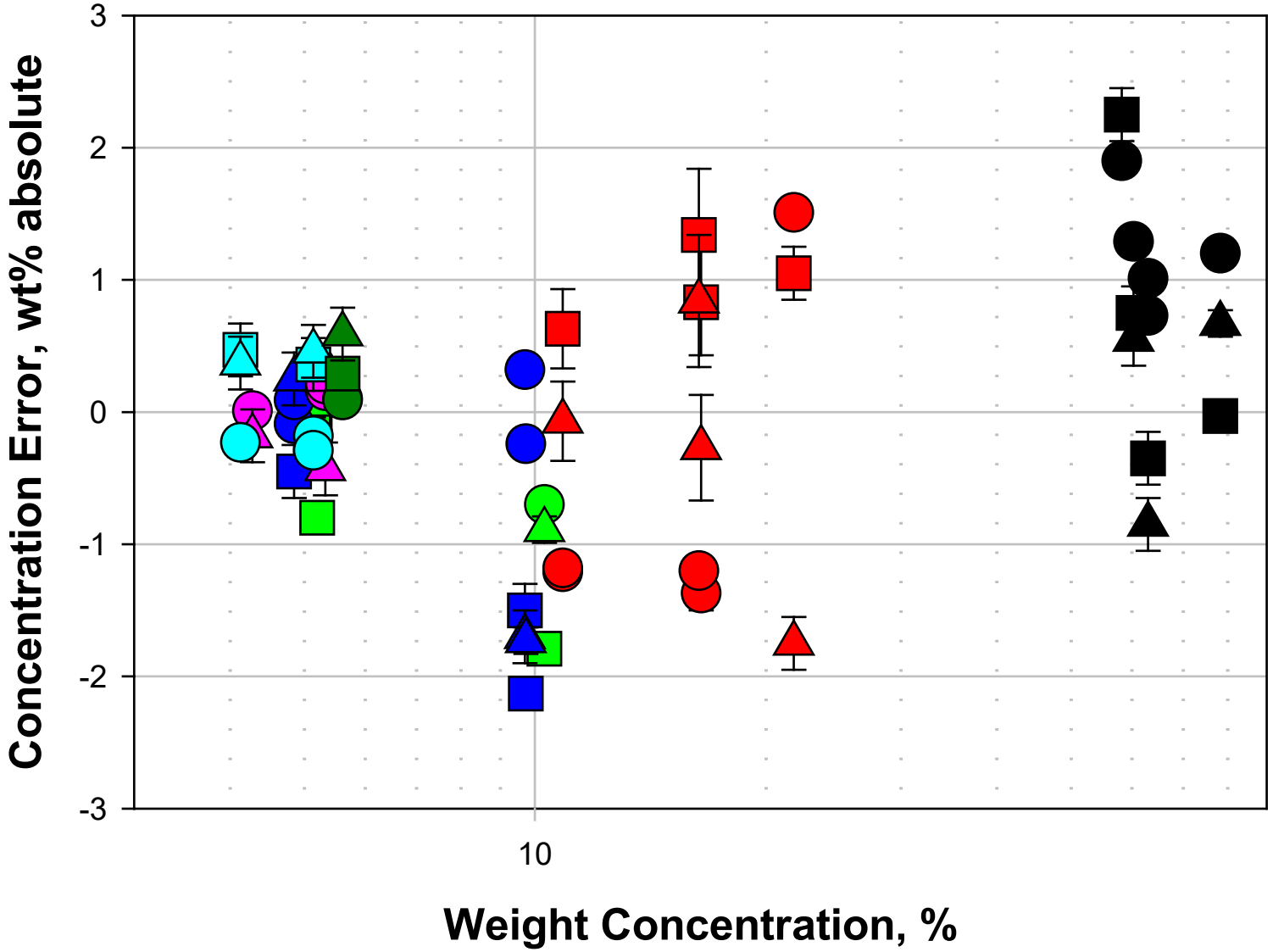

Accuracy in Rietveld quantitative phase analysis: a comparative study of strictly monochromatic Mo and Cu radiation, L. León-Reina, M. Garcia-Maté, G. Alvarez-Pinazo, I. Santacruz, O. Vallcorba, A. G. De la Torre, and M. A. G. Aranda, *J. Appl. Crystallogr.*, **49** (2016); http://dx.doi.org/10.1107/S1600576716003873, open access.

International Tables for Crystallography Volume H: Powder Diffraction, Chapter 3.10, pp. 374-384 (2019)

Table 3
Rietveld quantitative phase analyses for the crystalline inorganic mixtures measured with Cu $K\alpha_1$ and Mo $K\alpha_1$ radiations.

Weighed amounts (%Wt) are shown for the sake of comparison (in bold). The AKLDs for each mixture and the KLD values for i-anhydrite are also included.

	CGpQ_0.0A			CGpQ_0.25A			CGpQ_0.50A			CGpQ_1.0A			CGpQ_2.0A			CGpQ_4.0A		
Phases	%Wt	Mo trm	Cu rfl	%Wt	Mo trm	Cu rfl	%Wt	Mo trm	Cu rfl	%Wt	Mo trm	Cu rfl	%Wt	Mo trm	Cu rfl	%Wt	Mo trm	Cu rfl
C	**32.9**	32.6 (1)	30.4 (2)	**32.8**	32.0 (1)	33.6 (1)	**32.7**	33.2 (1)	32.8 (1)	**32.5**	32.8 (1)	32.6 (2)	**32.2**	31.3 (1)	31.4 (1)	**31.6**	31.2 (1)	31.8 (1)
Gp	**31.7**	31.7 (1)	34.5 (1)	**31.7**	32.5 (1)	31.6 (1)	**31.6**	30.1 (1)	30.7 (1)	**31.5**	30.4 (1)	30.7 (1)	**31.1**	32.1 (1)	32.3 (1)	**30.5**	30.7 (1)	30.5 (1)
Q	**34.2**	34.6 (1)	33.7 (1)	**34.1**	33.9 (1)	33.0 (1)	**34.0**	34.6 (1)	34.2 (1)	**33.8**	34.1 (1)	33.8 (1)	**33.5**	33.5 (1)	32.6 (1)	**32.8**	32.8 (1)	32.0 (1)
s-A	**0.8**	0.66 (3)	0.76 (5)	**0.8**	0.77 (4)	0.78 (5)	**0.8**	0.97 (3)	1.15 (5)	**0.8**	1.03 (4)	1.11 (5)	**0.7**	0.54 (3)	0.58 (5)	**0.7**	0.67 (3)	0.77 (4)
$SrSO_4$	**0.4**	0.44 (4)	0.70 (6)	**0.4**	0.44 (4)	0.67 (5)	**0.4**	0.39 (4)	0.56 (5)	**0.4**	0.43 (4)	0.68 (5)	**0.4**	0.48 (4)	0.68 (6)	**0.4**	0.45 (4)	0.63 (5)
i-A	–	–	–	**0.28**	0.42 (3)	0.42 (4)	**0.52**	0.71 (3)	0.71 (4)	**1.02**	1.23 (3)	1.17 (5)	**2.02**	2.05 (4)	2.38 (9)	**4.02**	4.30 (8)	4.33 (9)
AKLD sum		0.0089	0.0605		0.0198	0.0235		0.0295	0.0180		0.0214	0.0152		0.0218	0.0358		0.0095	0.0156
(i-A) KLD					–0.001	–0.001		–0.002	–0.002		–0.002	–0.001		0.000	–0.003		–0.004	–0.003

Table 4
RQPA for the crystalline organic mixtures measured with Cu $K\alpha_1$ and Mo $K\alpha_1$ radiations.

Weighed amounts (%Wt) are shown for the sake of comparison (in bold). The AKLDs for each mixture and the KLD values for xylose are also included.

	GFL_0.0X			GFL_0.25X			GFL_0.50X			GFL_1.0X			GFL_2.0X			GFL_4.0X		
Phases	%Wt	Mo trm	Cu rfl	%Wt	Mo trm	Cu rfl	%Wt	Mo trm	Cu rfl	%Wt	Mo trm	Cu rfl	%Wt	Mo trm	Cu rfl	%Wt	Mo trm	Cu rfl
G	**33.4**	33.8 (1)	33.5 (3)	**33.3**	33.6 (1)	33.1 (2)	**33.2**	32.3 (2)	33.5 (2)	**33.0**	34.7 (1)	33.6 (2)	**32.7**	32.2 (1)	31.5 (2)	**32.0**	32.8 (1)	33.6 (2)
F	**33.5**	31.7 (1)	32.7 (3)	**33.4**	32.3 (1)	34.3 (2)	**33.3**	32.1 (2)	33.4 (2)	**33.1**	32.6 (1)	33.7 (2)	**32.8**	31.7 (1)	34.4 (2)	**32.2**	30.7 (1)	32.5 (2)
L	**33.1**	34.5 (1)	33.7 (3)	**33.0**	33.7 (1)	32.0 (2)	**33.0**	35.0 (3)	32.5 (2)	**32.8**	31.6 (2)	31.4 (2)	**32.5**	34.3 (1)	32.0 (2)	**31.8**	32.9 (1)	30.5 (2)
X	–	–	–	**0.27**	0.33 (4)	0.57 (9)	**0.55**	0.53 (8)	0.61 (9)	**1.1**	1.10 (5)	1.3 (1)	**2.0**	1.76 (5)	2.1 (1)	**3.9**	3.70 (5)	3.4 (2)
AKLD sum		0.0362	0.0150		0.0216	0.0231		0.0410	0.0096		0.0338	0.0280		0.0363	0.0339		0.0361	0.0372
(X) KLD		–	–		–0.001	–0.002		0.000	–0.001		0.000	–0.002		0.003	–0.001		0.002	0.005

The Reynolds Cup

www.clays.org/SocietyAwards/RCIntro.html

An example of organic quantitative phase analysis – cellulose/sucrose mixtures

Sucrose/Cellulose Mixtures

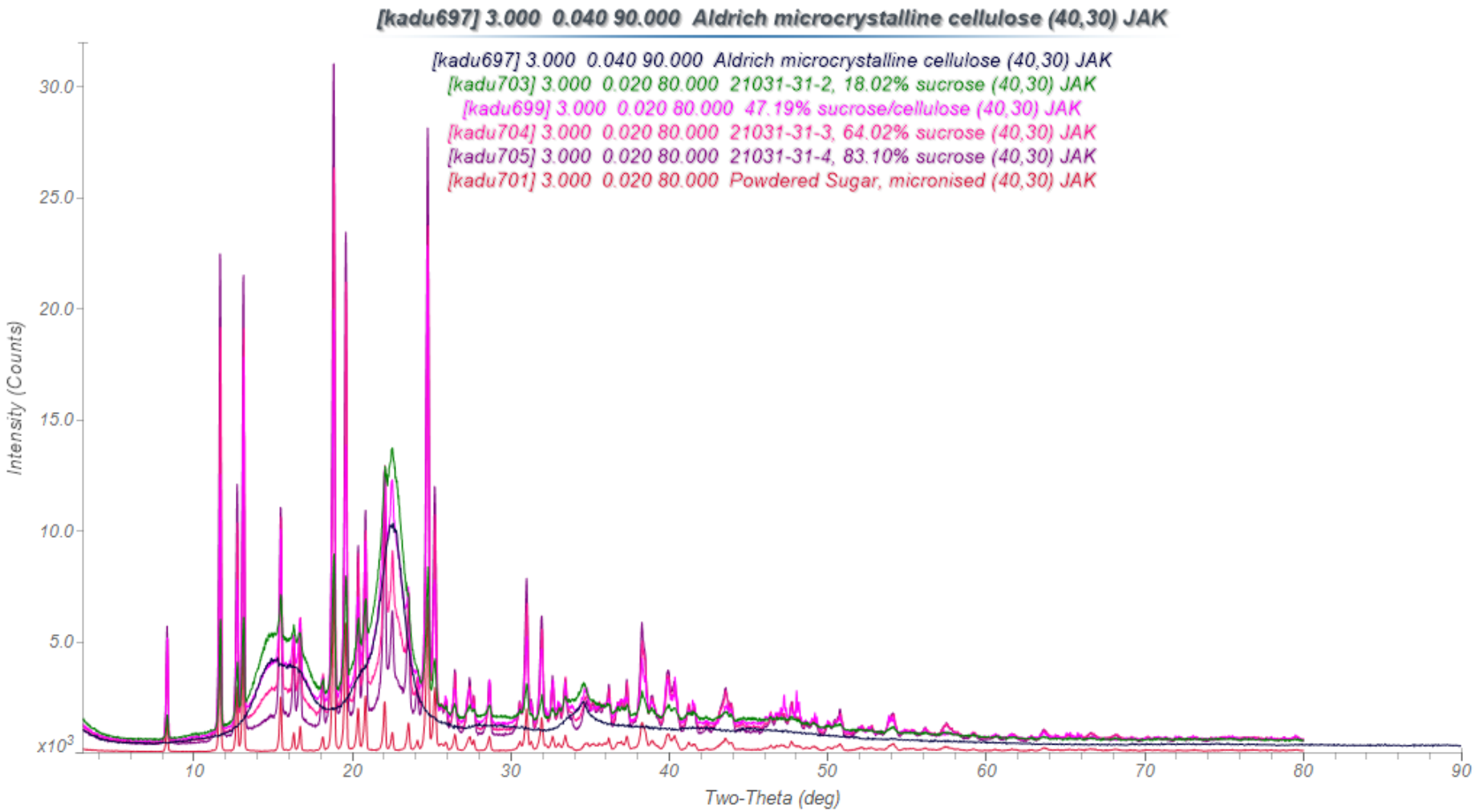

Sucrose/Cellulose Mixtures

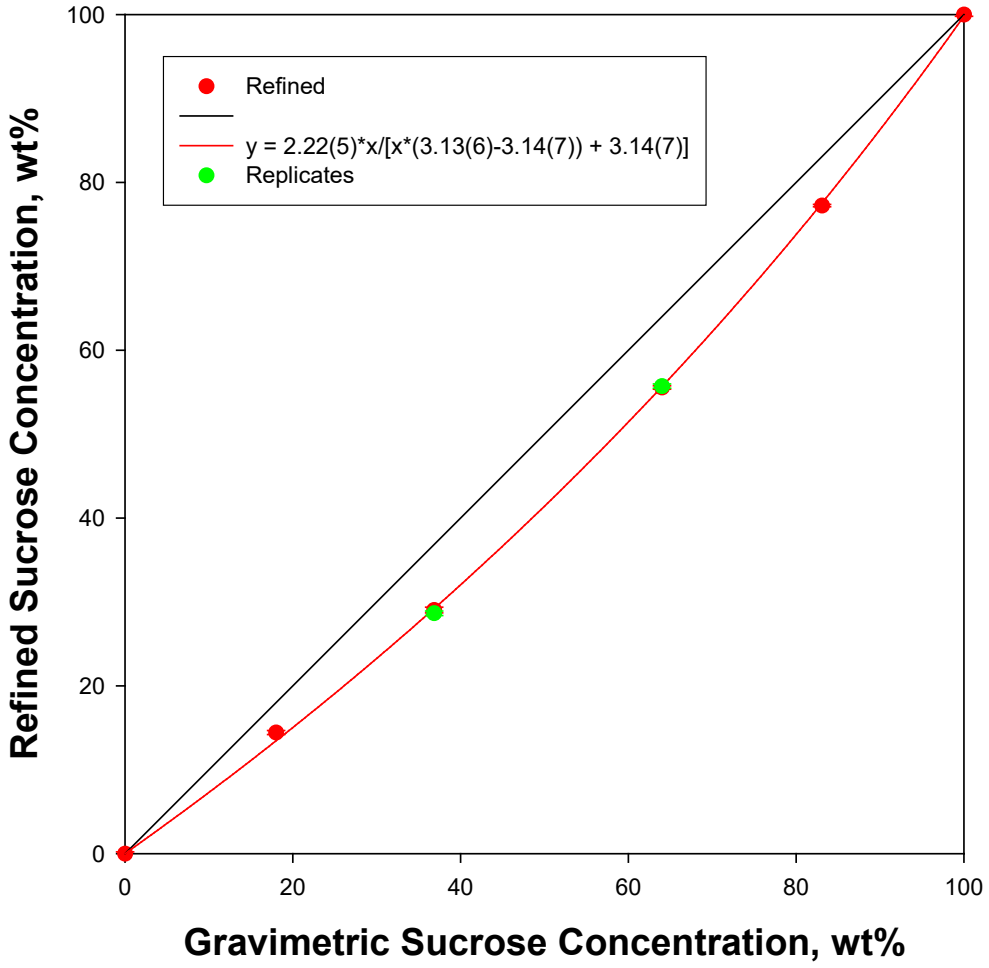

Error in Quantitative Analysis

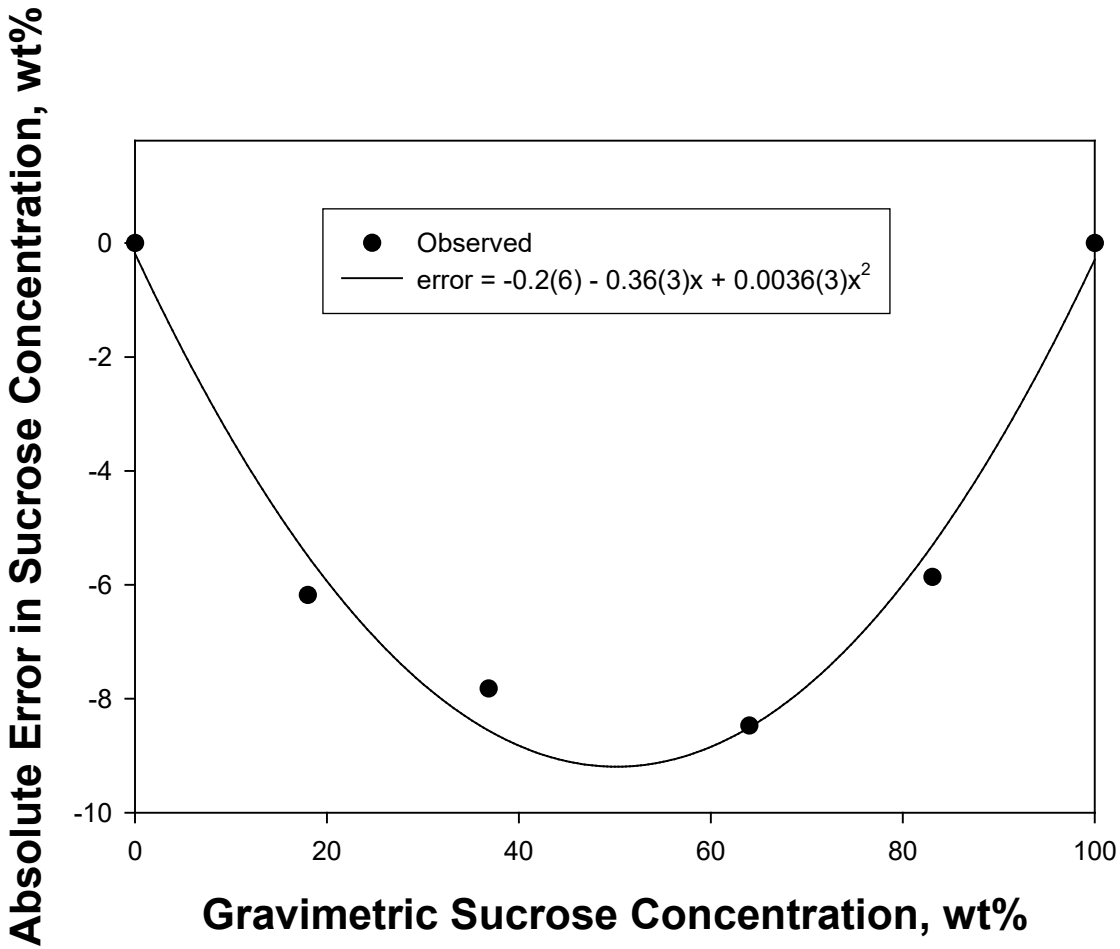

Better Specimen Prep

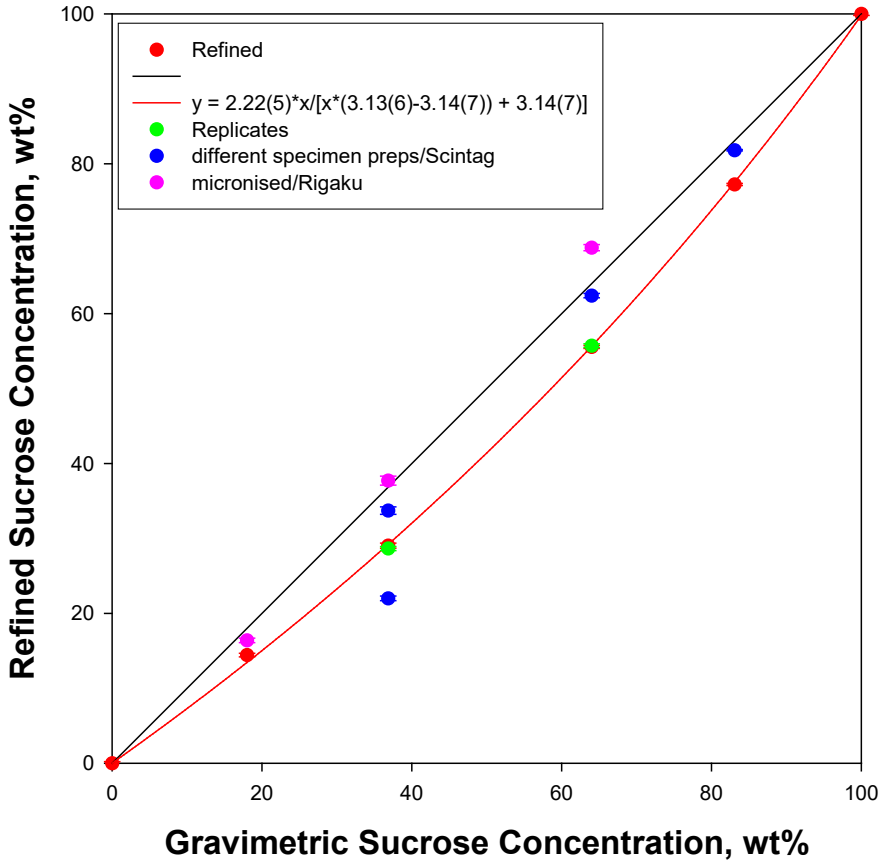

wt% sucrose =
-0.8(17) + 1.01(3)expected

95% confidence limits = ± 3 wt%

Specimen preparation can be especially-critical for organic samples!

Another Example of Organic QPA Duratuss GP 120-1200

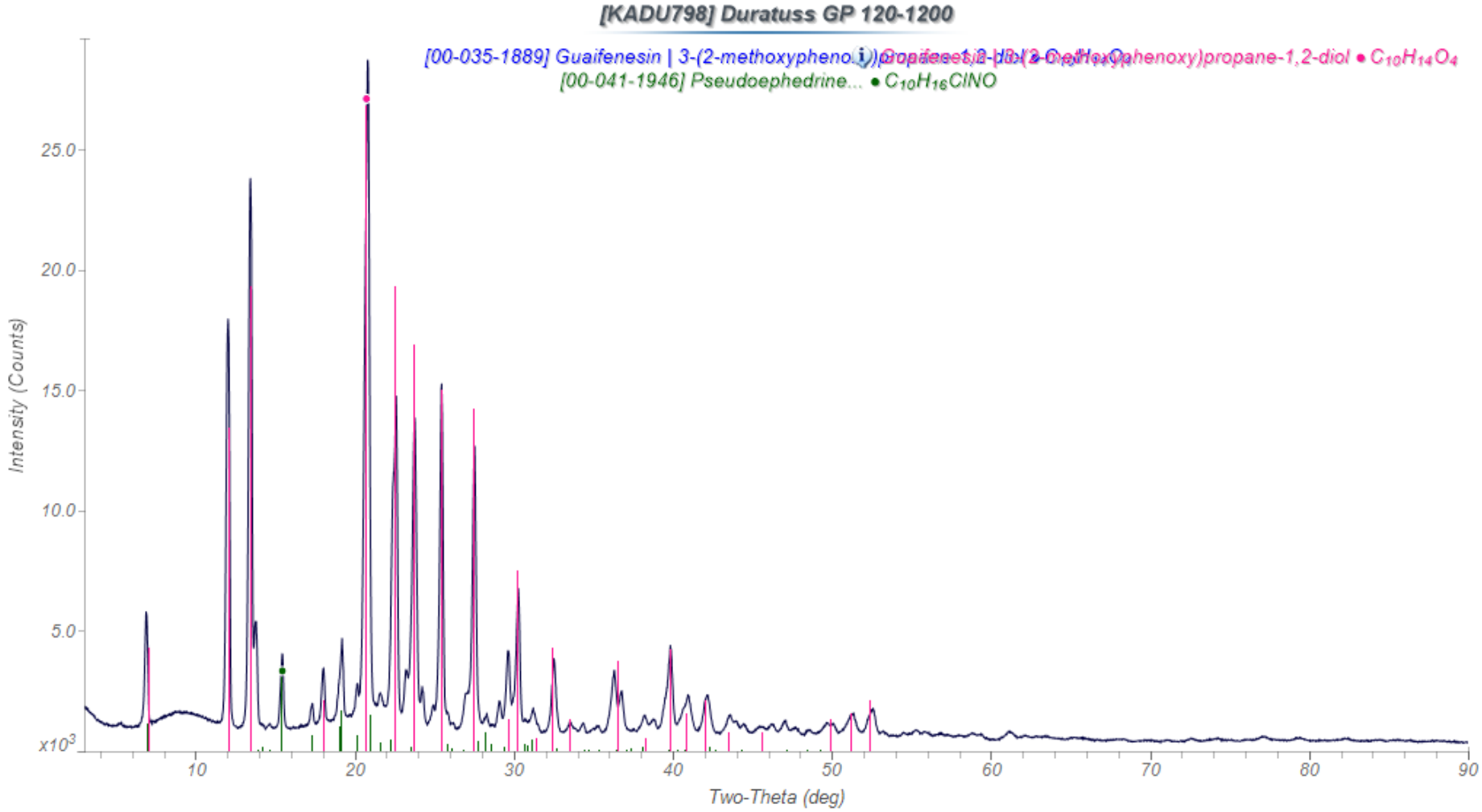
[KADU798] Duratuss GP 120-1200
[00-035-1889] Guaifenesin | 3-(2-methoxyphenoxy)propane-1,2-diol • C10H14O4
[00-041-1946] Pseudoephedrine... • C10H16ClNO
Intensity (Counts)
x10^3
25.0
20.0
15.0
10.0
5.0
10
20
30
40
50
60
70
80
90
Two-Theta (deg)

Quantitative Phase Analysis of Duratuss GP 120-1200

Phase	wt%	int. std. wt%	expected mg	wt%
guaifenesin	91.62(2)	90.4(4)	1200	90.9
pseudoephedrine hydrochloride	8.38(15)	7.7(4)	120	9.1
sum	100	98.1	1320	100

Actual tablets weigh ~1540 mg
120/1540 = 0.078!

Re-Visit the IUCr CPD QPARR Samples 1*n*

IUCr CPD QPARR – 2008 Results

Sample	Data Source	Al_2O_3 wt%	CaF_2 wt%	ZnO wt%		Sample	Data Source	Al_2O_3 wt%	CaF_2 wt%	ZnO wt%
1A	Ineos Weight	1.33(6) 1.15	95.1(1) 94.81	3.53(7) 4.04		1E	Ineos Weight	56.0(4) 55.12	29.3(3) 29.62	14.7(2) 15.25
1B	Ineos Weight	94.54(2) 94.31	4.13(2) 4.33	1.32(1) 1.36		1F	Ineos Weight	27.4(3) 27.06	17.9(0) 17.72	54.7(2) 55.22
1C	Ineos Weight	5.4(1) 5.04	1.27(2) 1.36	93.3(1) 93.59		1G	Ineos Weight	31.3(1) 31.37	34.9(0) 34.42	33.9(1) 34.21
1D	Ineos Weight	13.6(3) 13.53	54.3(1) 53.58	32.2(2) 32.89		1H	Ineos Weight	36.1(1) 35.12	34.5(1) 34.69	29.4(2) 30.19

IUCr CPD QPARR
Samples 1*n*
2008 Results

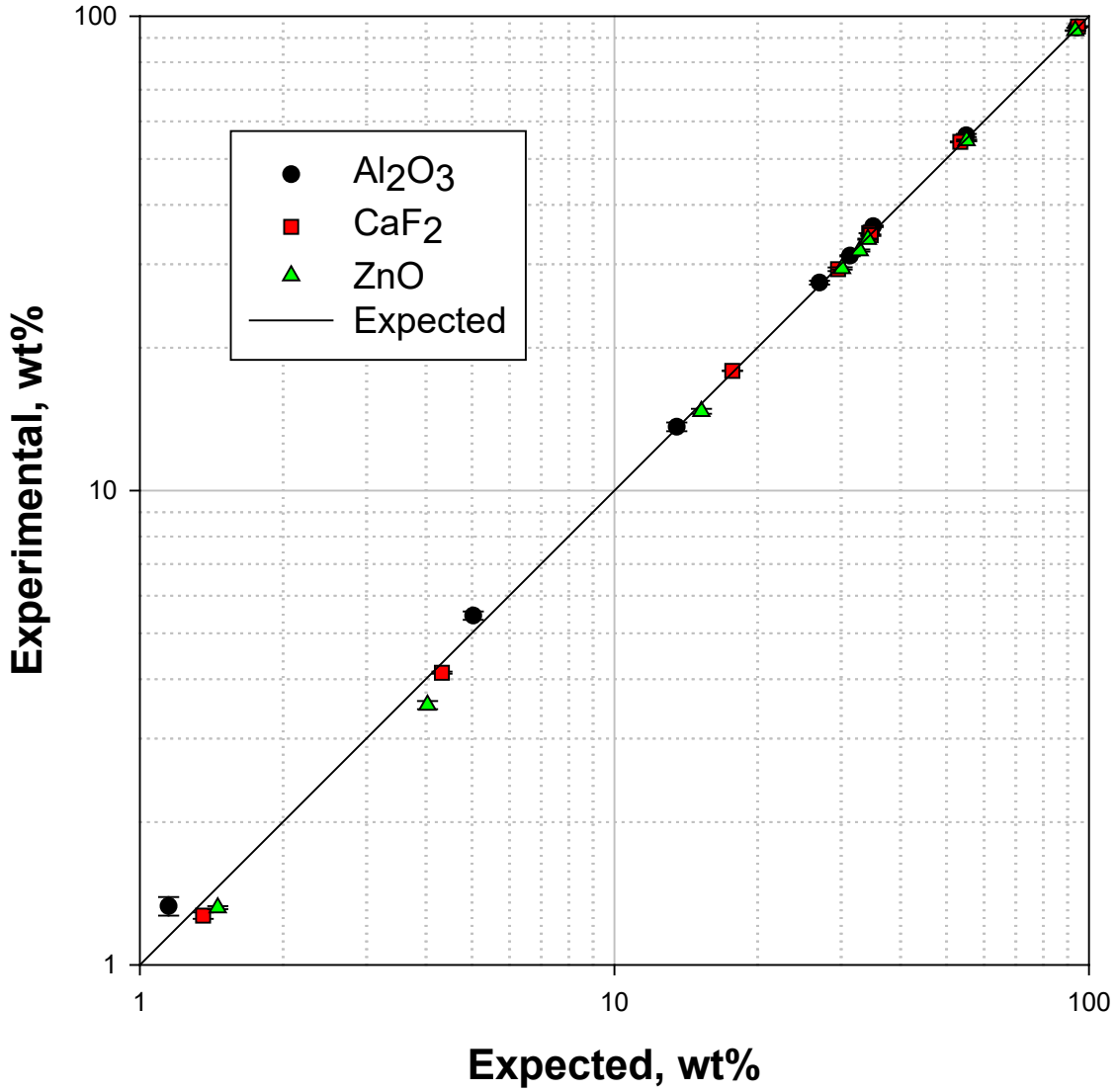

Absolute Concentration Errors
IUCr CPD QPARR Samples 1*n*
2008 Results, Triplicate Analyses

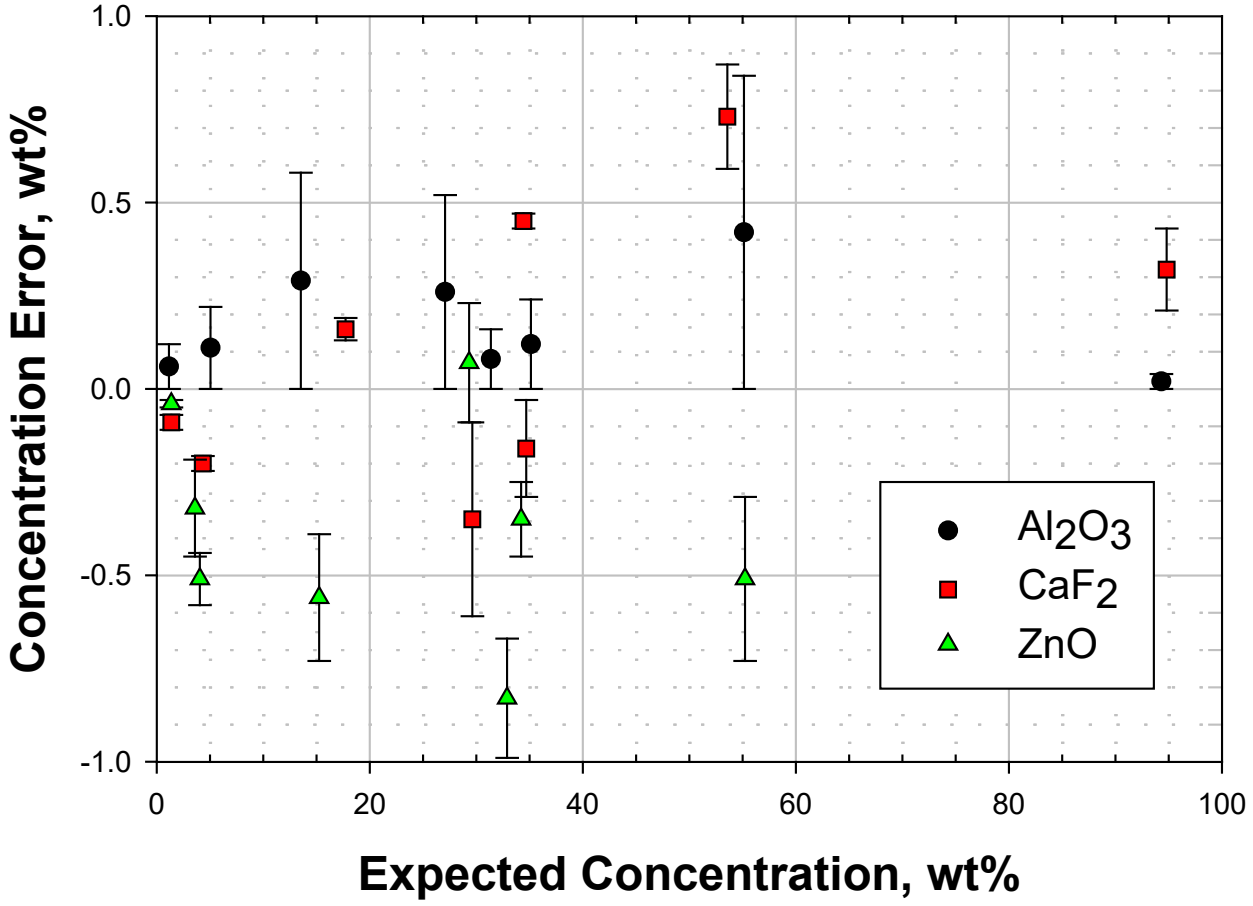

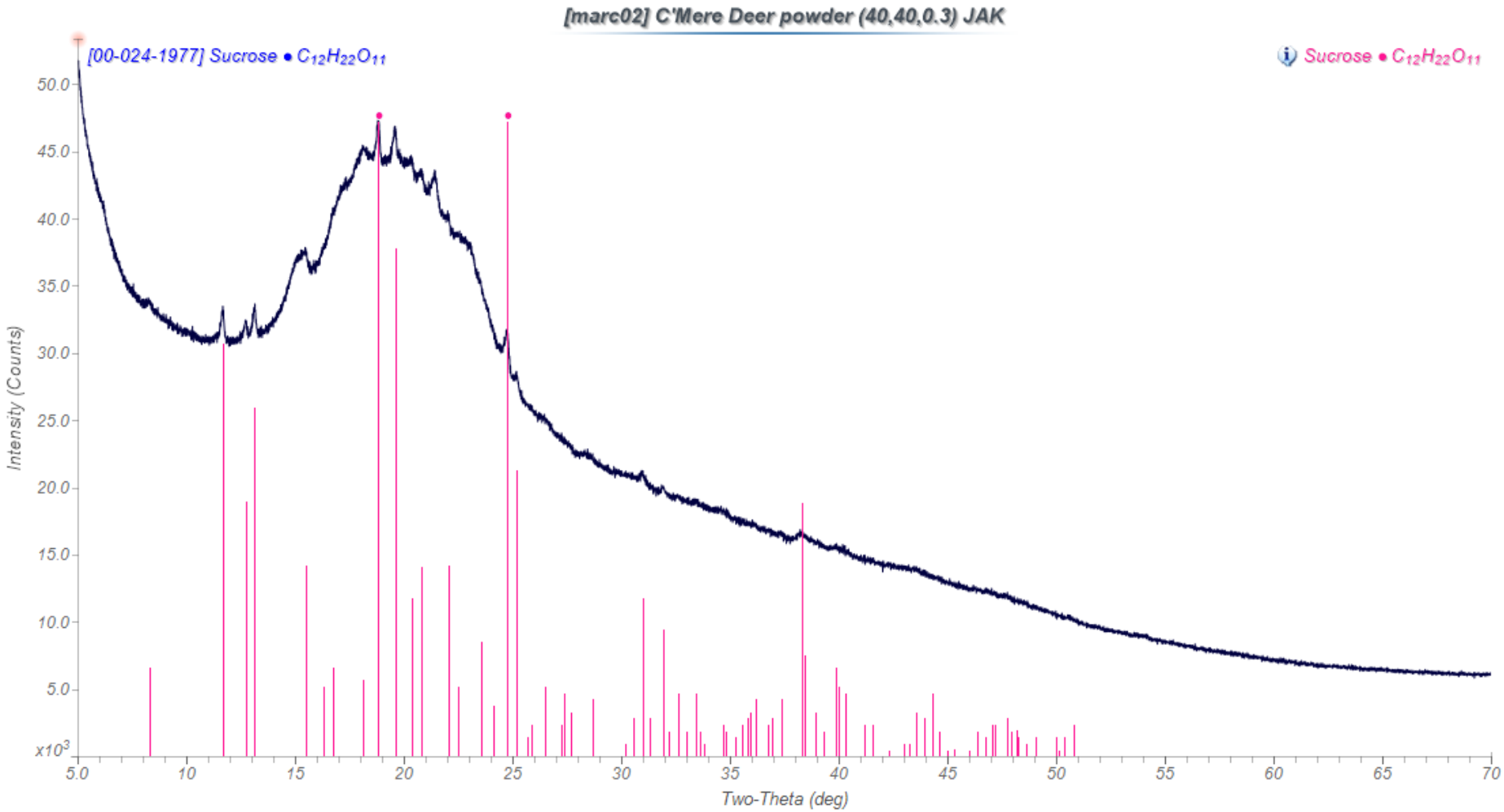
[marc02] C'Mere Deer powder (40,40,0.3) JAK
[00-024-1977] Sucrose • C12H22O11
Sucrose • C12H22O11
Intensity (Counts)
x10^3
50.0
45.0
40.0
35.0
30.0
25.0
20.0
15.0
10.0
5.0
5.0
10
15
20
25
30
35
40
45
50
55
60
65
70
Two-Theta (deg)

C’Mere Deer powder

rice bran, soybeans, corn, yeast,
trace minerals (< 2%),
artificial and natural flavorings

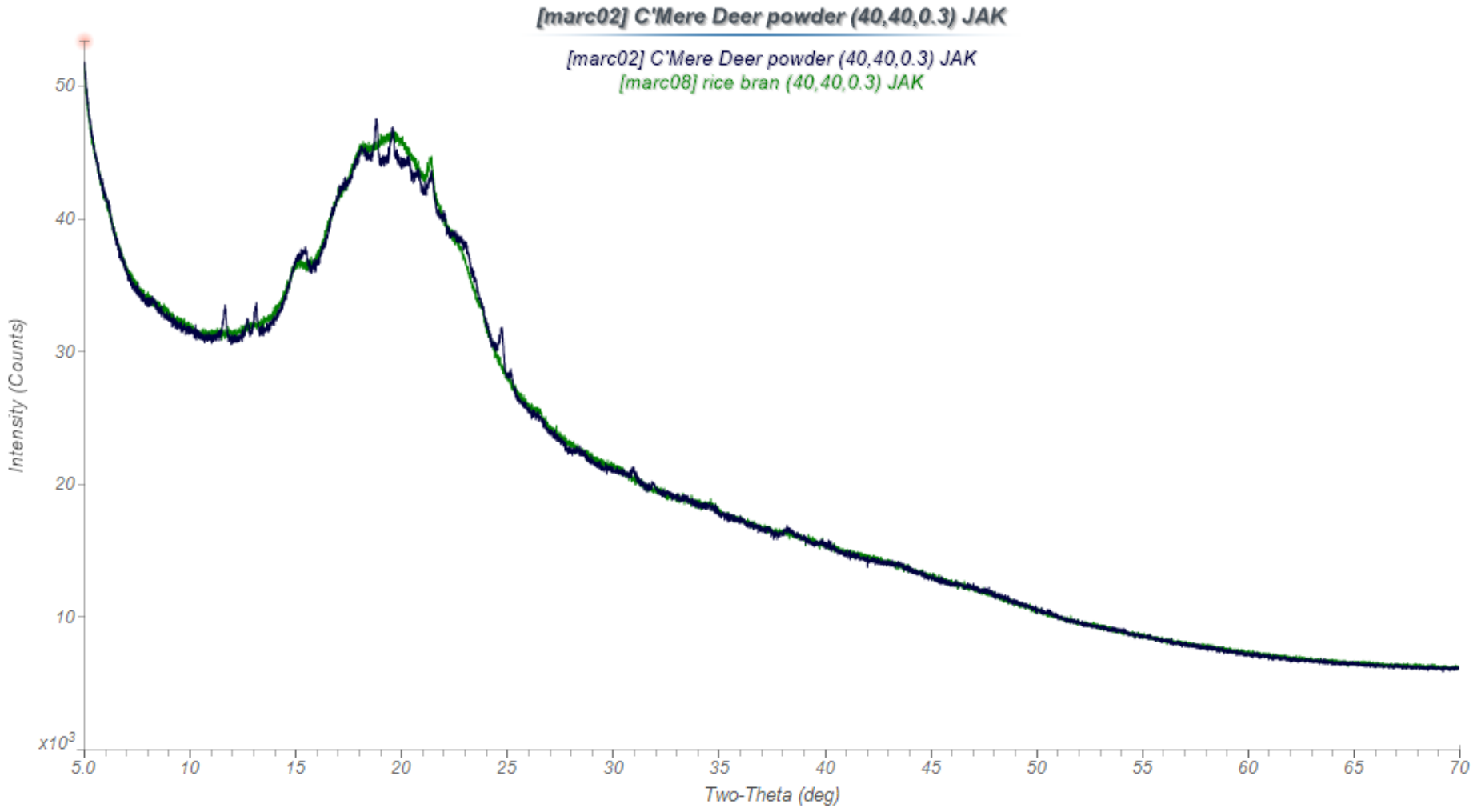
[marc02] C'Mere Deer powder (40,40,0.3) JAK
[marc02] C'Mere Deer powder (40,40,0.3) JAK
[marc08] rice bran (40,40,0.3) JAK
Intensity (Counts)
x10^3
50
40
30
20
10
5.0
10
15
20
25
30
35
40
45
50
55
60
65
70
Two-Theta (deg)

Address on the label is:
EST, LLC
205 Fair Ave.
Winnsboro LA 71295

Most US rice is grown in LA, so perhaps rice bran is cheap!

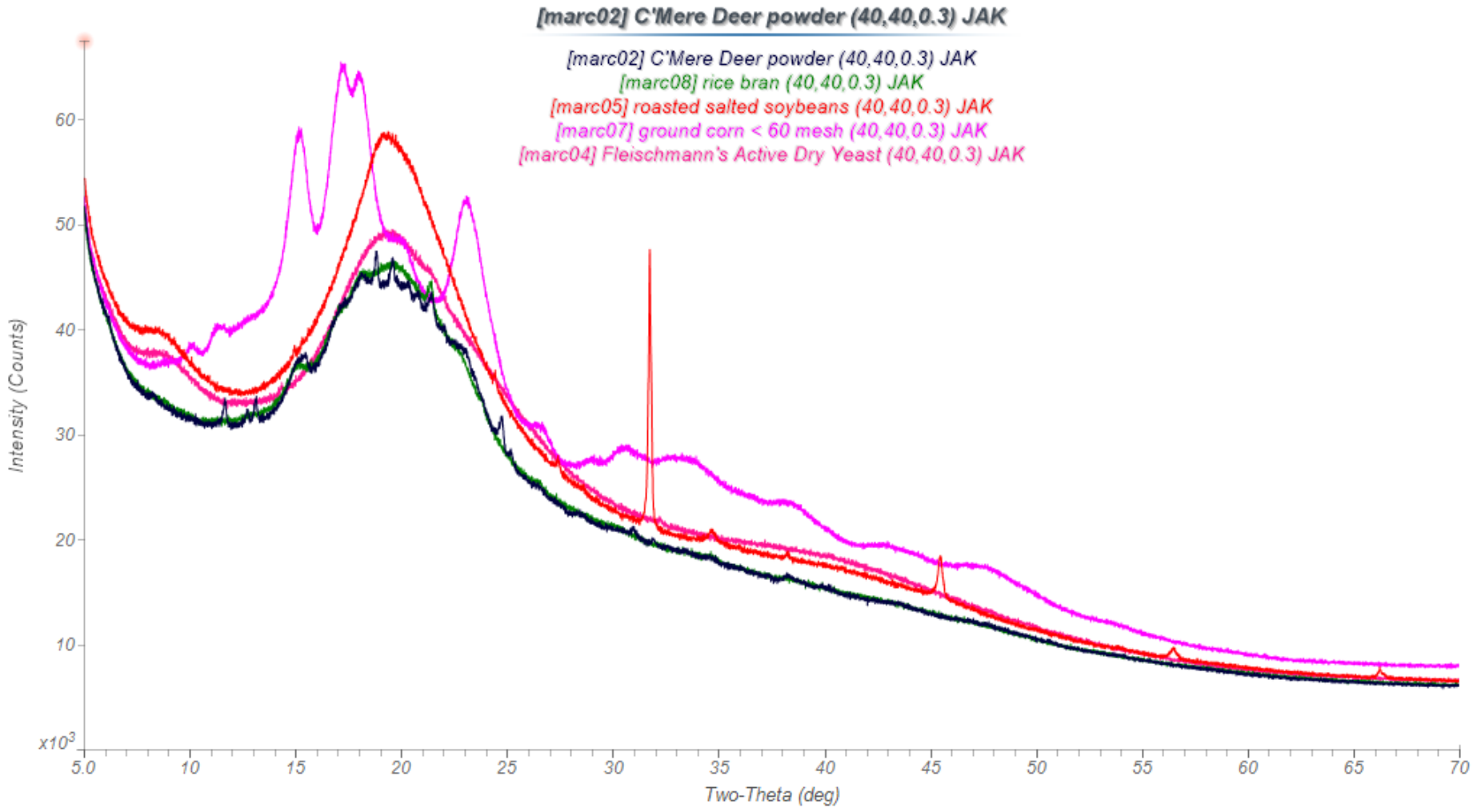
[marc02] C'Mere Deer powder (40,40,0.3) JAK
[marc02] C'Mere Deer powder (40,40,0.3) JAK
[marc08] rice bran (40,40,0.3) JAK
[marc05] roasted salted soybeans (40,40,0.3) JAK
[marc07] ground corn < 60 mesh (40,40,0.3) JAK
[marc04] Fleischmann's Active Dry Yeast (40,40,0.3) JAK
Intensity (Counts)
x10^3
60
50
40
30
20
10
5.0
10
15
20
25
30
35
40
45
50
55
60
65
70
Two-Theta (deg)

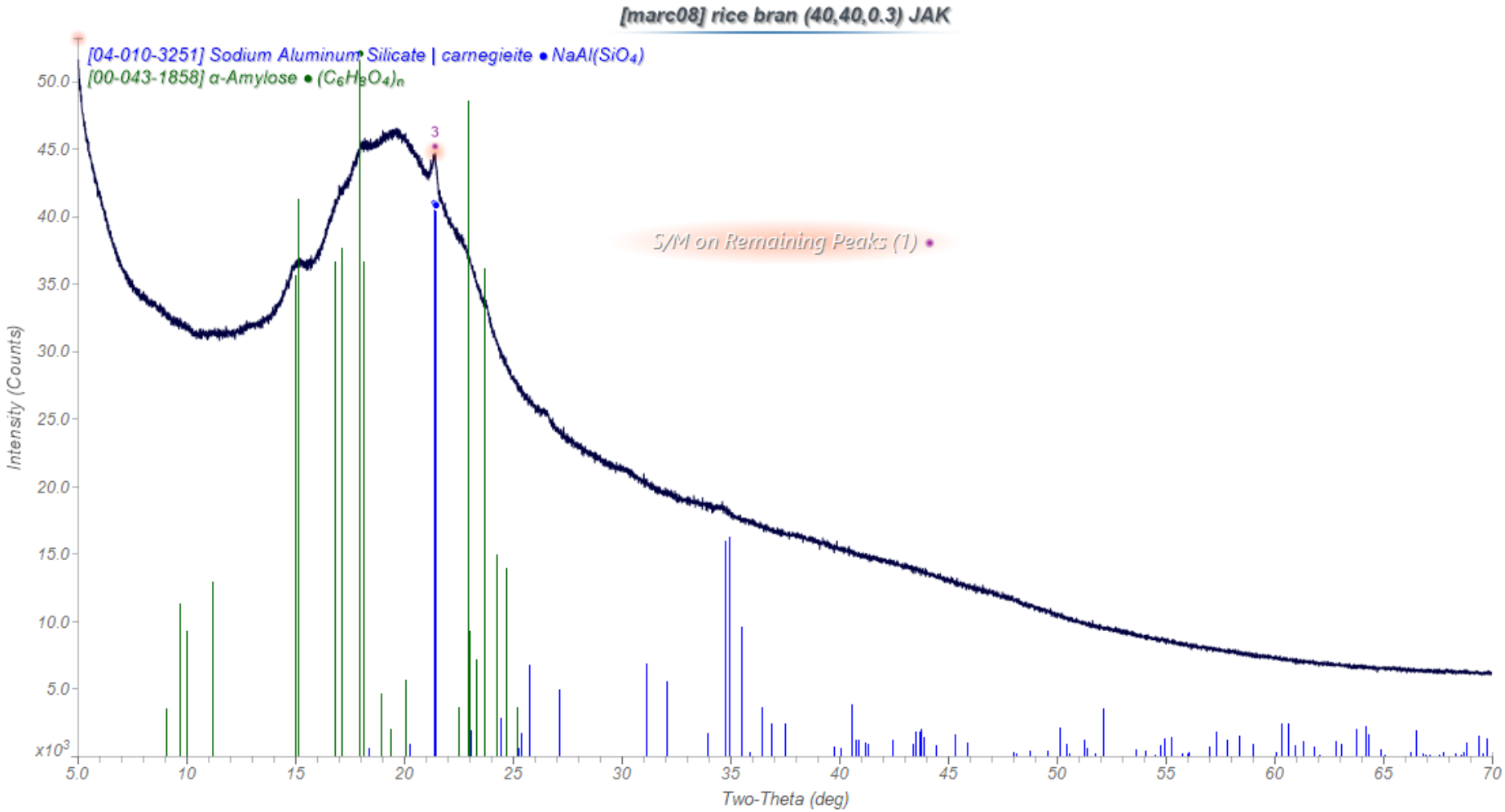
[marc08] rice bran (40,40,0.3) JAK
[04-010-3251] Sodium Aluminum Silicate | carnegieite • NaAl(SiO4)
[00-043-1858] α-Amylose • (C6H10O4)n
S/M on Remaining Peaks (1)
Intensity (Counts)
x10^3
Two-Theta (deg)

Rice is known to be good at extracting silica from the soil.

Maybe some quartz, too?

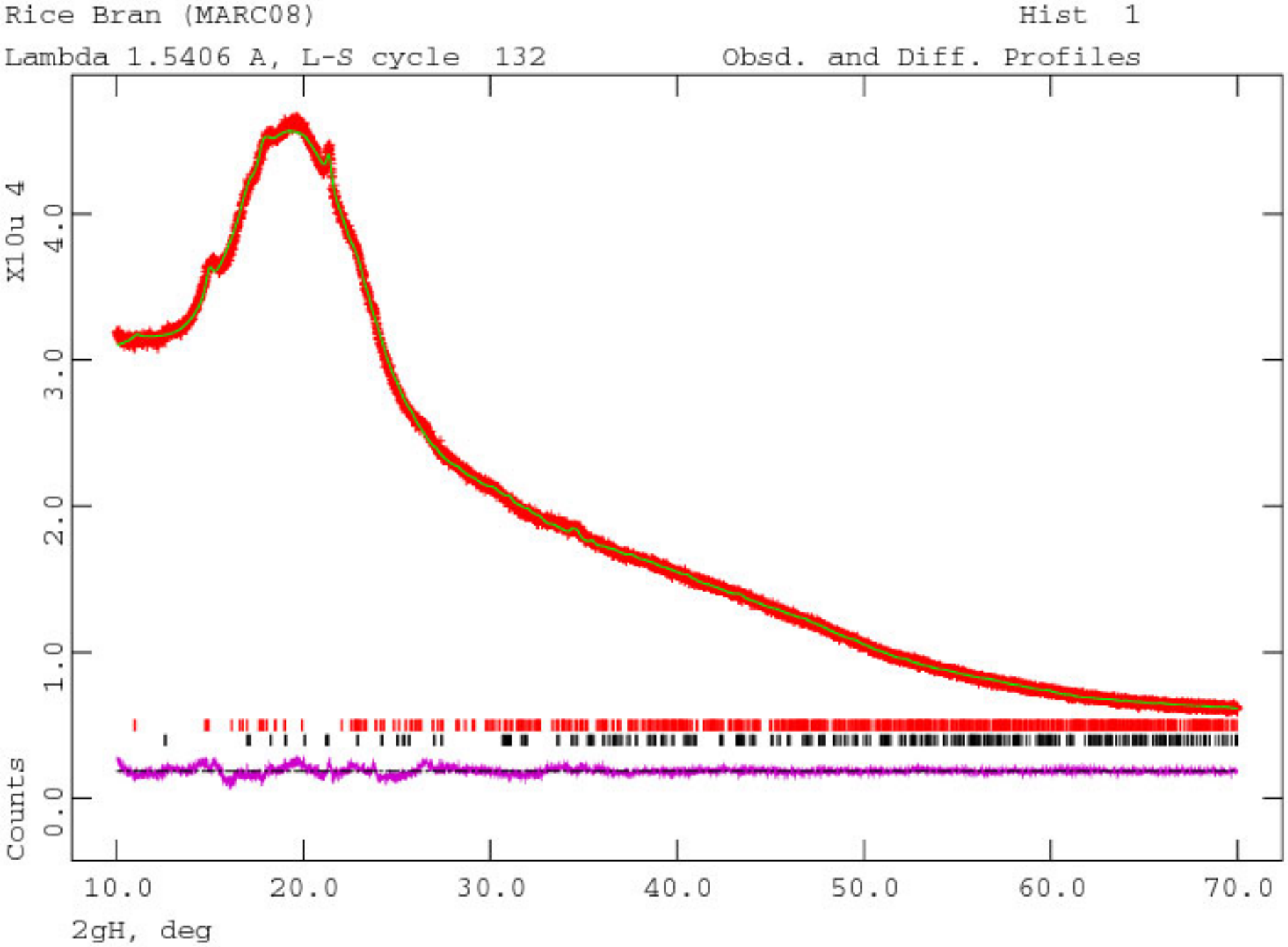
Rice Bran (MARC08)
Hist 1
Lambda 1.5406 A, L-S cycle 132
Obsd. and Diff. Profiles
X10u 4
4.0
3.0
2.0
1.0
0.0
Counts
10.0
20.0
30.0
40.0
50.0
60.0
70.0
2gH, deg

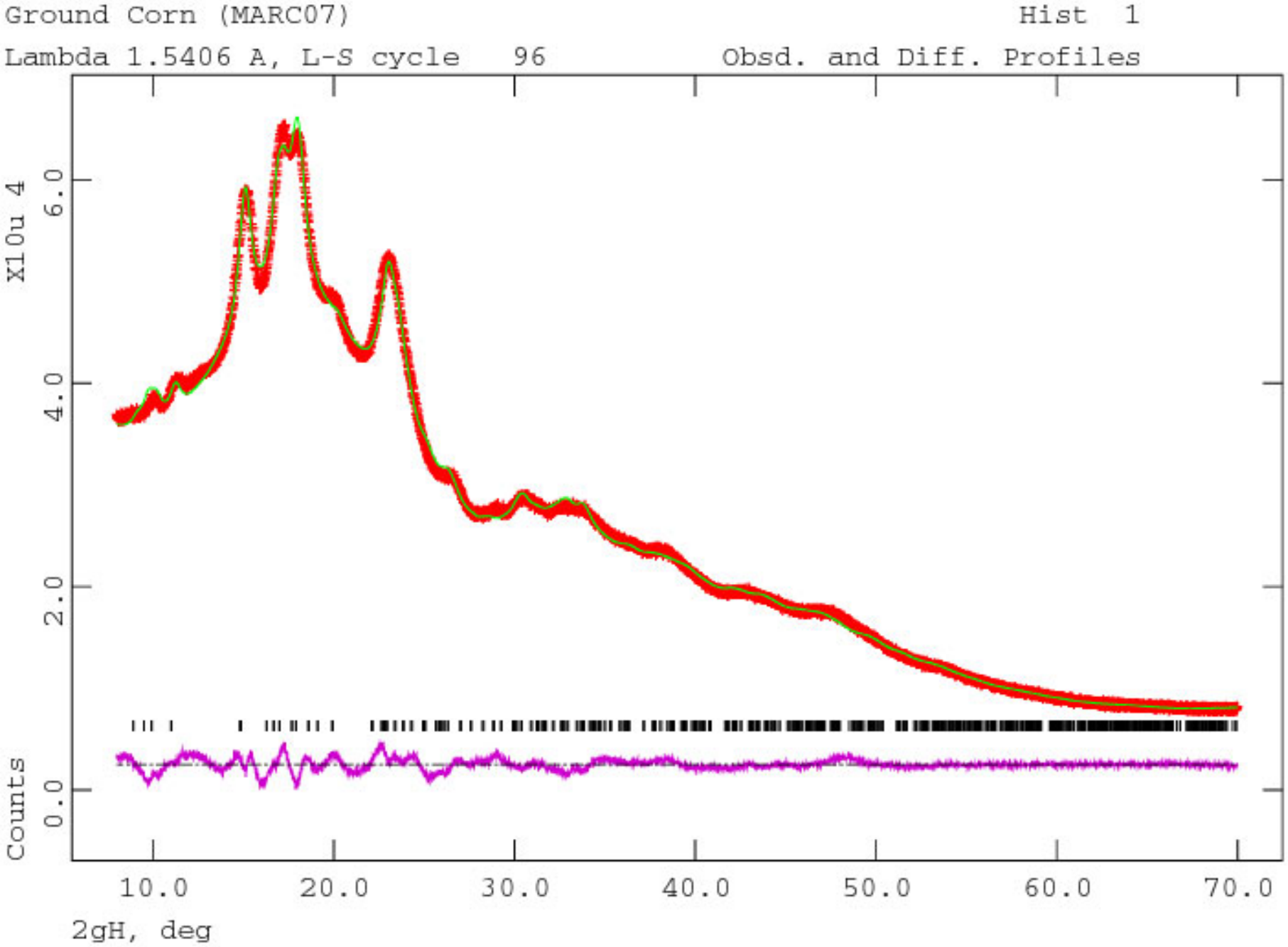
Ground Corn (MARC07)
Hist 1
Lambda 1.5406 A, L-S cycle 96
Obsd. and Diff. Profiles
X10u 4
6.0
4.0
2.0
0.0
Counts
10.0
20.0
30.0
40.0
50.0
60.0
70.0
2gH, deg

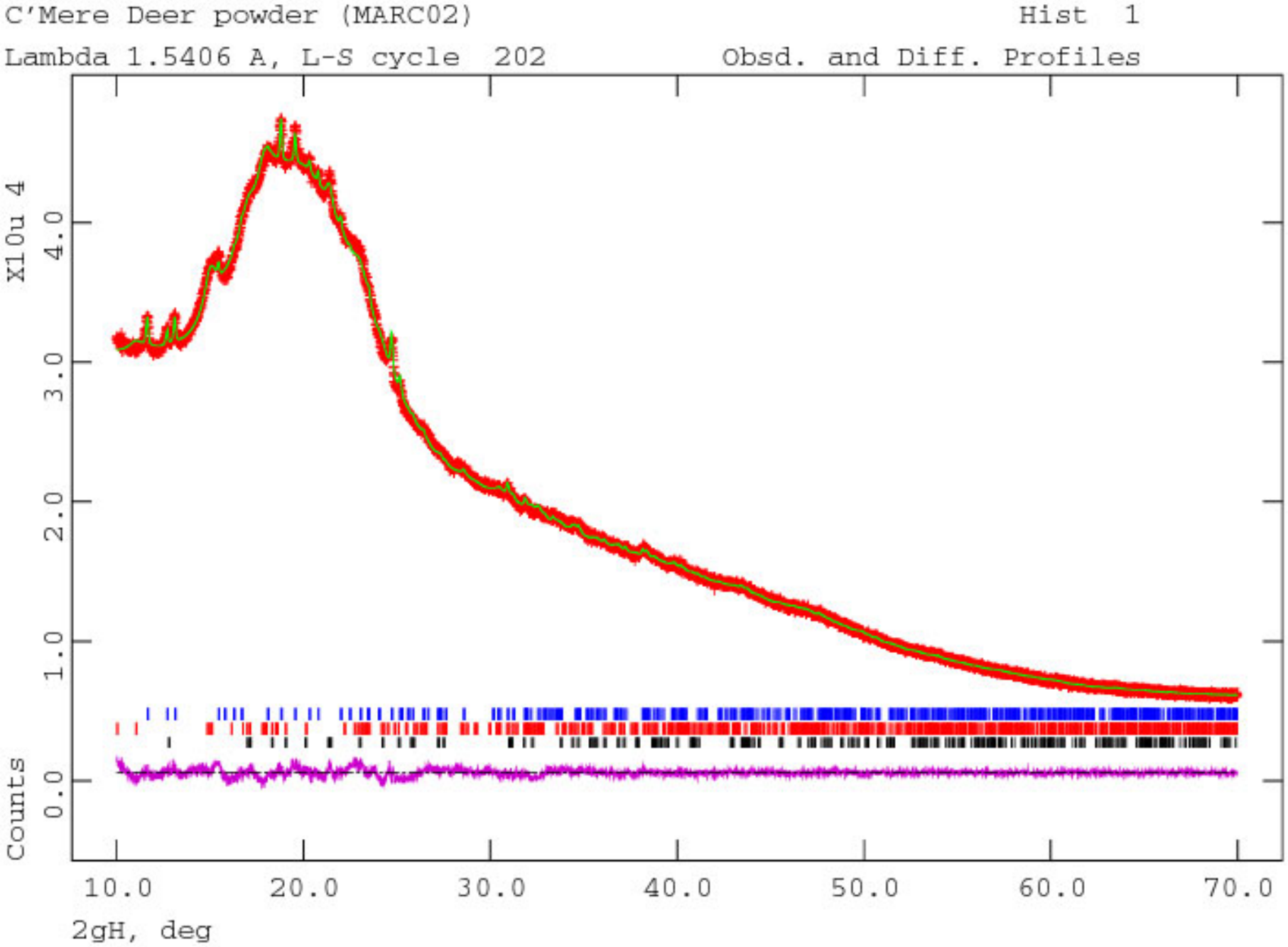
C'Mere Deer powder (MARC02)
Hist 1
Lambda 1.5406 A, L-S cycle 202
Obsd. and Diff. Profiles
X10u 4
4.0
3.0
2.0
1.0
0.0
Counts
10.0
20.0
30.0
40.0
50.0
60.0
70.0
2gH, deg

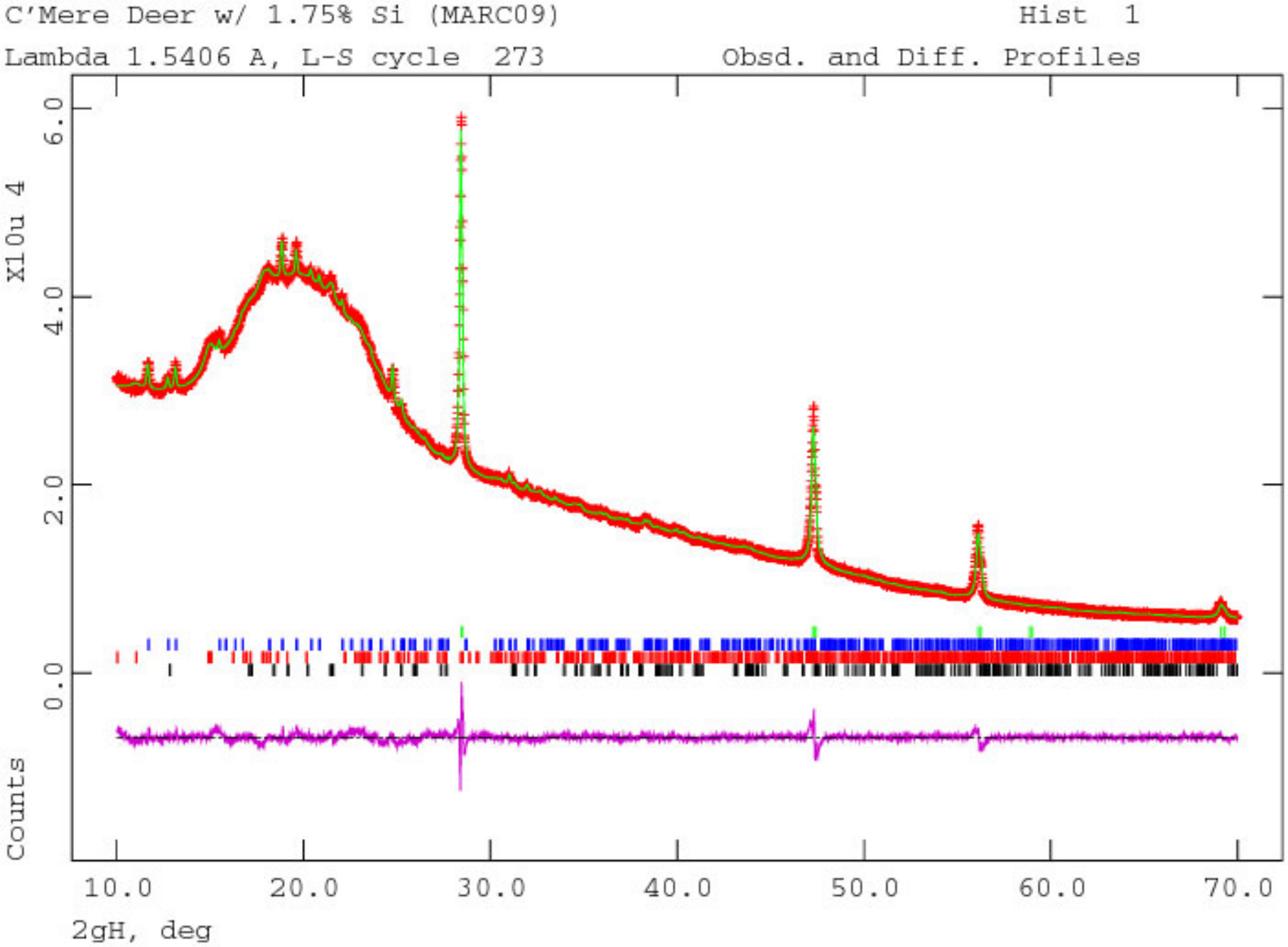
C'Mere Deer w/ 1.75% Si (MARC09)
Hist 1
Lambda 1.5406 A, L-S cycle 273
Obsd. and Diff. Profiles
X10u 4
6.0
4.0
2.0
0.0
Counts
10.0
20.0
30.0
40.0
50.0
60.0
70.0
2gH, deg

Quantitative Phase Analysis of C'Mere Deer Powder

Phase	Raw wt%	Abs. wt%	Real wt%
$NaAlSiO_4$	5.2(2)	0.42	0.4(1)
Amylose	56.9(4)	4.60	4.7(1)
Sucrose	16.3(2)	1.32	1.3(1)
Si	21.62(6)	1.75	-

The Merck Index says that corn is typically 27% amylose and 73% amylopectin, so this translates into ~17 wt% corn.

Scaling "Experiments"

Variable	Rice Bran	Corn	Soybeans	Yeast
(background-subtracted) raw patterns	70	10	10	10
Amylose scale factors		11		
Diffuse scattering amplitudes	83			
Best Guess	76	15	4	4

1.3% sucrose, and traces of minerals and flavors.